



00033040

## Volume I

U. S. Bureau of Mines  
Minneapolis, Minn.

LIBRARY

Development and Testing of an  
Electromagnetic Location System

A. J. Farstad  
C. Fisher, Jr.  
R. F. Linfield  
R. O. Maes  
B. Lindeman

Westinghouse Electric Corporation  
Friendship International Airport  
Baltimore, Maryland

May, 1973

Final report covering the period  
July, 1972 to April, 1973

Prepared for

The U. S. Bureau of Mines  
Under Contract H0220073

OFR  
74-41 (1)

Disclaimer

The views and conclusions contained in this document are those of the authors and should not be interpreted as necessarily representing the official policies of the Department of the Interior, Bureau of Mines, or the U. S. Government.



## PREFACE

This report is one of a series of four volumes of a final report prepared for the Bureau of Mines under Contract H0220073. The report contained herein includes that work done on electromagnetic direction finding systems between July of 1972 and April of 1973. Two design approaches were included in this effort; (1) a prototype pulse system was fabricated and subjected to limited testing, and (2) a CW system was fabricated and tested at three operating mine sites. The latter included testing in conjunction with a helicopter. In late 1972 the pulse system effort was discontinued in favor of the CW system approach. After modifications, the latter was subjected to limited testing which was completed in May of 1973.

Part I below constitutes the final report in the CW direction finding system. Part II is devoted to the pulse system.

## PART I

### DEVELOPMENT AND TESTING OF A CW ELECTROMAGNETIC LOCATION SYSTEM

#### CONTENTS

<u>Section</u>		<u>Page</u>
1.0	INTRODUCTION	1
2.0	SIGNAL PROPAGATION	3
3.0	LOCATION SYSTEM DESIGN	6
	3.1 Optimization of Operating Frequency	6
	3.2 Transmitting System Tradeoffs	15
	3.3 Receiving System Tradeoffs	19
4.0	SYSTEM PERFORMANCE	27
	4.1 Manpack EM Transmitter Model 837-A	27
	4.2 EM Location Receiver Model C836-A	28
	4.3 EM Location Receiver Model C842	29
5.0	FIELD MEASUREMENTS	30
	5.1 Test Coal Mines	30
	5.1.1 Island Creek Coal Co. Guyan No. 1A	30
	5.1.2 Union Carbide Co. Putnam Mine	42
	5.1.3 Robena #4 Mine (U.S. Steel)	57
	5.2 Hardrock Mine	78
	U. S. Tunnel, Idaho Springs, Colorado	78
6.0	MINE LOCATION SYSTEM CHARACTERIZATION	83
7.0	ALTERNATE LOCATION SYSTEM CONFIGURATION	94
8.0	IMPROVED LOCATION SYSTEM SPECIFICATIONS	102
9.0	CONCLUSIONS AND RECOMMENDATIONS	104
	REFERENCES (PART I)	113

## PART I

## LIST OF FIGURES

Page



PART I  
LIST OF FIGURES

	<u>Page</u>
Figure 5-5      Field Intensity Profile above Vertical Magnetic Dipole at the Guyan No. 1A Mine, Amherstdale, W. Va. (North-South Profile)	40
Figure 5-6      Field Intensity Profile above Vertical Magnetic Dipole at the Guyan No. 1A Mine, Amherstdale, W. Va. (East-West Profile)	41
Figure 5-7      Earth Conductivity Sounding , Putnam Mine, Elmwood, West Virginia	43
Figure 5-8      Surface EM Noise vs. Frequency (Surface Location G)	44
Figure 5-9      Surface EM Noise vs. Frequency (Surface Location G <sub>1</sub> )	45
Figure 5-10     EM Location Experiments at the Putnam Mine, Elm- wood, West Virginia	47
Figure 5-11     Field Intensity Profile above Vertical Magnetic Dipole at Putnam Mine, Elmwood, West Virginia (East-West Profile Location A).	51
Figure 5-12     Field Intensity Profile above Vertical Magnetic Dipole at Putnam Mine, Elmwood, West Virginia (North- South Profile Location A).	52
Figure 5-13     Field Intensity Profile above Vertical Magnetic Dipole at Putnam Mine, Elmwood, West Virginia (North- South Profile, Location C)	53
Figure 5-14     Field Intensity Profile above Vertical Magnetic Dipole at Putnam Mine, Elmwood, West Virginia (East-West Profile, Location C)	54
Figure 5-15     Field Intensity Profile above a Vertical Magnetic Dipole at Putnam Mine, Elmwood, West Virginia (North-South Profile, Location G)	55
Figure 5-16     Field Intensity Profile above a Vertical Magnetic Dipole at Putnam Mine, Elmwood, West Virginia (East-West Profile, Location G)	56
Figure 5-17     Robena Mine No. 4 Mine Map	58
Figure 5-18     Robena Mine No. 4 Conductivity Sounding	60
Figure 5-19     Oscilloscope photographs of receiver IF output after 53 hours of continuous transmitter operation.	64



PART I  
LIST OF FIGURES

	<u>Page</u>
Figure 5-20 Surface EM Noise vs. Frequency Robena Mine, 30 ft. from Compressor	65
Figure 5-21 Surface EM Noise vs. Frequency Location D & E, (Mine Operating)	66
Figure 5-22 Surface EM Noise vs. Frequency Location D & E, (Mine not operating)	67
Figure 5-23 Surface EM Noise vs. Frequency - Location B & C	68
Figure 5-24 Surface EM Noise vs. Frequency - Location B & C	69
Figure 5-25 EM Noise vs. Frequency Directly Beneath Enstrom F28A Helicopter	70
Figure 5-26 EM Noise vs. Frequency 35 ft. behind Enstrom F28A Helicopter	71
Figure 5-27 EM Noise vs. Frequency Directly beneath Bell Jet Ranger 206A Helicopter	72
Figure 5-28 EM Noise vs. Frequency 35 ft. behind Bell Jet Ranger 206A Helicopter	73
Figure 5-29 Theoretical Field Profiles for Airborne Fields over Robena Mine	76
Figure 5-30 Transit-Tape Survey of the U. S. Tunnel	79
Figure 5-31 Earth Conductivity Sounding, U. S. Tunnel, Idaho Springs, Colorado	81
Figure 5-32 Surface EM Noise vs. Frequency U. S. Tunnel Idaho Springs, Colorado - Data Processing Bandwidth 9.8 Hz.	82
Figure 6-1 Multiple Access Trade-Off Curves for Mine Location System Characterization	84
Figure 6-2 Conductivity & Frequency Effects on Performance for one Antenna Configuration	86
Figure 6-3 Detection Depth vs. Frequency for Estimated Noise Models	87
Figure 6-4 Field Strength vs. Depth for Antenna Configuration used at Robena	89
Figure 6-5 System Performance Characteristics using Multiple Antenna Elements in Series	91

PART I  
LIST OF FIGURES

		<u>Page</u>
Figure 6-6	Wire Weight vs. Battery Life for Different Antenna Antenna Configurations.	92
Figure 7-1	Full Wave Switching Arrangement	96
Figure 7-2	Current vs. Supply Voltage for a Full Wave Switching Amplifier into a 0.4 Ohm Resistive Load	99

PART II  
TABLE OF CONTENTS

<u>Section</u>		<u>Page</u>
1.0	Introduction	114
	1.1 Basic Phenomenon	114
	1.2 Summary	114
2.0	Theory	116
	2.1 Introduction	116
	2.2 Analysis	118
	2.3 Terrain Slope Considerations	128
	2.4 Noise Effects	129
3.0	Equipment Design	132
	3.1 Instrumentation	132
	3.2 Transmitter	132
	3.3 Transmitter Antenna	135
	3.4 Receiver	135
4.0	Experimental Results	144
	4.1 Island Creek Mine 1A, Blair, W.Va.	144
	4.2 Union Carbide Mine, Leon, W.Va.	153
	4.3 Operation	153
	4.4 Intrinsic Safety	158
	4.5 Endurance	158
	← 4.6 Equipment Calibration	163
5.0	Conclusions and Recommendations	166
	5.1 Conclusions	166
	5.2 Recommendations	166
6.0	Administration	167
	6.1 Rights in Data	167
	6.2 Inventions and Disclosures	167
7.0	References	168
 APPENDIX A		
1.0	Transmitter Parts List	A-1
2.0	Receiver Parts List	A-4



## PART II

### LIST OF ILLUSTRATIONS

<u>Figure</u>	<u>Page</u>
2.1-1 Buried Transient Source Received Waveform	117
2.2-1 Geometry of Location System	119
2.2-2 Propagation Factor	122
2.2.3-2 Pulse Waveform	126
2.2.3-3 Received Field Intensity	127
2.4-2 Frequency Variation of Atmospheric Noise	131
3.1-1 Transmitter Waveform	133
3.2-1 Mine Location Transmitter	134
3.4-1 Mine Location Receiver Main Frame	137
3.4-2 Input Amplifier A	138
3.4-3 Filter Modules $B_1$ and $B_3$	139
3.4-4 Typical Active Filter	140
3.4-5 $B_2$ and $B_4$ Filter Module	142
3.4-6 Output Amplifier (Module C)	143
4.1-1 Island Creek Mine	145
4.1-2 Island Creek Mine Location #1 N-S	146
4.1-3 Island Creek Mine Location #1 E-W	147
4.1-4 Island Creek Mine Location #1 N-S	149
4.1-5 Island Creek Mine Location #2 N-S	150
4.1-6 Island Creek Mine Location #2 E-W	151
4.1-7 Coverage	152
4.1-8 Putnam Mine, Location #1 E-W	154
4.1-9 Union Carbide Mine, Leon, W.Va.	155
4.1-10 Putnam Mine, Location #2 E-W	156
4.1-11 Putnam Mine, Location #2 N-S	157
4.1-12 Minimum Ignition Current (Voltage)	159
4.1-13 Minimum Ignition Current (Capacitance)	160
4.1-14 Minimum Ignition Current (Inductance)	161



List of Illustrations (Continued)

<u>Figure</u>		<u>Page</u>
4.5-1	Calibration Loop	164
4.5-2	Loop Characteristics	165
A-1	Transformer A3T1	A-3

PART I  
DEVELOPMENT AND TESTING OF A CW  
ELECTROMAGNETIC LOCATION SYSTEM

1.0 INTRODUCTION

The principle objective of the research effort described herein was to identify as rapidly as possible a practical trapped miner location system. Much effort has been expended in the past on the development of a highly sophisticated seismic location system [1] for trapped miners. Field tests of this system have shown that the location accuracy is limited by a combination of seismic velocity anomalies, timing errors, and in general by the relatively weak nature of the signals received at the surface. It was first felt that similar propagation anomalies would be experienced by electromagnetic systems, but to a greater extent than the seismic. However, preliminary tests performed by Westinghouse on the Operations and Maintenance Program, Contract No. H0210063 in 1971 and 1972, indicated that an electromagnetic solution to the location problem may be more feasible than a seismic solution. Thus a more concentrated effort was launched in 1972 and 1973 to more completely determine the feasibility of electromagnetic location systems for trapped miners. Two different approaches to the location problem were undertaken on this program: (1) A pulsed electromagnetic system was developed by the Special Systems Division of Westinghouse in Baltimore, and (2) a Continuous Wave (CW) System was developed by Westinghouse Georesearch Laboratory (WGL) in Boulder, Colorado. Part I of this report will deal only with the development and results of CW Location System developed by WGL.

The CW Location System was field tested at three eastern coal mines and at one western hardrock mine. The maximum overburden depth penetrated during these tests was 990 feet at the Robena No. 4 mine near Waynesburg, Pennsylvania. The earth conductivity at this mine was measured to be  $1.1 \times 10^{-2}$  mhos/m, which combined with the deep overburden make this mine representative of expected worst case conditions for a coal mine EM location exercise.

Equipment developed on this project consist of the following:

1. Westinghouse EM Manpack Location Transmitter Model C 837A.
2. Westinghouse EM Location Receiver Model C 836A.
3. Westinghouse Manpack Locator Model C 842A.

For complete descriptions of these systems, refer to Section 3 of the report. Additional breadboard development was undertaken following the field test period to produce a full wave solid state transmitter capable of operating closer to the limits of intrinsic safety and thus be capable of generating stronger field strengths at the surface. The results of this development are given in Section 7.0.



## 2.0 SIGNAL PROPAGATION

Formal expressions for the electric and magnetic fields excited by a vertical magnetic dipole placed below the surface of a semi-infinite conducting half space have been given by Wait and Campbell [2] and Sinha and Bhattacharya [3]. The results of these expressions are shown as a normalized frequency dependent attenuation factors (G, D & A) in Figure 2-1. The G factor\* applies to the attenuation experienced by the vertical magnetic field ( $H_z$ ) measured directly above a vertical magnetic transmitting dipole, separated by the indicated number of skin depths ( $\delta$ ). A skin depth is defined by

$$\delta \approx \frac{503.3}{(f \sigma)^{1/2}} \quad \text{meters}$$

where

$f$  is the frequency in Hertz, and

$\sigma$  is the earth conductivity in mhos/m.

The strength of the dipole source is measured by its dipole moment:

$$M \equiv \text{magnetic dipole moment} = I \cdot N \cdot A$$

where

$I$  is the loop current in amperes

$N$  is the number of turns in the transmitting loop

$A$  is the loop area in square meters.

Although Figure 2-1 applies only to the special case of the observer being located directly above the source, Westinghouse has developed computer programs to compute the fields anywhere on, in or above the air-earth interface. These programs were utilized in predicting the signal to noise ratios shown in Section 3.

\* See Appendix, page A9.



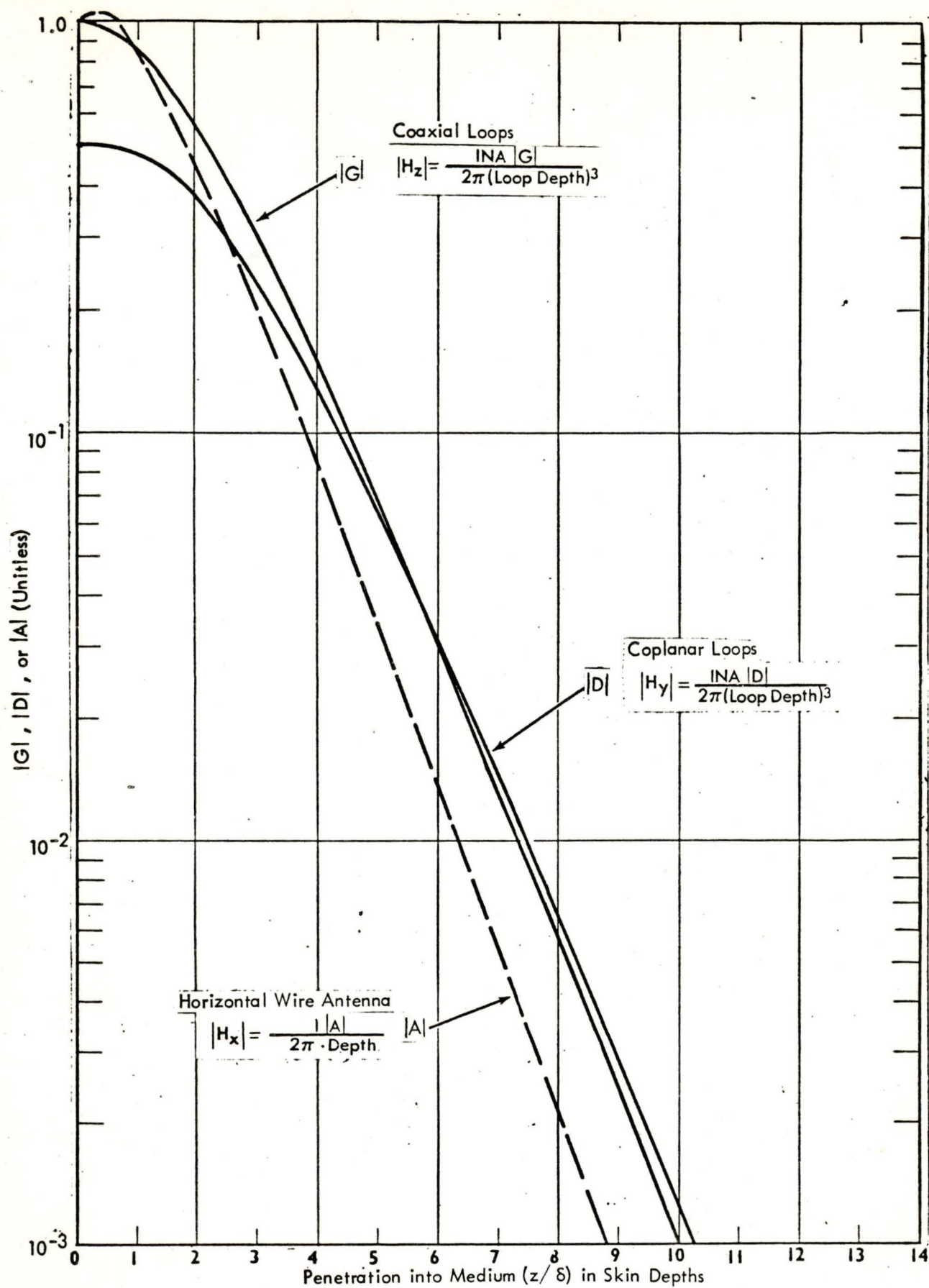


Figure 2-1 . Loop Antenna and Horizontal Coupling Relationships

The rapid decrease in  $|G|$  and  $|D|$  with increasing frequency shown in Figure 2-1 illustrates the large attenuation that signals above the VLF band incur in propagating through the earth. These propagation characteristics were taken into account along with an estimate of the frequency dependent background noise to arrive at a choice of optimum operating frequency for a practical coal mine EM manpack location system. The design of a practical system is described in detail in Section 3.

### 3.0 LOCATION SYSTEM DESIGN

Before entering into a detailed hardware design of an EM Location System, a design study task was undertaken to resolve some of the fundamental questions regarding optimization of (1) frequency (2) antenna configurations, and (3) receiver design concepts. A re-evaluation of typical coal mine parameters, and in particular, overburden depth and ground conductivity, was undertaken and a design goal for penetration capability was established as 1200 ft. of overburden (366 meters) with a conductivity of  $10^{-2}$  mhos/m. Surface signal to noise ratios for practical manpack transmitter moments were computed based on the atmospheric noise model for the spring season in Boulder, Colorado given in USBM Summary Report Contract H0210063, May 1971-June 1972. Surface noise will vary widely in time and space; this atmospheric noise model was adequate for preliminary design work. Curves showing transmitter dipole movement required to produce surface signal to noise ratios of 10 dB are also given.

#### 3.1 Optimization of Operating Frequency

An optimum frequency band was chosen for the EM Location System based on which frequencies gave the maximum surface signal to noise ratio after taking into account all propagation losses for a range of overburden depths from 10 meters to 1000 meters and a range of overburden conductivities from  $3 \times 10^{-4}$  mhos/m to  $3 \times 10^{-1}$  mhos/m. These curves, shown in Figures 3-1 to 3-5, indicate that for shallow overburdens (10-30 meters) the maximum signal to noise ratio is observed at 2kHz for all of the conductivities represented. However, for deeper overburdens and in particular those with the higher conductivities the optimum frequencies tend to shift to lower frequencies. The 300 meter curve (984 ft.) is most indicative of our design goal for an EM Location System and the  $10^{-2}$  mho/m conductivity curve peaks broadly between



Figure 3-1 MAGNETIC FIELD STRENGTH/ATMOSPHERIC NOISE

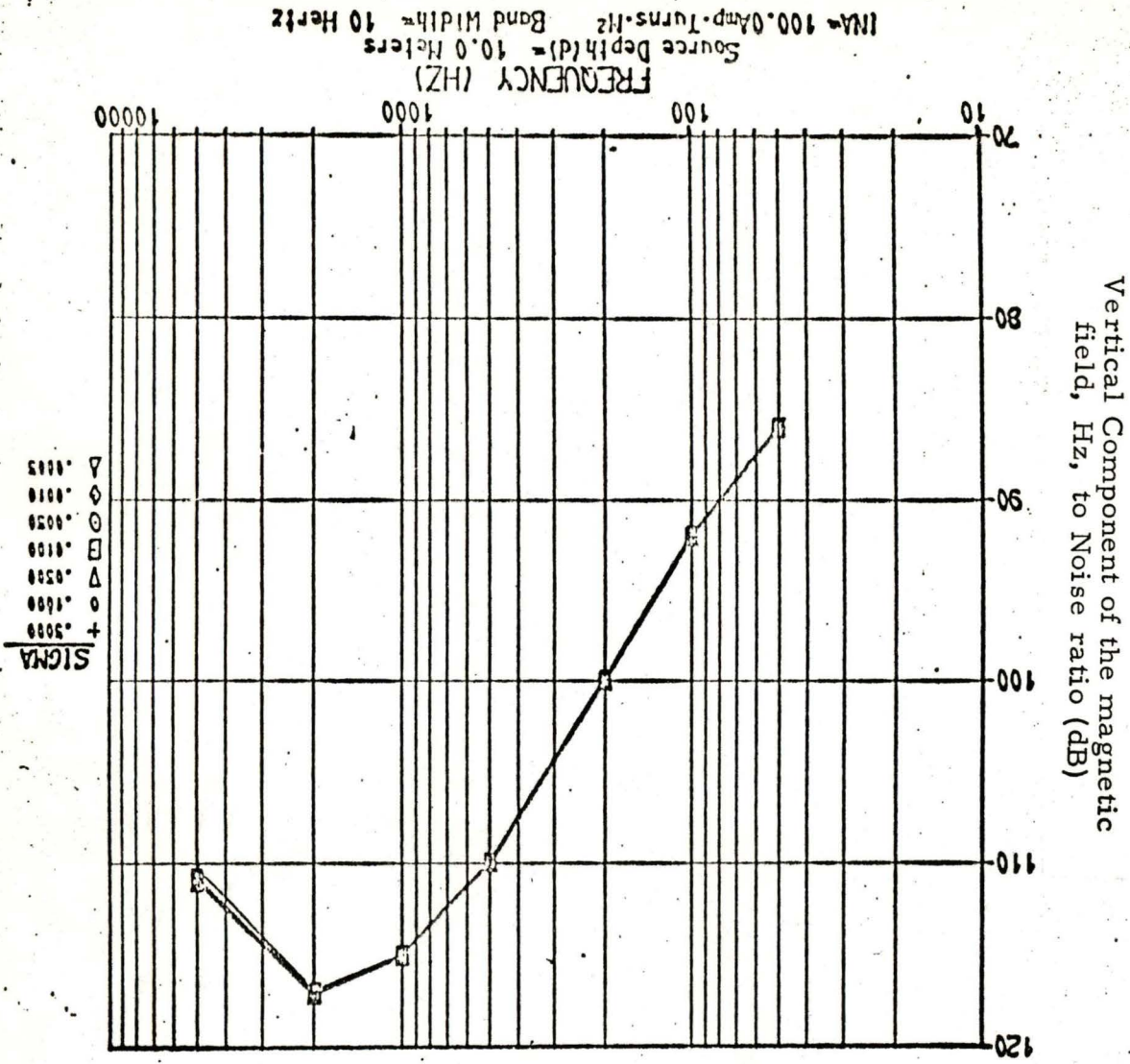




Figure 3-2 MAGNETIC FIELD STRENGTH/ATMOSPHERIC NOISE  
SUBSURFACE VERTICAL MAGNETIC DIPOLE SOURCE

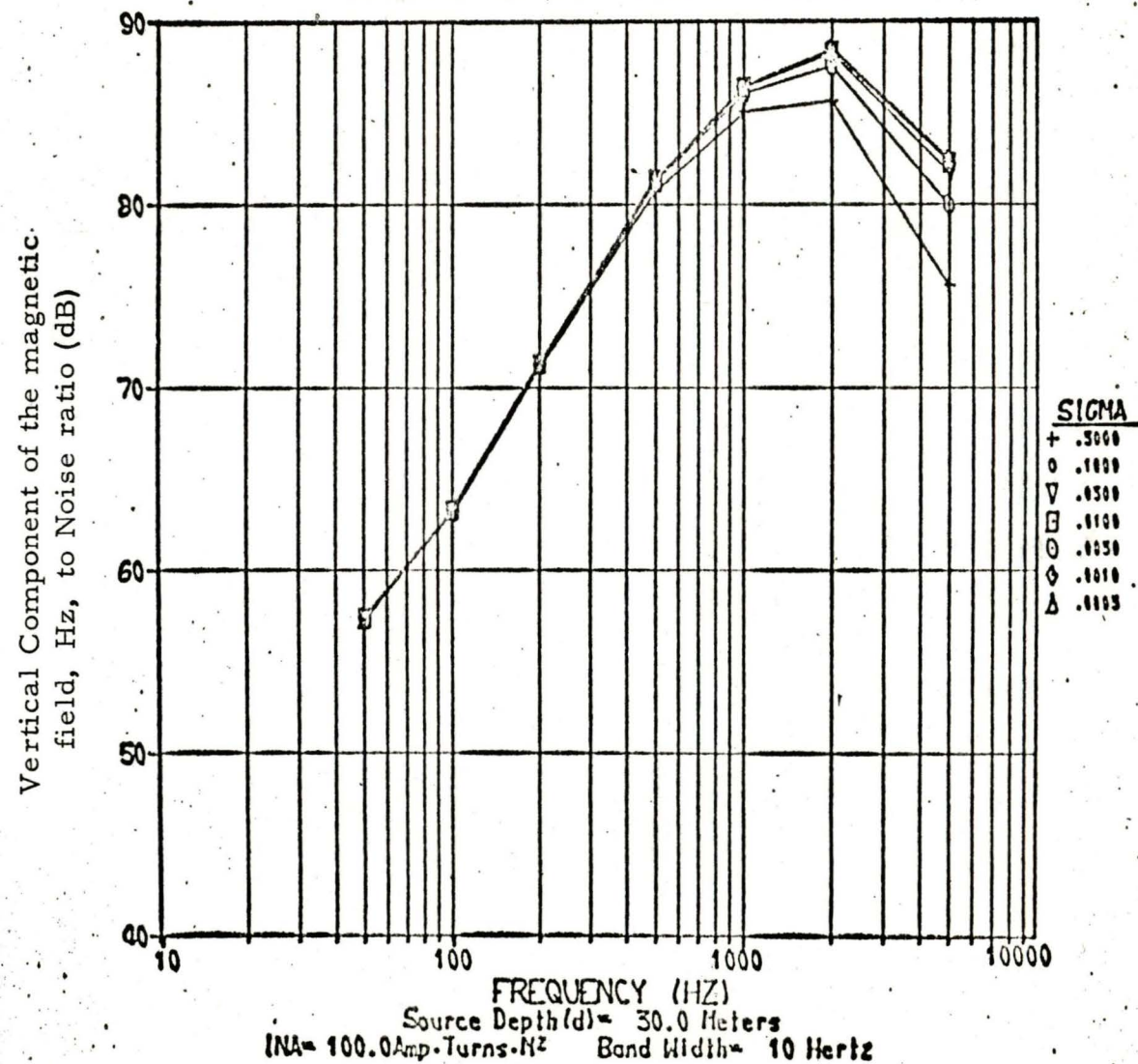


Figure 3-3

# MAGNETIC FIELD STRENGTH/ATMOSPHERIC NOISE SUBSURFACE VERTICAL MAGNETIC DIPOLE SOURCE

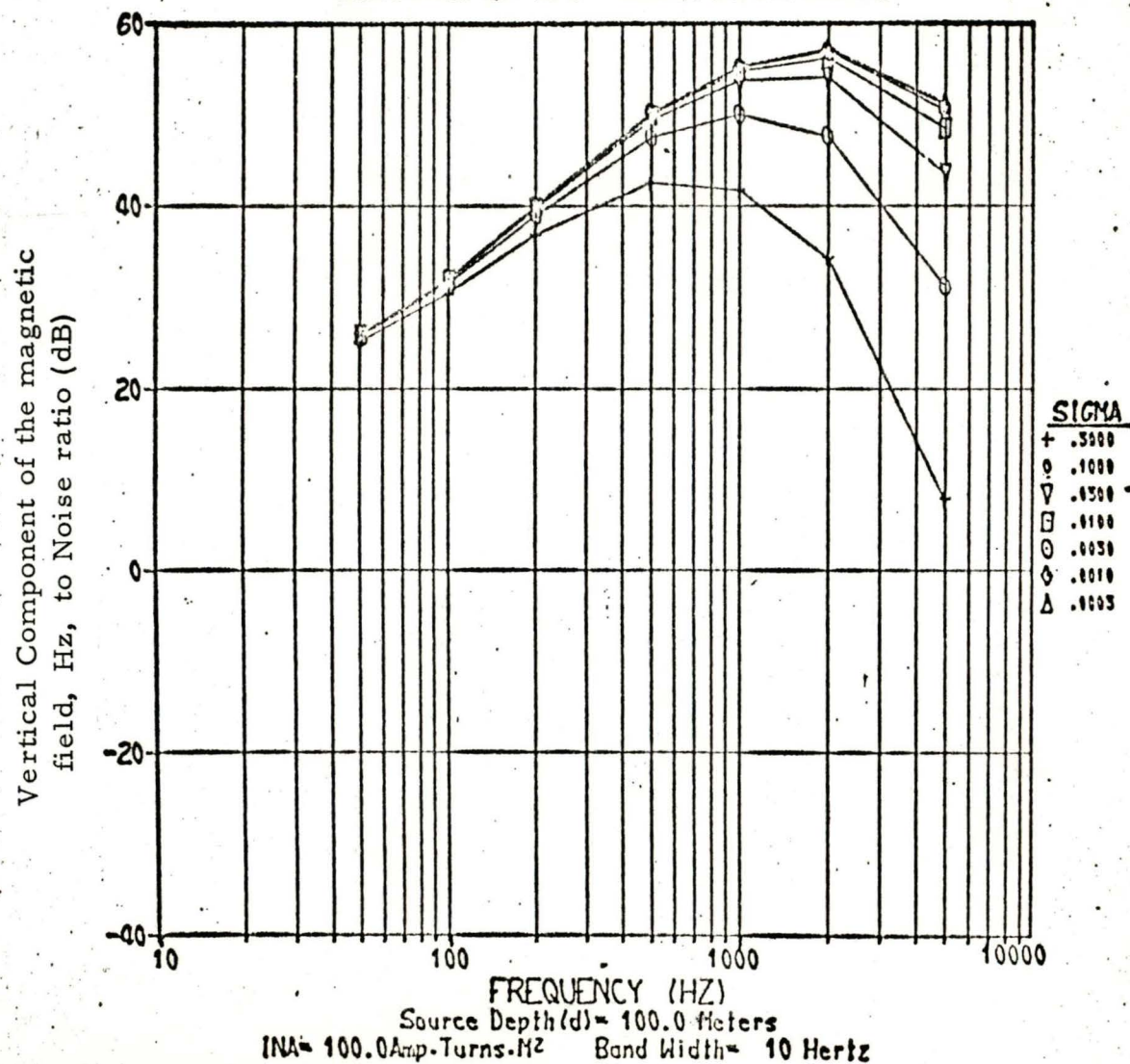




Figure 3-4 MAGNETIC FIELD STRENGTH/ATMOSPHERIC NOISE  
SUBSURFACE VERTICAL MAGNETIC DIPOLE SOURCE

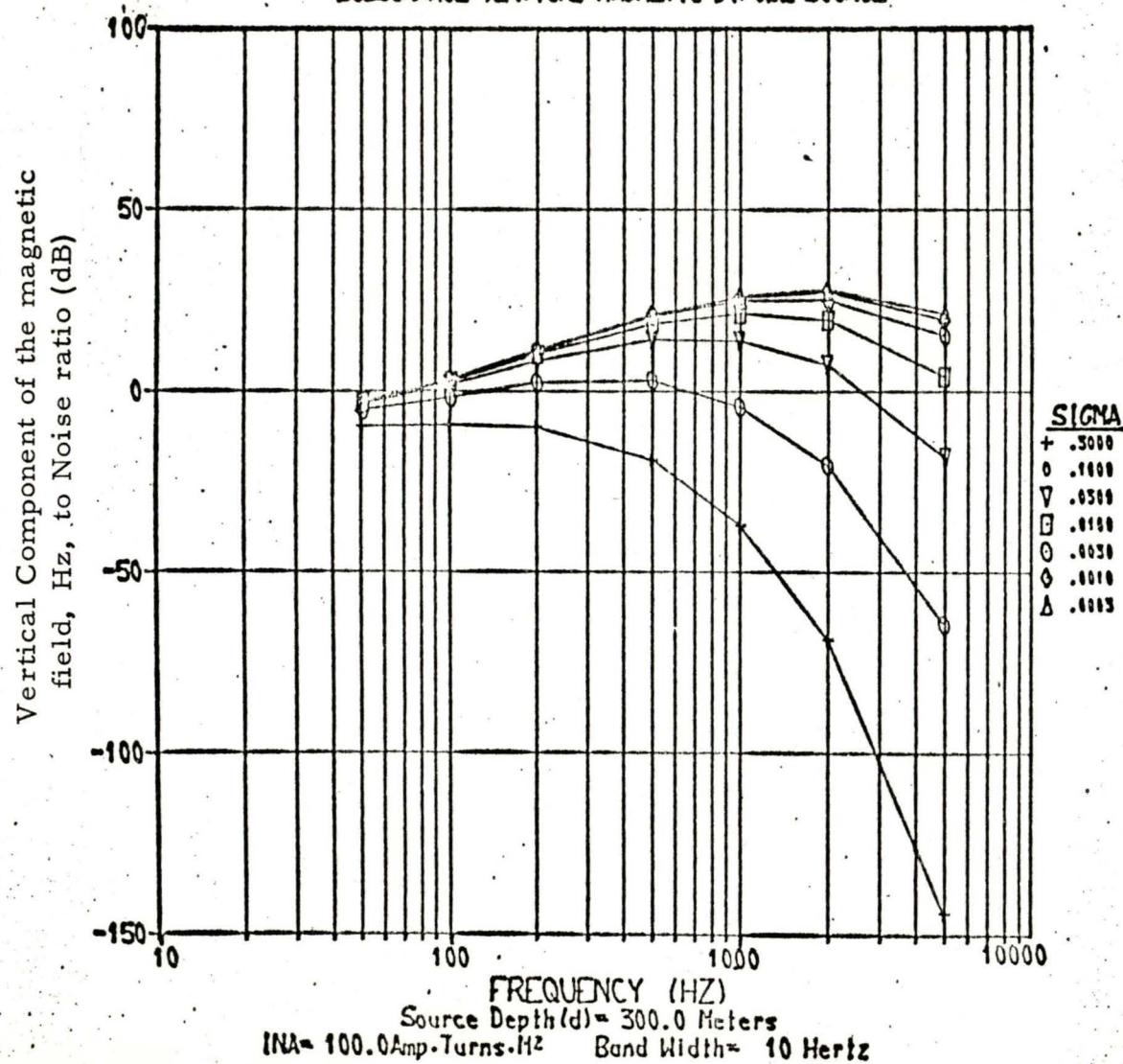
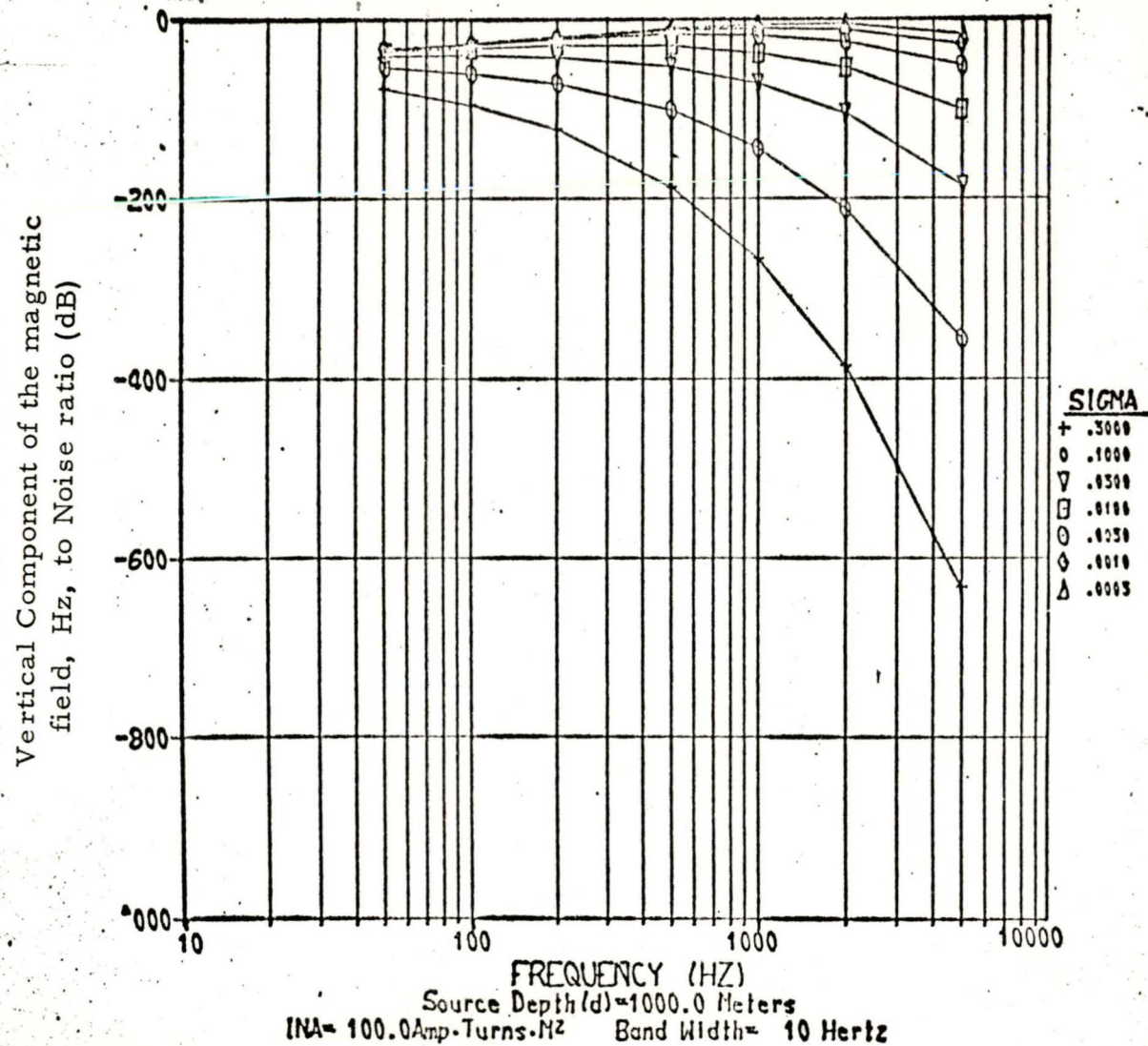




Figure 3-5

# MAGNETIC FIELD STRENGTH/ATMOSPHERIC NOISE SUBSURFACE VERTICAL MAGNETIC DIPOLE SOURCE



500 Hz and 2000 Hz.

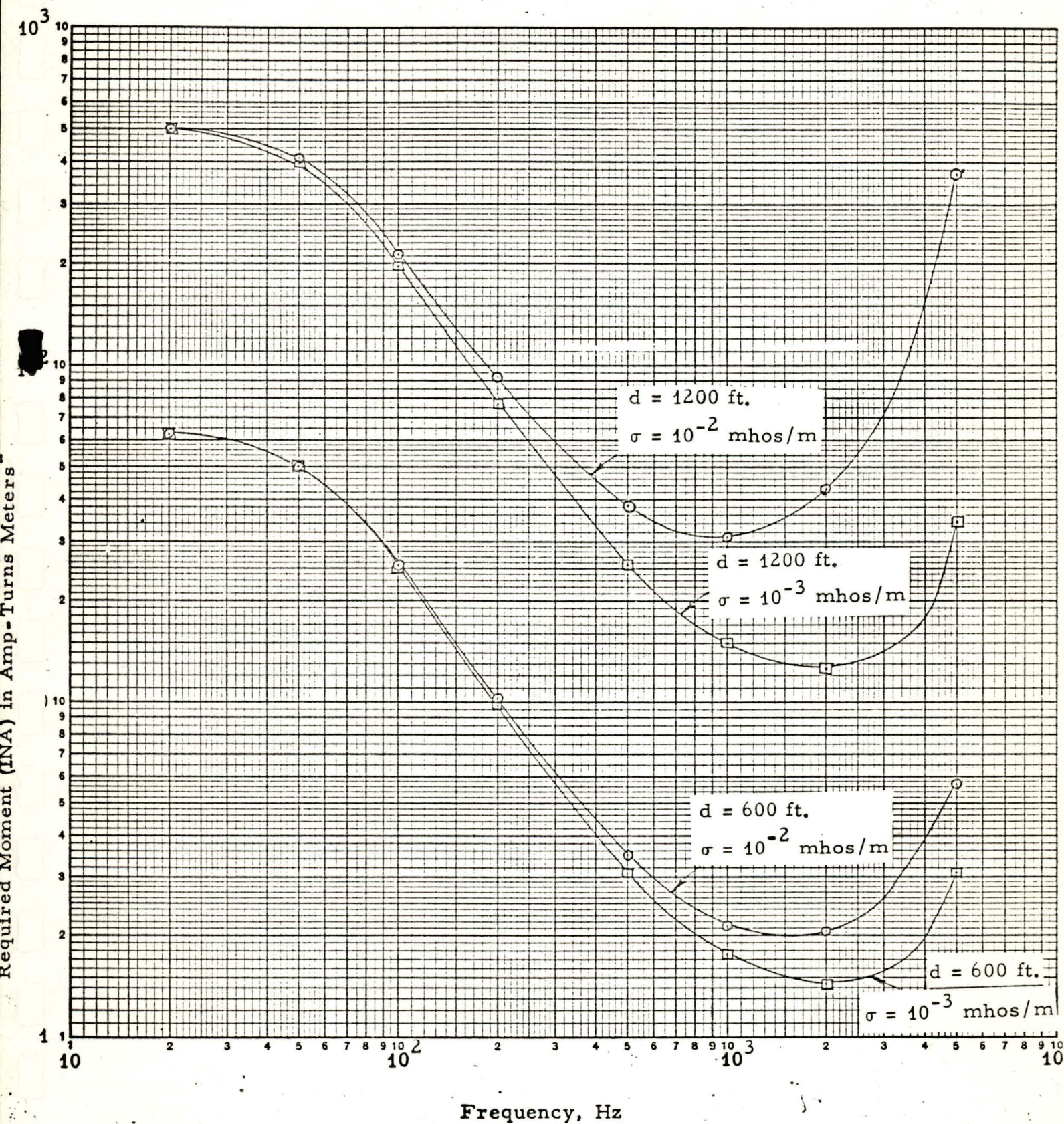
There may be times when an uplink EM Location System could be limited by man-made noise rather than atmospheric noise. Based on noise curves shown by Bensema [4], man-made noise as seen on the surface above typical coal mines in Colorado, generally peaks at harmonics of 60 Hz and these harmonic peaks become less pronounced for frequencies above 1 kHz. Consequently our assessment of optimum operating frequency based on atmospheric noise limiting is inclined to be on the low side for operation in man-made noise.

Figures 3-6 and 3-7 indicate an optimum frequency band based on a required antenna moment to produce a 10 dB signal to atmospheric noise ratio at the surface above the transmitting loop. It is apparent that for earth conductivities between  $10^{-2}$  and  $10^{-3}$  mhos/m and overburden depths between 600-1200 feet, the optimum frequency band would lie somewhere between 500 Hz and 3 kHz. One condition which would force the optimum frequency to lower values would be significantly higher conductivities such as 1 mho/m as shown in Figure 3-7. This condition is not expected to occur in coal mining regions so the lower frequencies indicated here have not been seriously considered in the design of the present system. Furthermore, past experience with an experimental 25 Hz Manpack Location System proved to be largely unsuccessful due to excessive noise induced by motion of the receiving coil in the earth's magnetic field.



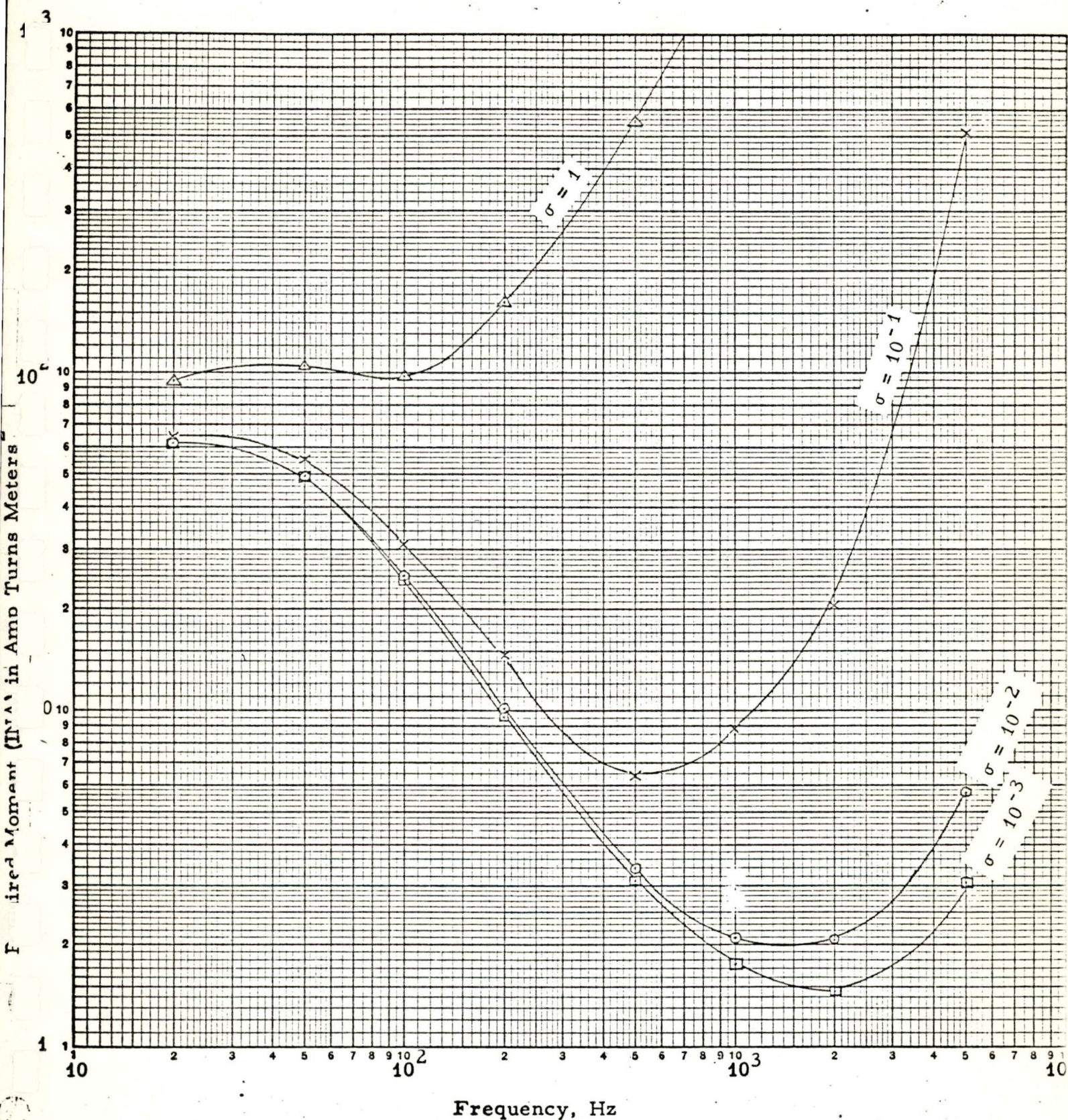
Figure 3-6

Required Transmitting Moment to Provide 10 dB Signal/Atmospheric Noise Ratio at the Surface in a 10 Hz Band.





Required Transmitting Moment to Provide 10 dB Signal/Atmospheric Noise  
Ratio at the Surface in a 10 Hz Bandwidth with an Overburden Depth of 600 Feet.





### 3.2 Transmitting System Tradeoffs

#### Transmitting Antenna

The transmitting system for the EM Location Transmitter was designed on the basis of obtaining a maximum transmitting moment to weight ratio. To focus on a configuration which would give this, we proceed as follows:

- 1) Assume that our interrupted source of power is a miner 4 volt battery whose current output is chopped through a solid state transistor switch. Assume a total source resistance of 1 ohm.

Then 
$$I = \frac{E}{1 + R_l}$$

where  $R_l$  = loop resistance  
 $E$  = battery voltage.

The weight of the loop (W) is given by

$$W = a \cdot l \cdot d_o$$

where  $a$  = the wire cross sectional area  
 $l$  = the wire length  
 $d_o$  = the density of the wire material.

We want to maximize  $INA/W$ .

$$\frac{INA}{W} = \frac{\left( \frac{E}{1 + R_l} \right) NA}{a l d_o}$$

however,  $R_l = \frac{\rho l}{a}$

where  $\rho$  = the resistivity of the wire

and

$$\frac{INA}{W} = \frac{ENA}{(a + \rho l)(l d_o)}$$

The area of a circular loop (A) is given by

$$A = \pi r^2$$

and

$$l = 2\pi rN$$

$$r^2 = \frac{l^2}{4\pi^2 N^2}$$

and

$$A = \frac{l^2}{4\pi N^2}$$

$$\frac{INA}{W} = \frac{E l}{4\pi d_o (a + \rho l) N} \quad (3-1)$$

making the assumption that  $l$  is a constant length of wire. The above expression was differentiated with respect to  $N$  to give:

$$\frac{d}{dN} \left( \frac{INA}{W} \right) = \frac{E l}{4\pi d_o (a + \rho l) N^2} \quad (3-2)$$

However, this does not go to zero for any finite  $N$  so we must evaluate the original formula in (3-1) to determine the optimum value of  $N$  for a constant wire length. It is apparent from this expression that the best choice for  $N$  is 1 turn of wire. However, it must be kept in mind that the primary objective for this system is source location, and if extremely long wires are used for



antennas, it would be advantageous from a location accuracy standpoint to use more than one turn to minimize the area\* of the transmitting loop. A reasonable trade-off parameter here would be to use 1 turn of wire if the total wire length were equal to or less than the overburden depth, if the wire length was twice the overburden depth use a 2 turn configuration and so on. In the present transmitting antenna system, a switch is included so that the operator may choose between 1 or 2 turns of wire.

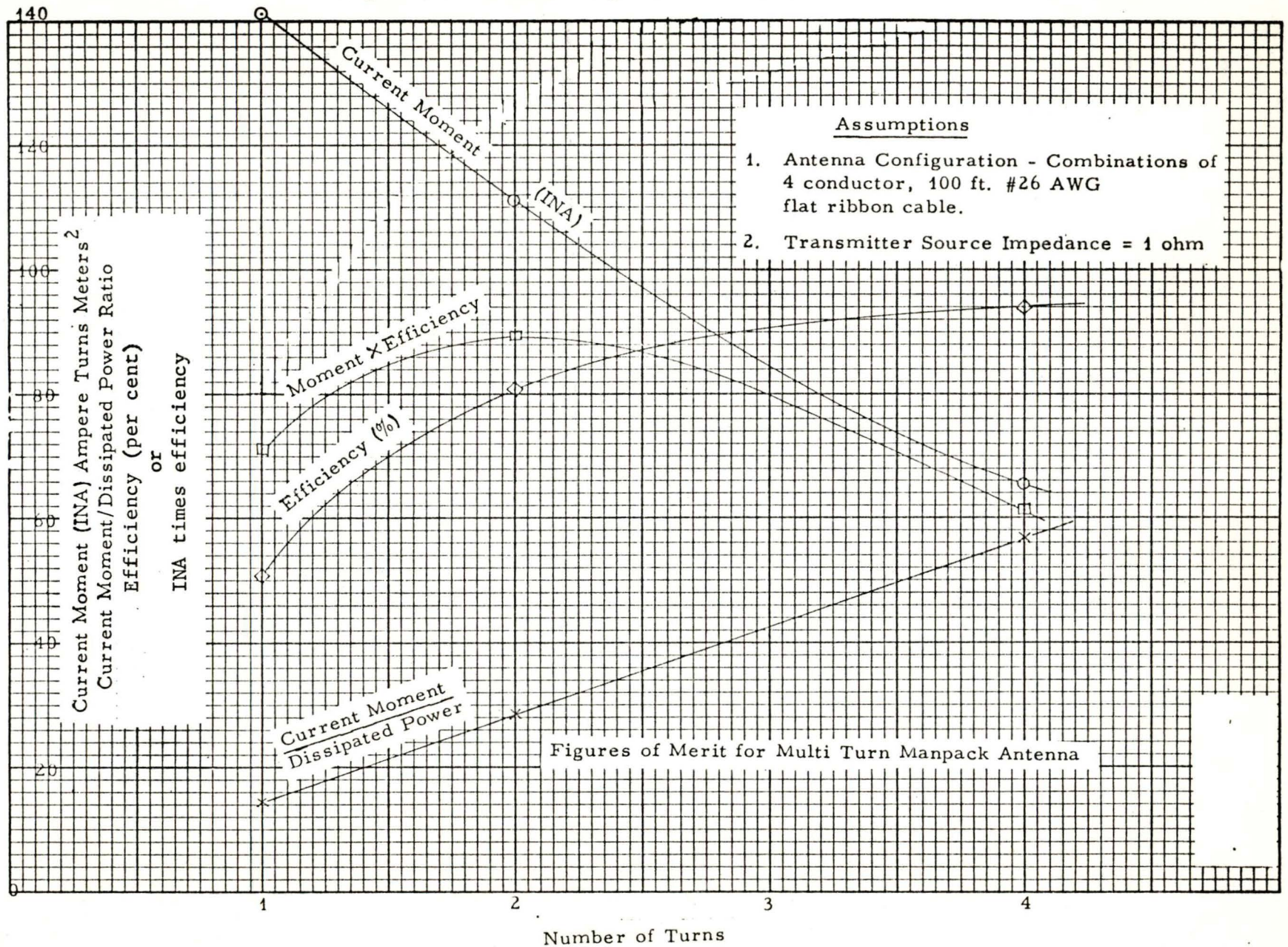
Another optimization factor that was examined for the manpack transmitting system was the transmitter efficiency which is given by the AC power into the transmitting loop divided by the DC power drawn from the battery. The importance of this quantity is apparent when one considers that a miner's lamp battery has only a limited service duration after each charge cycle. Efficiency was evaluated for a 100 foot length of 4 conductor #26 ribbon cable. It turned out that as the number of turns increased (as governed by the different ways of connecting the conductor ends) the resistance of the load increased exponentially and the efficiency approached 100% asymptotically. However at the same time the transmitting antenna moment decreased as the number of turns increased. Since transmitting moment is equally if not more important than transmitting efficiency, the product of these two quantities was also evaluated and was found to reach a peak for a configuration of 2 turns. (See Figure 3-8). Consequently, the design approach was modified slightly to incorporate a two conductor ribbon cable with provision for using either a one or two turn loop configuration. It cannot be concluded that a 2 turn antenna is, in general, the optimum. In a deeper mine, for example, and in order to maximize the current moment, one turn might be superior, and may well mean the difference between penetration and not penetrating the overburden.

---

\* The theoretical implications of loop size have been evaluated by Wait and Spies. J. R. Wait and K. P. Spies - Sub-surface Electromagnetic Fields of a Circular Loop of Current Located Above Ground. Report to the Bureau of Mines, November, 1971.



Figure 3-8. Transmitting Antenna Tradeoffs





### Transmitting Antenna Packaging

The package chosen to house the antenna cable is a modified version of a 100 ft. measuring tape enclosure. We removed the steel measuring tape and replaced it with an equivalent length of flat ribbon cable. The cable contains two conductors with copper cross section equivalent to AWG #22. Its thickness is slightly greater than that of the measuring tape; consequently only 90 feet could be wound in the carrying case. However, this length should be sufficient to produce a current moment needed to successfully operate the EM Location System.

A junction box is attached to the underside of the antenna package and allows for the switching of antenna and power terminals to produce the antenna configurations desired. See Figure 3-9.

### Transmitter Electronics

In designing the electronic circuitry to be incorporated into the man-pack location transmitter, emphasis was placed on size, weight, and portability criteria as well as frequency stability of the transmitting source. An effort was made to package the electronics into the underside of the miners lamp battery cap and thus require no additional package for the miner to carry. A printed circuit card was fabricated to incorporate a tuning fork oscillator and switching amplifier with a unijunction transistor pulsed interrupter to aid the receiver operator in discriminating between the resulting transmissions and power line harmonic interference at neighboring frequencies. A schematic diagram of the Westinghouse Manpack Transmitter Model C837-A which evolved from this effort is shown in Figure 3-10.

### 3.3 Receiving System Tradeoffs

Two receiving systems were developed during the course of this project. Receiver No. 1 (Westinghouse EM Location Receiver Model C836-A) was designed on the basis of providing a research tool to measure several field parameters simultaneously at the expense of increased complexity, size and weight. Receiver No. 2 (Westinghouse Manpack Locator Model 842A



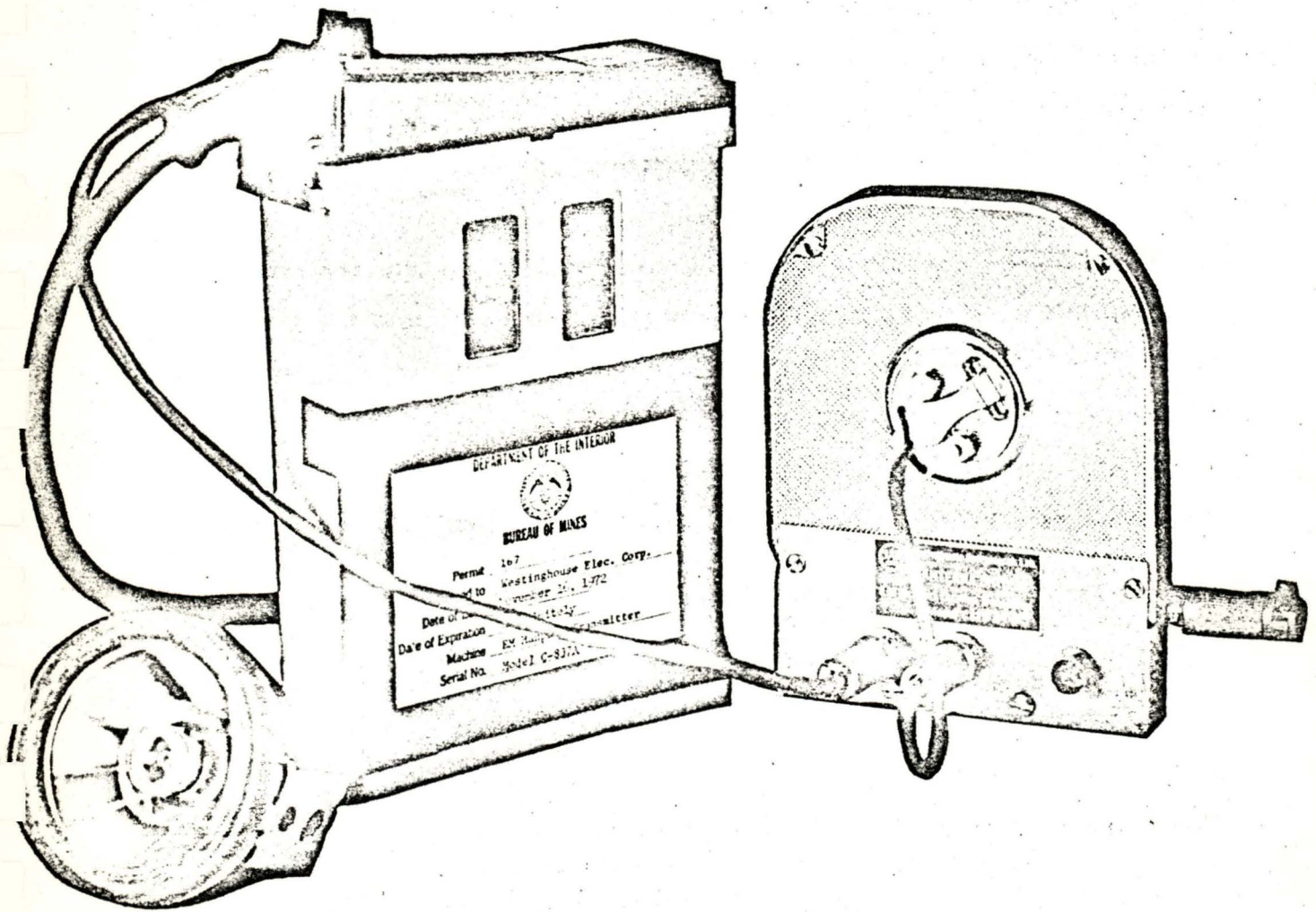
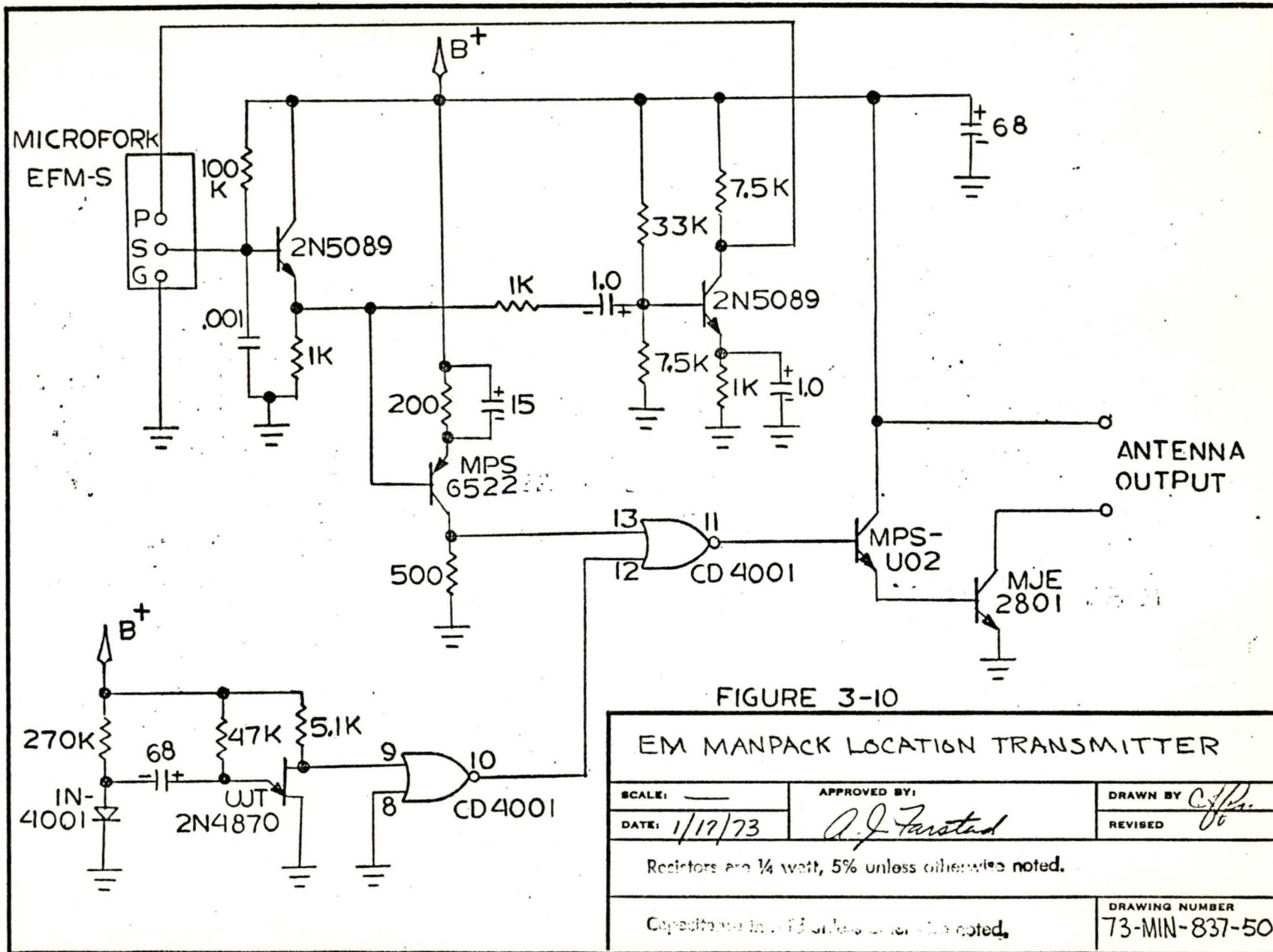


Figure 3-9. Westinghouse EM Location Transmitter Model C837A





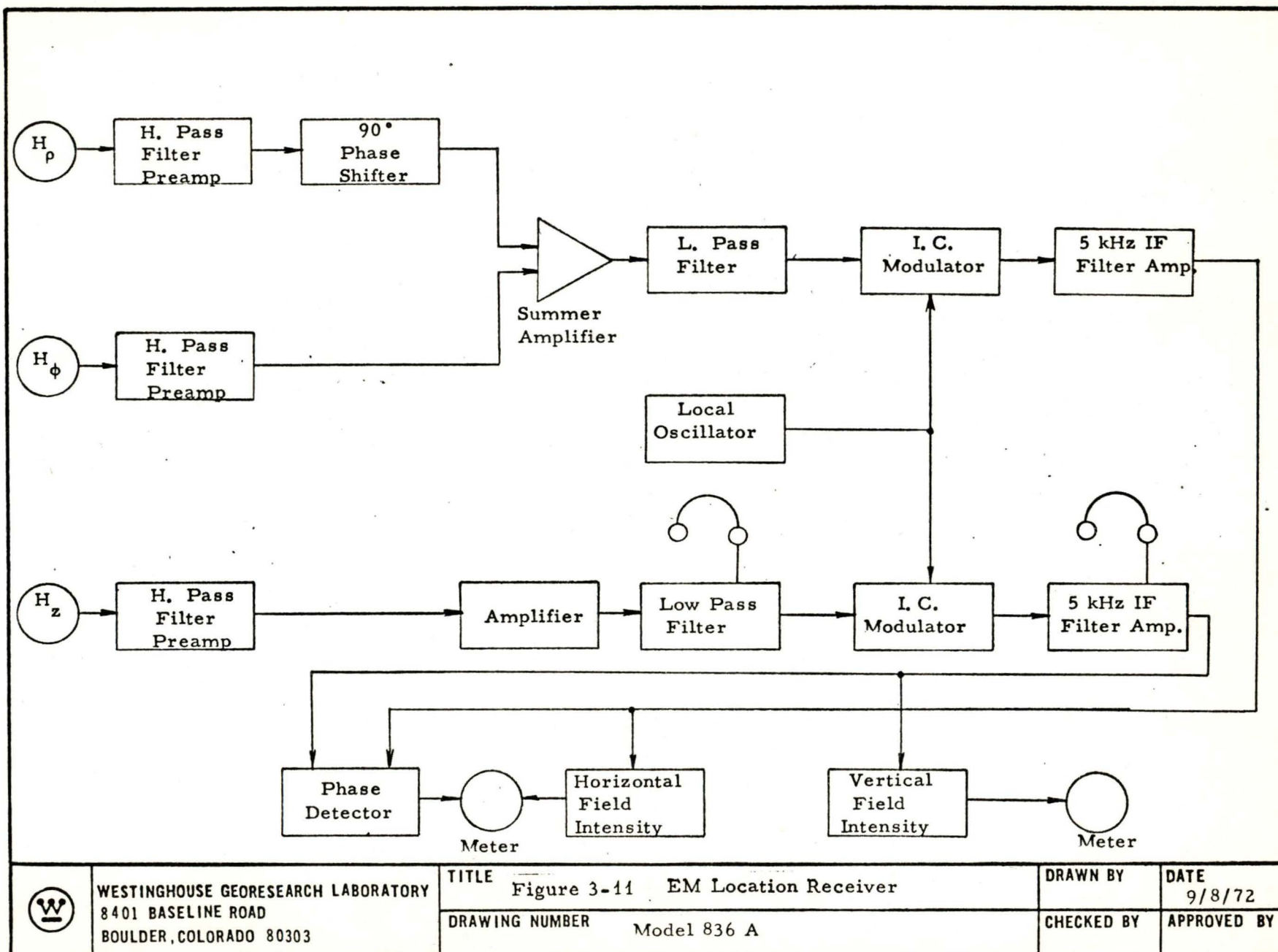
was designed on the basis of minimum size, weight and complexity without sacrificing such necessary performance characteristics as received signal to noise ratio. Each receiver will be described separately and each concept has proven itself from an operational standpoint to have a unique set of advantages and disadvantages.

#### Westinghouse Receiver Model C836-A

A block diagram of the receiver is shown in Figure 3-11 and a photograph is shown in Figure 3-12. Three orthogonal ferrite core loop antennas are housed in a nonconducting fiberglass case which also contained the output meters for the vertical and horizontal magnetic fields as well as the phase angle between them. A 12 conductor cable is used to connect the antenna/meter package with the receiver chassis.

In the receiver front end, separate low noise preamps are included in each of the 3 field component channels ( $H_\rho$ ,  $H_\phi$ , and  $H_z$ ). However the outputs of the two horizontal field strength amplifiers are combined in an active summer network after one of them is shifted  $90^\circ$  in time phase. This essentially produces an omnidirectional horizontal field receiver pattern when both of the horizontal field loops are connected. Provision was made for alternately eliminating the signal from one or the other of the horizontal field amplifiers to produce a figure 8 receiving pattern in either the  $H_\rho$  or  $H_\phi$  direction. The  $H_z$  or vertical magnetic field channel is connected at all times to its output meter while the horizontal magnetic field must be selected as either component separately or both combined. Noise reduction is accomplished by 1) tuning the loop antennas to the desired frequency, 2) high pass and low pass filtering in the amplifier channels at 1 kHz and 4 kHz respectively and 3) mixing the signals up to an intermediate frequency of 5 kHz and filtering both horizontal and vertical field signals with separate high Q double tuned LC filters at 5 kHz. To accomplish the mixing process, a Signetics 581 integrated circuit oscillator was used to modulate a pair of TI SN76514 integrated circuit modulators. Because of the inherent instability of the oscillator and IF filter and the extremely





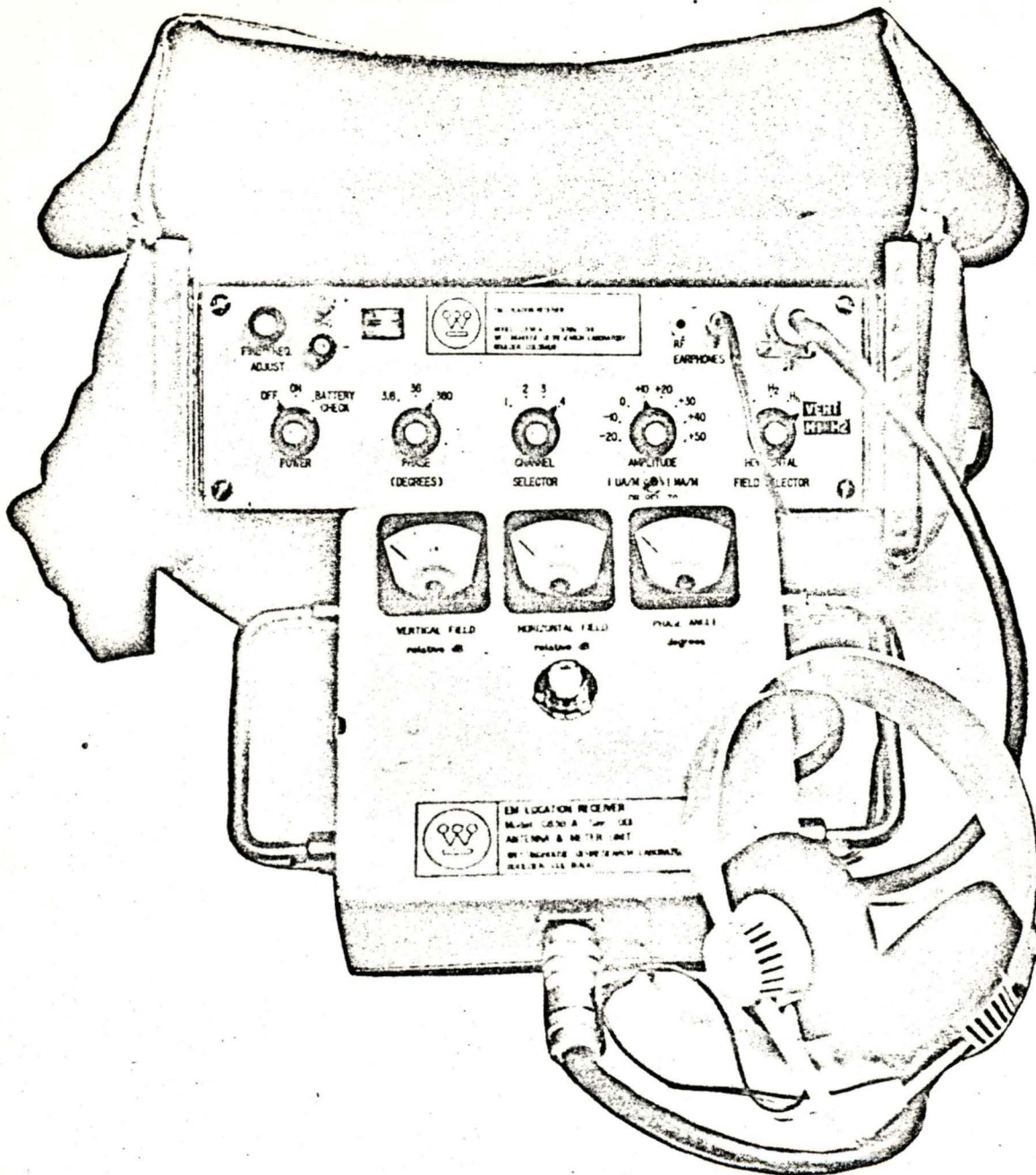


Figure 3-12 Westinghouse EM Location Receiver Model C836A



narrow bandwidth of the IF filter (5 Hz), provision was made for variable tuning above and below the 4 switched channel frequencies of 1050 Hz, 2010 Hz, 2070 Hz and 3030 Hz. A digital phase detector circuit was used to monitor phase angle between the vertical and horizontal fields utilizing zero crossing detectors, integrated circuit timers and low pass filters. The amplitudes of the two field components were monitored by a solid state transistor meter/detector circuit. In addition to output metering, earphone outputs are provided for aural monitoring of both the RF and IF signals. The receiving system described above was somewhat cumbersome in that it weighed 17 pounds and measured 5" X 10" X 10".

#### Westinghouse Receiver Model C842-A

This receiver was conceived and fabricated after spending several weeks at each of two coal mines and one hard rock mine under difficult weather and field conditions. It is infinitely simpler, and lighter weight than the Model C836-A receiver, yet it performs all of the necessary functions required to obtain a surface fix on an underground CW transmitter. A photograph of this receiver is shown in Figure 3-13. It uses a single 15" air core loop antenna tuned to one frequency inside the receiver chassis and followed by a series of high gain filter amplifiers and a single stage tuning fork filter tuned to the same operating frequency. Thus, the receiver is capable of detecting and determining the surface fix of one and only one transmitter frequency, which is its main disadvantage. However, because of its simplicity and single frequency tuning capability, it is extremely simple to operate and could be effectively used by untrained personnel. This receiver comes equipped with earphone jacks for aural monitoring of signals and for metering with the aid of an external AC meter (not provided). The receiver is packaged in a case  $3 \frac{5}{8}'' \times 4 \frac{5}{8}'' \times 2''$ , weighs  $2 \frac{1}{4}$  pounds and can be conveniently strapped to the operators belt leaving both hands free to handle the 15" diameter air core antenna. One of the advantages of air core antennas over ferrite core antennas is their much improved core stability with temperature. This receiver will operate on its internal rechargeable 12 volt batteries for a period of 40 hours between charges.

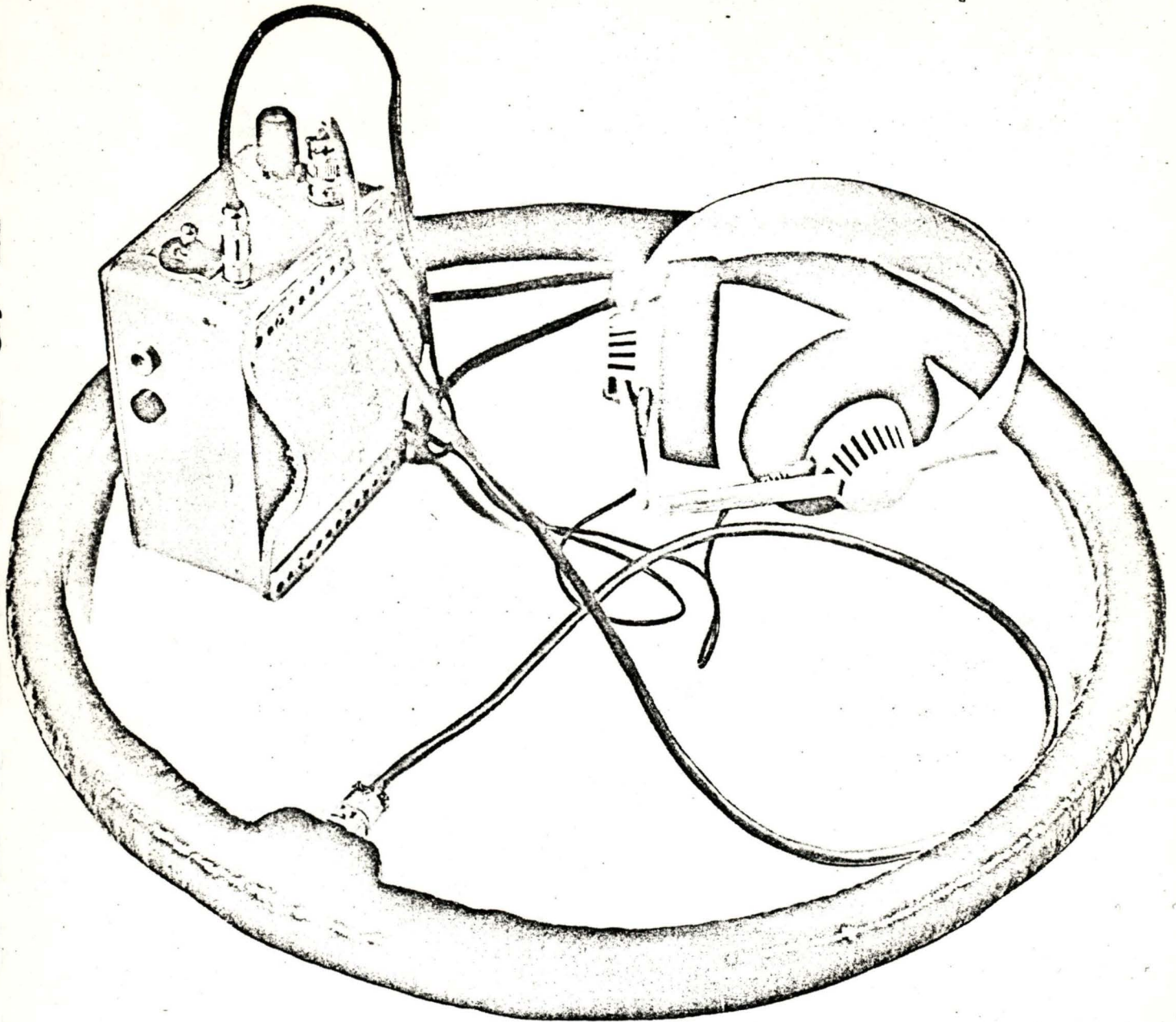


Figure 3-13. Westinghouse Manpack Locator Model C842A



#### 4.0 SYSTEM PERFORMANCE

##### 4.1 Manpack EM Transmitter Model 837-A

The manpack transmitter was tested in a temperature chamber over a range from  $-20^{\circ}$  to  $+60^{\circ}$  C. The total discernable frequency drift over this range was less than 2 Hz for the 2010 Hz transmitter. This falls well within the requirements for an operational system, since such a frequency drift will not in anyway hamper unique identification of individual transmitter channels in the mine. The transmitting antenna was deployed in an open field and its voltage and current characteristics were observed over an 8 hour period in an ambient temperature of  $0^{\circ}$  C. At the beginning of the 8 hours, the rms current in the single turn loop configuration was 1.5 amperes rms with a voltage of 4.2 volts. After 8 hours of continuous operation, the current had dropped to 1.43 amperes rms at a voltage of 4.0 volts. With the two turn deployment of the the loop antenna, the rms current was reduced by a factor of 3 to 0.5 amperes rms.

Initially the duty cycle of the transmitter was set for a 200 millisecond tone interruption every 2 seconds. This proved to be somewhat difficult to hear in the narrowband receiver output so it was later adjusted for a 200 millisecond tone burst every 2 seconds. This latter arrangement improved detectability and increased battery life.

##### Intrinsic Safety Tests

With the helpful cooperation of Robert Wolfe of the Approval and Testing Group of U. S. B. M. , we were able to run laboratory tests on the transmitter to determine its intrinsic safety. With the actual transmitter and antenna configuration as designed, the system was tested in a 8.5% Methane air mixture and allowed to break circuit 6,000 times with no resulting ignition. The switching transient into the inductive load was considerably larger than the peak square wave current but because of its very short duration

(less than 2  $\mu$ sec) was of no consequence in meeting intrinsic safety criteria.

The portable ribbon antenna packing was later replaced with an equivalent length of No. 14 AWG insulated wire and the peak current increased to approximately 12 amperes as measured on the oscilloscope. This configuration also did not produce ignition of the Methane air mixture. However, if such current drains were to be practical from a miners battery, they would have to be pulsed in a low duty cycle pulse train to conserve battery life.

#### 4.2 EM Location Receiver Model C836-A

This receiver by virtue of its variable tuning control and low noise front end was able to detect transmitted signals down to as low as - 20 dB relative to 1  $\mu$ a/m. Its phase metering circuits performed adequately on uncontaminated signals in the laboratory, however it was subject to transient interference pulses in the field and consequently no significant phase measurements were obtained with this receiver under field conditions. In view of the fact that phase data was not considered to be a vital requirement for location, no further effort was put forth to make the phase detectors less sensitive to noise.

One problem which was observed in this receiver after the unit was utilized in the field was the amplitude instability of the ferrite receiving antenna with temperature. Tests had been performed in the laboratory on a ferrite core antenna similar to the ones used in this receiver and they proved to be reasonably stable. However, the  $H_z$  receiving antenna for this receiver was fabricated using two ferrite blocks cemented together as a core and it was suspected that the joint expansion and contraction was responsible for the amplitude instability. This was the main reason that air core antennas were used in the next receiver design (Model C842-A).



#### 4.3 EM Location Receiver Model C 842A

This receiver is an ultra stable fixed frequency device designed to receive only one unique frequency. Its stability was tested over a  $-20^{\circ}\text{C}$  to  $+60^{\circ}\text{C}$  range and found to be stable to less than 2 cycles from its specified frequency. Its sensitivity for full scale output was  $1\text{ }\mu\text{A/m}$ . However, the output tone could easily be heard with signal levels below  $0.1\text{ }\mu\text{A/m}$ . Initially there was a problem with feedback between the electromagnetic earphones and the air core loop antenna. However, this was corrected by applying a copper screen shield to the outside of the coil form and replacing the electromagnetic earphones with crystal earphones. Battery life was found to be 40 hours between recharge. Other outstanding advantages are clearly evident in this receiver: 1) Its simplicity of operation, 2) its portability, and 3) its relatively low cost.

## 5.0 FIELD MEASUREMENTS

The EM Location System, described in Section 3.0, was field tested and evaluated at three coal mines in the Appalachian region of West Virginia and Pennsylvania and one hard rock mine in the Rocky Mountains of Colorado.

Testing and evaluation consisted primarily of location exercises, and included those tests and experiments necessary to establish location correction factors, establish the validity of the location data and tests to acquire the data needed for comparison with theoretical predictions. This includes conductivity surveys and measurement of man-made and natural EM noise and field intensity profiles. At one coal mine, exercises were conducted to determine the feasibility of helicopter reconnaissance in locating the subsurface transmitter signal.

### 5.1 Test Coal Mines

#### 5.1.1 Island Creek Coal Company Guyan No. 1A

This first mine selected for a test site is located in the 65 inch Island Creek seam beneath Kelly Mountain in Logan County, West Virginia. Mine depth in the test area ranges from 400 to 450 feet. The overburden consists of weathered surface, sandstone, slate, shale and coal. The terrain above the mine is hilly with steep slopes of 30° or better. The area is sparsely populated with rural power lines in the vicinity. Vegetation is mostly pine trees, brush and grass.

The weather during the test period was extremely humid with rain showers frequently approaching torrential proportions. Temperatures ranged from 25° to 70° F.



### Overburden Conductivity

Conductivity measurements were conducted using the Westinghouse short range induced polarization transmitter and receiver with copper-clad steel stakes for electrodes. The standard Eltran and dipole array configurations were used out to a distance of  $n = 3$  (300 meters). Average overburden conductivity was determined to be  $9 \times 10^{-4}$  mhos/m; calculations and conductivity sounding data are shown on the graph of Figure 5-1.

### EM Noise Measurements

Noise recordings were made using a Wollensak Model 4300 battery-operated tape recorder, a wideband noise preamplifier and ferrite loop antenna in a 0-5 kHz frequency range. The recordings were subsequently played back, plotted and analyzed.

Measurements were made at three different points in the test area, although transmitter location exercises were conducted at only two of these points. The first measurement was made in the immediate vicinity of a local power line; the second and third measurements were made at distances of 100 meters and 300 meters from the power line. In all cases, measurements were made with three orientations of the ferrite loop: (1) loop axis vertical, (2) loop axis parallel to the power line, (3) loop axis perpendicular to the power line.

The plot of Figure 5-2 shows the noise spectrum for a location immediately adjacent to the power line with the ferrite loop axis perpendicular to the line. The plot of Figure 5-3 shows the same spectrum for the same antenna orientation at a distance of 100 meters from the power line. Transmitter location attempts failed at the first site, while at the latter point location attempts were quite successful. This will be discussed further in subsequent sections of this report.

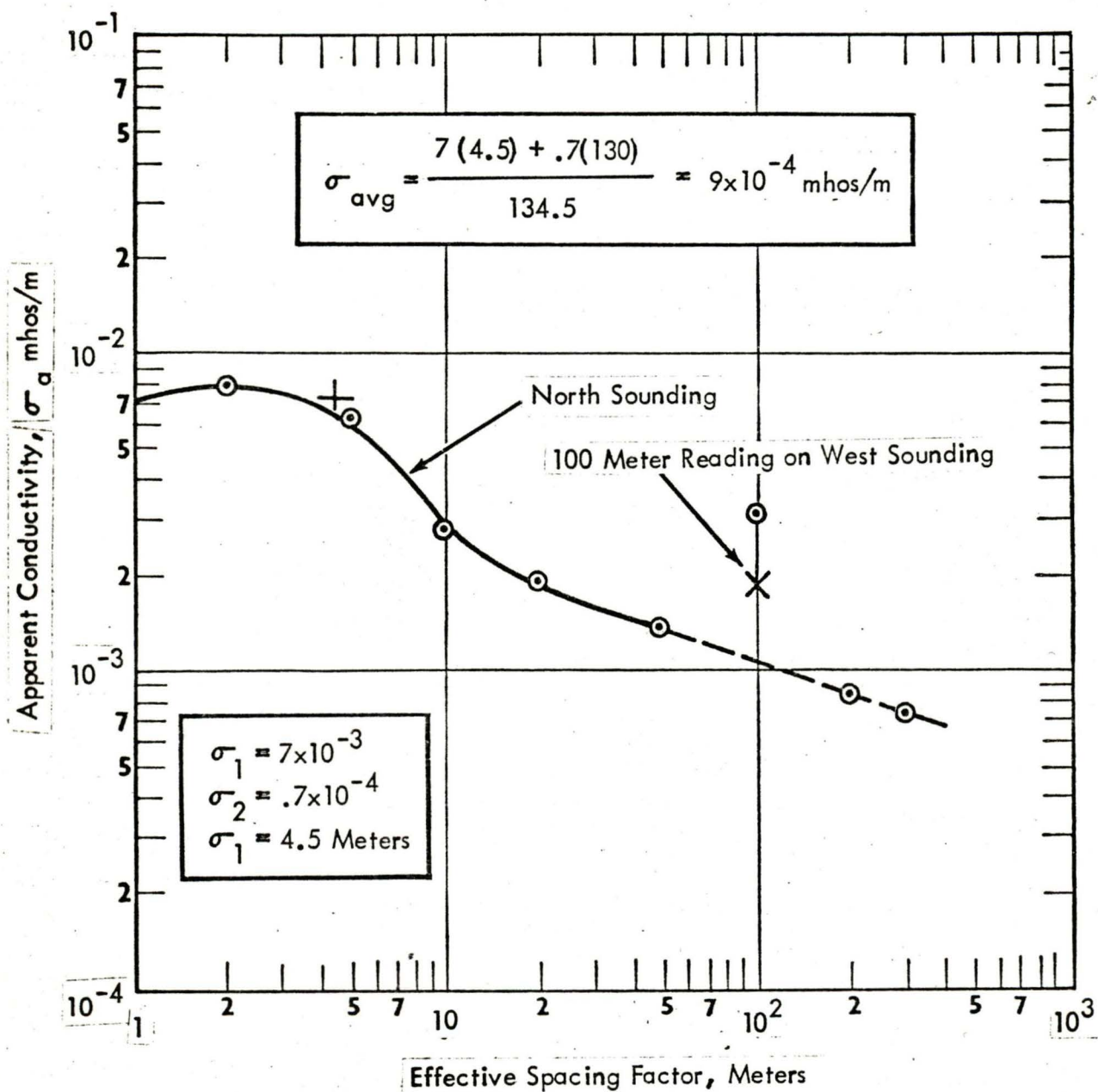
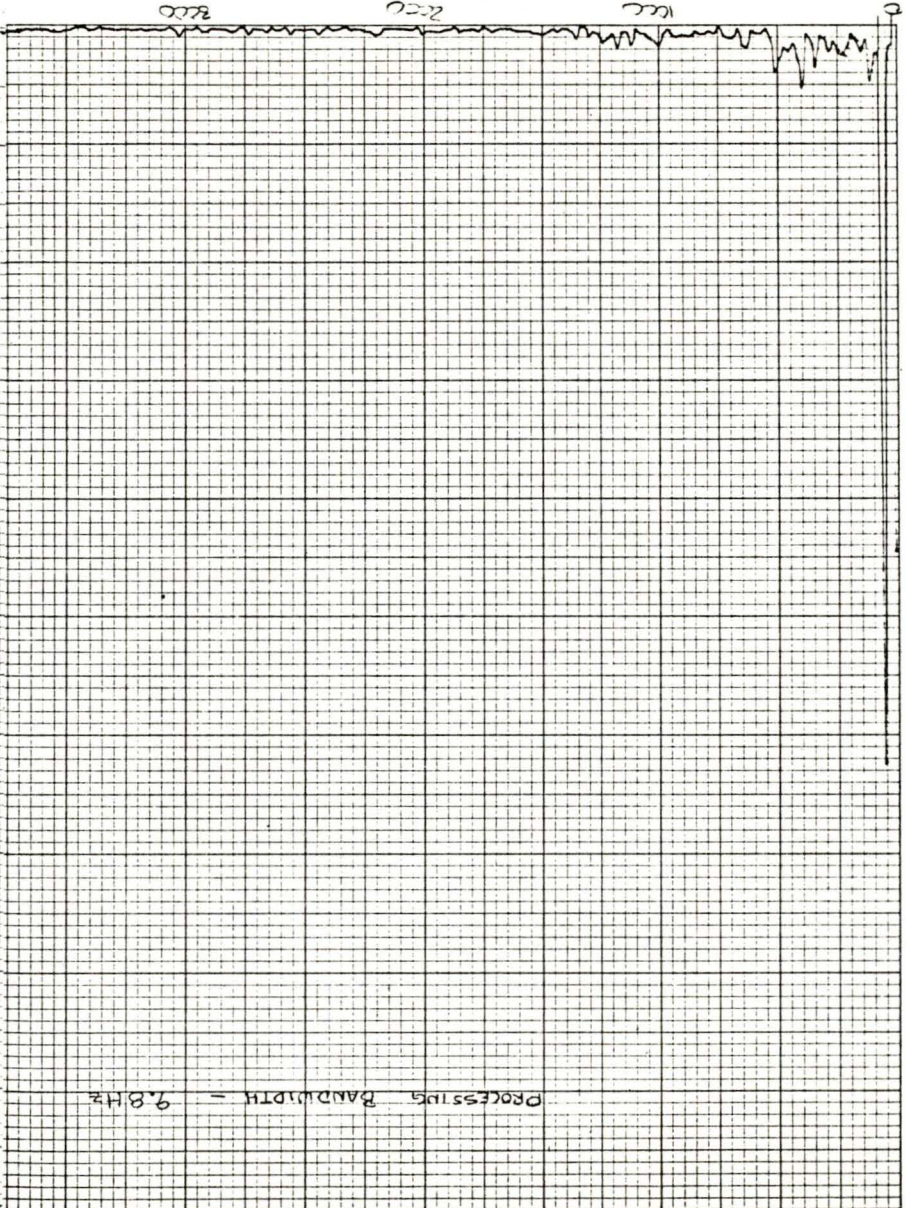


Figure 5-1. Earth Conductivity Sounding, Island Creek No. 1A Mine, Logan, W. Va.



FIGURE S-2 SURFACE EM NOISE VS FREQUENCY

PROCESSING BANDWIDTH = 9.8 Hz



Plot #12 Island Creek Mine ③ 12/12/72  
 Guyana J-A Mine  
 Amherst, W. Va.  
 TAPET SIDE 2 50-70  
 Hz (1 to 200 lines)  
 Above #86 Break

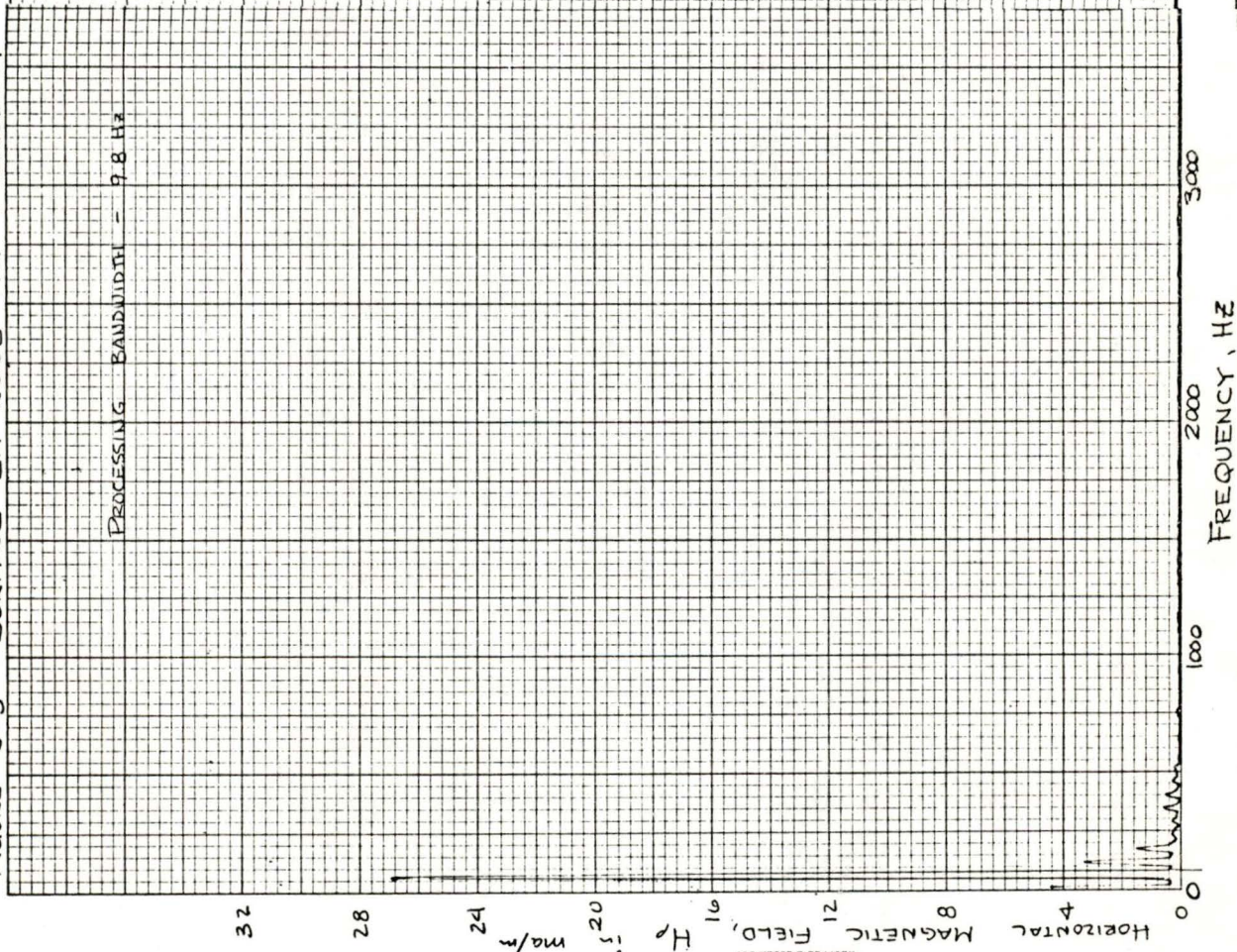
HORIZONTAL MAGNETIC FIELD STRENGTH,  $H_p$  in mV/m  
 K&E 10 X 10 TO THE INCH 47 0780  
 10 X 10 INCHES KUFFEL & ESSER CO. 200 000 000

FREQUENCY, Hz

Plot #12



FIGURE 5-3 SURFACE EM NOISE VS. FREQUENCY



Plot #17 Island Creek Mine ③ 12/12/72  
 GUYAN 1-A Mine  
 Amherstdale, W. Va.  
 TAPE 1 SIDE 2 175-195  
 H<sub>1</sub> (1 to PWR Lines)  
 AT Surface location B<sub>1</sub>

Plot #17

KEUFFEL & ESSER CO.  
 10 X 10 TO THE INCH  
 47 0780  
 MADE IN U.S.A.



### EM Location and Signal Identification Tests

For the first location exercise the 1050 Hz and 2010 Hz Manpack Location Transmitters and associated ribbon antennas were deployed in the vicinity of break #86 on the east side of the north-south mine tunnel directly below the surface power lines at a mine depth of 130 meters. See the map of Figure 5-4. Signal location attempts on the surface were made using the C-836A Location Receiver. No signals were detected that could be positively identified as the subsurface transmitters. Further efforts were made to detect and identify the signals utilizing the Hewlett Packard Model 302A Wave Analyzer in conjunction with the Location Receiver. (The output of the Location Receiver was fed into the H. P. Wave Analyzer for further filtering.) Signal detection still proved impossible in the presence of the interference fields created by the power lines.

For the second location exercise, the 1050 Hz and 2010 Hz transmitters were moved to the west side of the north-south mine tunnel parallel to but some 100 meters removed from the surface power lines at a mine depth of 123 meters. See map of Figure 5-4. No difficulty was encountered in locating the transmitter signals or the points of maximum and minimum intensities of the vertical and horizontal fields.

After the null locations were established and marked, a land survey was conducted to determine the actual transmitter location. The null offset errors (shown in Table 5-1) for both locations are negligible.

A = 1650 Hz X-MITER  
B = 2010 Hz X-MITER

$B = 2010 \text{ H2 X-MTEB}$

$$A, B,$$

Null Location:

• TRANSMITTER LOCATION

✱ SURFACE HULL PT. LOCATION

WORKING FILE

NV

PETAL

Island Creek Coal Co.  
Guyana # 1A Mine  
Amherstdale, W. Va.

Figure 5-4.



Table 5-1

Mine Name	Location Description	Frequency	Overburden Depth (ft.)	Conductivity (mhos/m)	Slope	Null Offset (ft.)	
						Uncor- rected	Corrected
Guyan Mine No. 1A Amherstdale, W. Va.	A <sub>1</sub> profiled	2010	403	$9 \times 10^{-4}$	3°	0	0
	B <sub>1</sub>	1050	439	$9 \times 10^{-4}$	7°	0	1
	{ A <sub>1</sub> B <sub>1</sub> profiled	2070	403	$9 \times 10^{-4}$	3°	0	0
		2010	439	$9 \times 10^{-4}$	7°	0	1
	C <sub>1</sub> profiled	3030	403	$9 \times 10^{-4}$	8°	13	10

Transmitters  
are 150 feet  
apart in mine.

(It should be noted that while such small errors as several feet speak well for both equipment design and implementation, there is a degree of operator proficiency to be considered. Null locations in this particular instance, for example, could have been established and marked anywhere within a 2.5 meter radius of the chosen point, but by careful observation of the field intensity meter, antenna tilt and diametric distances between points of equal field intensities a location can be selected as the most probable center of the circle of ambiguity.)

For all succeeding location exercises at this test site, the transmitting antennas were left as deployed (locations A and B on the map); the transmitters were changed to include the 2070 Hz and 3030 Hz signals in the location tests. Location errors for these frequencies were negligible also. Null offset figures are shown in Table 5-1.

Signal identification tests to evaluate the capability of the system to identify one subsurface transmission in the presence of another nearby subsurface transmission were conducted using the 2070 Hz and 2010 Hz transmitters in simultaneous operation separated by a distance of approximately 50 meters. Both signals were readily identifiable and there was no noticeable shift in null location produced by the presence of the adjacent transmitter.

The only problem encountered during the signal identification tests was on a day when two in-mine, pulse-type transmitters operating at 470 Hz and 510 Hz were being tested in the vicinity of the 2070 Hz and 2010 Hz CW transmitters. (Locations are designated E and D on the map of Figure 5-4.) The interaction of the harmonics of one or both of these pulse transmitters caused the null location of the 2010 Hz transmission ( $B_1$ ) to shift 55 meters in the direction of the pulse transmitters. Removing the 470 Hz and 510 Hz transmitters eliminated the problem, and no further investigation of the phenomenon was conducted.



## Magnetic Field Profiles

Field intensity measurements of the horizontal ( $H_{\rho}$ ) and vertical ( $H_z$ ) fields were made in the area above the 2010 Hz transmitter at location A on the map of Figure 5-4. Measurements of the relative field strengths were taken and recorded every five meters in four radial directions from the surface null location ( $A_1$ ). The direction of the first radial was established by choosing the direction of maximum hill slope with the second radial displaced  $180^\circ$  from the first. The third and fourth radials were  $180^\circ$  apart and perpendicular to the first two. By coincidence, the radials ran in the directions of the four cardinal compass headings. The radials were extended to the point where the transmitter signal was no longer discernible. In the east direction the range was limited to 40 meters because of the previously mentioned power line interference. A clinometer was used to measure hill slope so that slope corrections could be applied where necessary.

The measured profiles are plotted in Figures 5-5 and 5-6. Transmitter depth and frequency, radial direction, overburden conductivity and the general contour of the terrain are shown in the upper right hand corner. Because of the extreme irregularity of the terrain at this location, a simple slope computer model could not be used to determine theoretical profiles. A summary of the location offsets at the Guyan No. 1A mine is given in Table 5-1. The slopes used in correcting the null location was the average slope in the immediate vicinity of the site. The data shows that the amount of slope correction was insignificant, and that the null determined directly by the field instruments was sufficiently accurate to be used in mine rescue operations.

After the null locations were established, using the C836A Location Receiver, they were checked with the absolute field intensities obtained using the H-P Model 302A Wave Analyzer and Beacon uplink air core loop antenna designed for the USBM mine rescue system. Differences in field strength

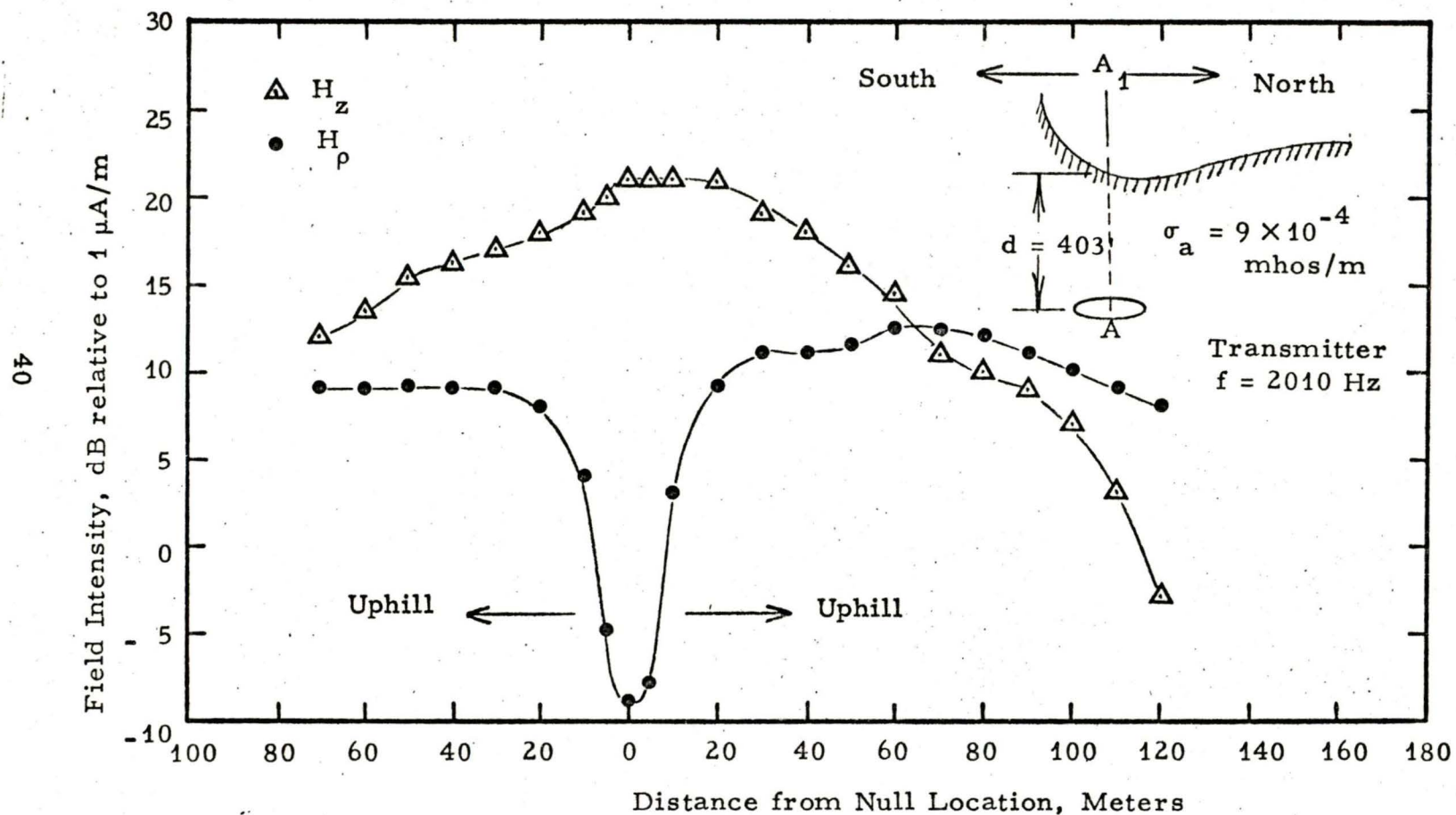


Figure 5-5. Field Intensity Profile above Vertical Magnetic Dipole at the Guyan No. 1A Mine, Amherstdale, West Virginia (North-South Profile)



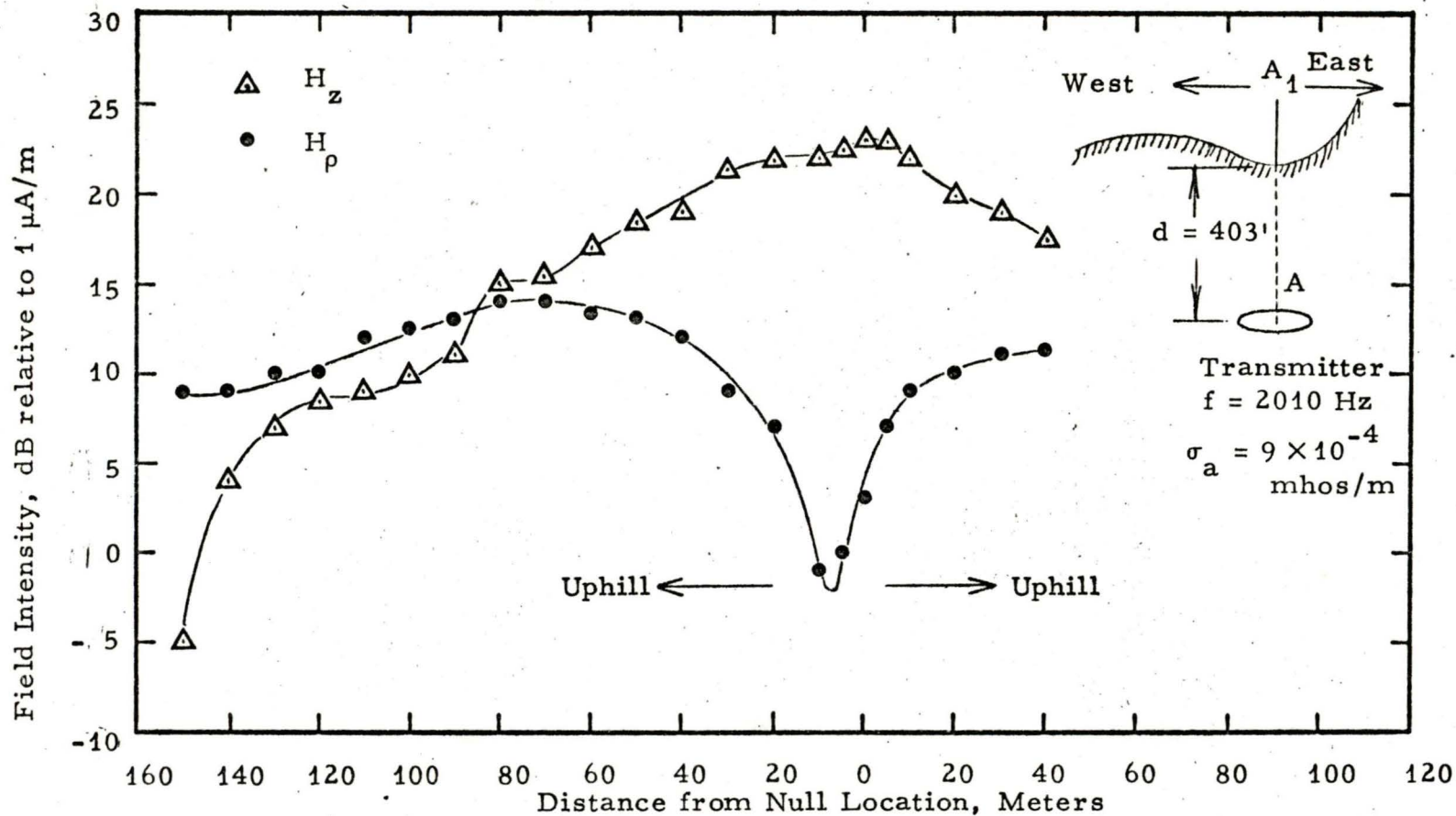


Figure 5-6. Field Intensity Profile above Vertical Magnetic Dipole at the Guyan No 1A Mine, Amherstdale, West Virginia. (East-West Profile)

measurements between the C836A and the calibrated Beacon loop and Wave Analyzer were noted and the C836A readings were corrected accordingly. Null resolution was noticeably improved using the air-core loop system; that is, the null radius was reduced to one meter and null depth increases of as much as 15 dB were noted. However, the null locations determined by each of these systems were essentially the same.

#### 5.1.2 Union Carbide Company Putnam Mine

The Putnam Mine is located in the 72" Pittsburgh No. 8 seam in Mason County, West Virginia. Mine depth in the test area ranges from 112 to 160 meters. The surface area above the mine is characterized by rolling hills. The immediate test area is mostly grassy pasture land with a few timbered tracts around the perimeter. The mine was in the process of closing down so there was no significant mine power or mine machinery interference to contend with. There is only one farm house in the area so the test site is devoid of live power lines. The weather during the test period was mostly humid with intermittent rain showers. Temperatures ranged from 15° to 50° F.

#### Overburden Conductivity

Conductivity measurements were conducted employing the same equipment and procedures as those used in the Guyan No. 1A mine. The conductivity of the overburden was determined to be  $2.8 \times 10^{-2}$  mhos/meter. Conductivity sounding data are shown in Figure 5-7.

#### EM Noise Measurements

Again the same procedures and equipment as those employed at the previous test site were employed here. This equipment included a ferrite loop antenna input to a wideband noise preamplifier feeding a Model 4300 battery powered tape recorder. The Model 4300 tape recorder includes additional signal conditioning circuitry. Typical noise patterns for the test area are shown in Figures 5-8 and 5-9; magnitudes are generally low at the frequencies of interest and power line interference was of no appreciable significance at any of the location sites in the test area.



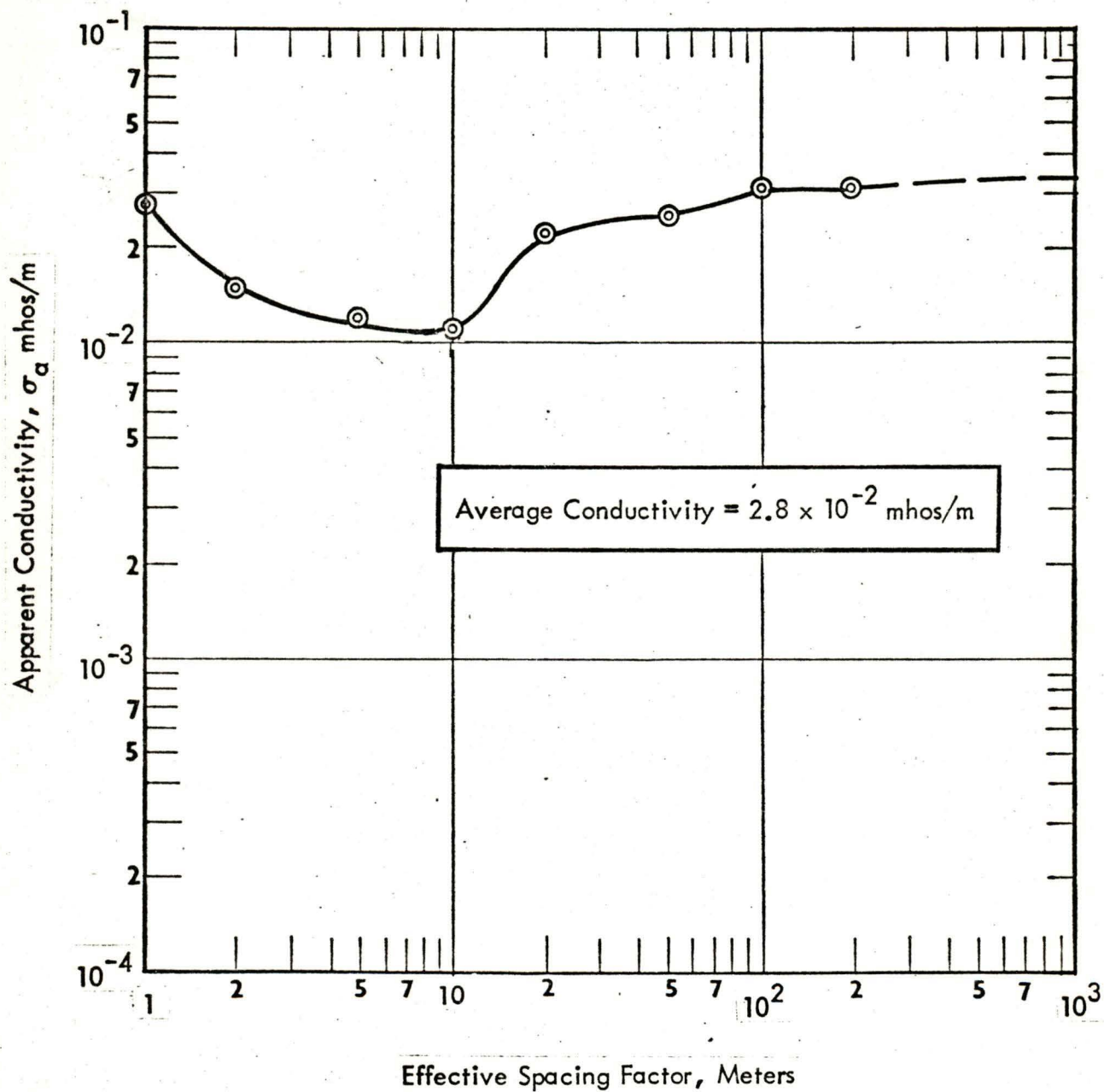


Figure 5-7. Earth Conductivity Sounding, Putnam Mine, Elmwood, West Virginia



FIGURE 5-8 SURFACE EM NOISE VS FREQUENCY

Plot No. 19

POTNAM MINE

12/18/71

PROCESSING BANDWIDTH = 9.8 HZ

POTNAM MINE  
SURFACE LOCATION G.

VERTICAL MAGNETIC FIELD,  $H_z$ ,  $\mu amp/m$

FREQUENCY, HZ

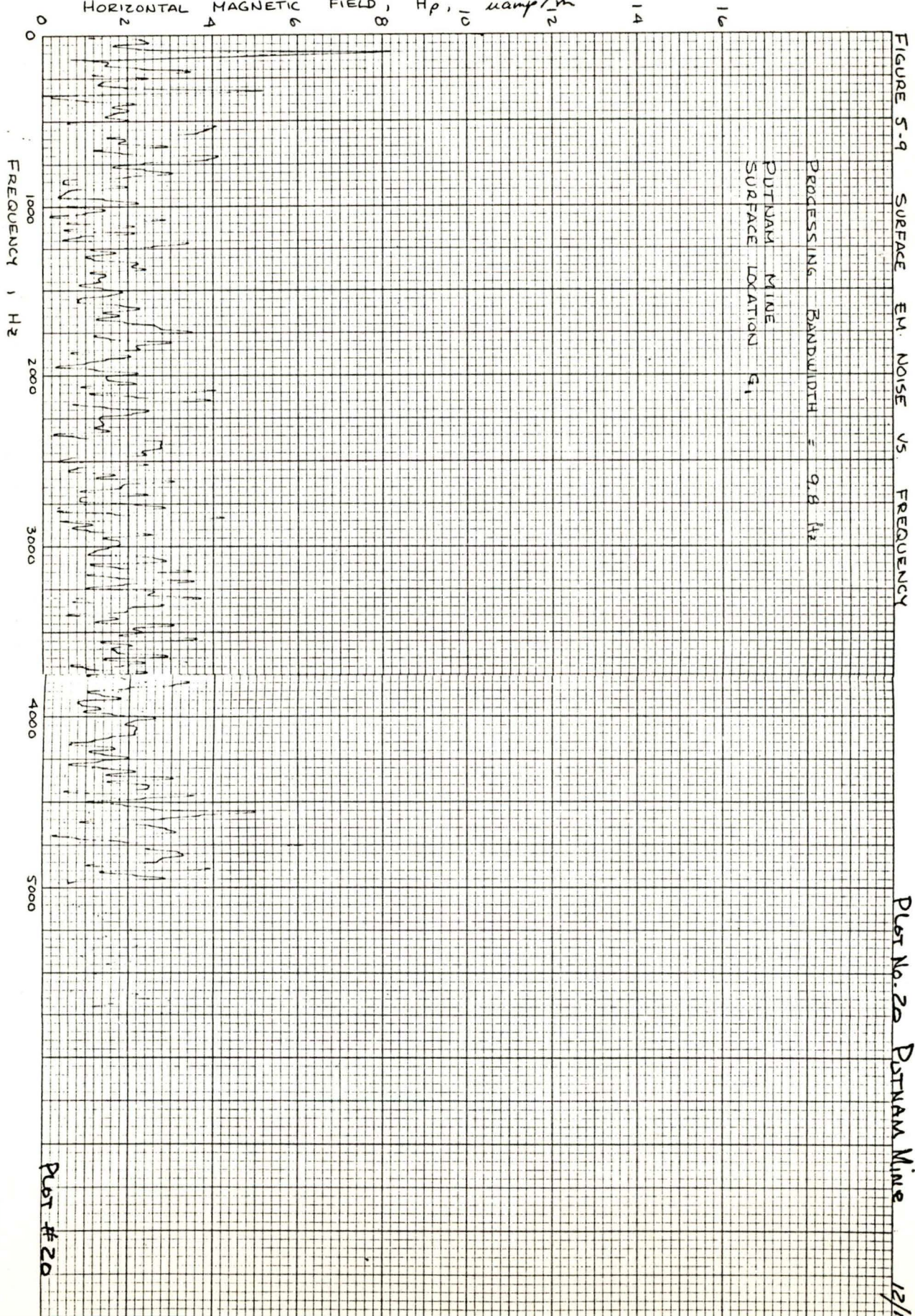
Plot # 19

K&E 10 X 10 TO THE INCH 47 0780  
KEUFFEL & ESSER CO  
MADE IN U.S.A.



K·E 10 X 10 TO THE INCH 47 0780  
10 X 10 INCHES  
KEUFFEL & ESSER CO. MADE IN U.S.A.

HORIZONTAL MAGNETIC FIELD,  $H_p$ ,  $\mu\text{amp}/\text{m}$





## EM Location and Signal Identification Tests

Seven location exercises were conducted at this site; four were conducted to cover a variety of mine depths and hill slopes, two for the purpose of signal identification and one to determine the effect of tilting the plane of the transmitting antenna from its normal horizontal position.

The transmitter locations and corresponding surface null locations are shown on the map of Figure 5-10. Frequencies, null offset errors, mine depths and average local hill slopes are shown in Table 5-2. The mine depth for the 2070 Hz transmitter at location A is comparatively shallow; the terrain above the transmitter is essentially flat; no difficulties were encountered either in detecting the signal or locating the surface null. At location B, there was no problem in locating the 1050 Hz transmitter signal; however, the surface null location occurred on a steep slope leading down to a creek bed. The null offset error indicates that some slope correction is required to account for the steep hill slope. The terrain above location C is a constant, gradual slope without steep or ragged interruptions. The null offset error at this location was actually increased by applying a slope correction. Part of this can be attributed to the fact that in these deep mines, the slope is not continuing down to the mine level and this represents a departure from the simple theoretical model used to calculate the slope correction. At location D the slope is gentle and smooth, also, but because of the low field intensity meter readings some difficulty was encountered in establishing the surface null location. It is suspected that the mine depth at that location is approaching the performance limitation for this transmitter antenna moment in this particular conductivity and noise environment making accurate location difficult.

Signal identification tests to test the system's ability to discern two signals in close proximity, both in frequency and distance, were conducted at locations E and F. The transmitters were 60 Hz apart in frequency (2070 Hz and 2010 Hz) and approximately 10 meters distant from one another. Both



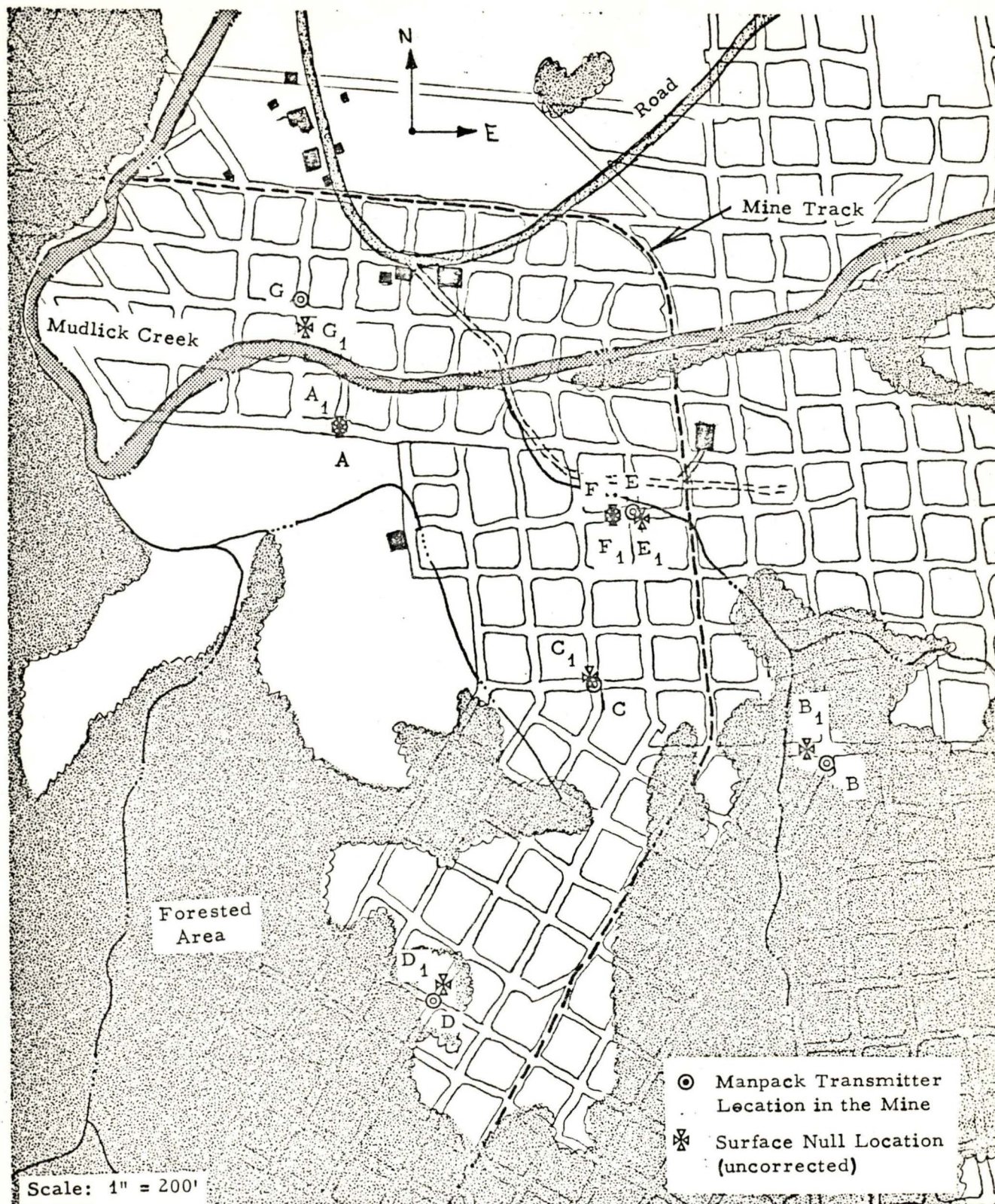


Figure 5-10. E. M. Location Experiments at the Putnam Mine, Elmwood, West Virginia.



Table 5-2

Mine Name	Location Description	Frequency	Overburden Depth (ft.)	Conductivity (mhos/m)	Est. Slope	Null Offset (ft.)	
						Uncor-rected	Corrected
Putnam Mine Elmwood, W. Va.	A <sub>1</sub> profiled	2070	380	$2.8 \times 10^{-2}$	0°	0	0
	B <sub>1</sub>	1050	440	$2.8 \times 10^{-2}$	32°	40	29
	C <sub>1</sub> profiled	2070	460	$2.8 \times 10^{-2}$	24°	12	34
	D <sub>1</sub>	2010	540	$2.8 \times 10^{-2}$	8°	30	24
	Manpack transmitters are located only 33 ft. apart in the mine.	E <sub>1</sub>	2010	$2.8 \times 10^{-2}$	0°	16	16
		F <sub>1</sub>	2070	$2.8 \times 10^{-2}$	0°	0	0
	G <sub>1</sub> profiled	1050	380	$2.8 \times 10^{-2}$	0°	44	44
Plane of Transmitting Antenna Tilted Approx. 30° in Direction of Null Offset.							



transmissions were readily detectable and it was verified that neither transmitter had any effect on the null location of the other.

For the tilted antenna test, the flat terrain at location G was selected; the subsurface transmitter loop was laid on the incline of roof fall rubble such that the antenna axis was tilted off the vertical in a southerly direction. The surface null location was shifted south by about 44 ft. This is consistent with the expected shift in location for a loop tilted by  $20^\circ$  in the mine. The slope of the transmitting loop was not precisely measured but was estimated to be on the order of  $20^\circ \pm 5^\circ$ .

### Magnetic Field Profiles

Field intensity measurements were made using the Location Receiver and the same procedures as those used at the previous test site. Two profiles were plotted using the 2070 Hz transmitter at two different locations, A and C, so that comparisons could be made between flat terrain and hill slope. A profile was also made of the tilted antenna transmitter at location G. The measured and theoretical profile plots for  $A_1$  are shown in Figures 5-11 and 5-12, and the measured profile for  $C_1$  is shown in Figures 5-13 and 5-14. The profile measured for the slanted antenna,  $G_1$ , is shown in Figure 5-15. There is no theoretical plot for this location; however, a location shift in the direction of the loop axis tilt was apparent in the measurement. For those cases where the slope was reasonably constant, the theoretical profiles were computed and are shown to be consistent with the measured results. For highly irregular terrain, the location accuracies, as a rule, were not improved by applying slope corrections based on average slope. In most cases the error was over-corrected by an amount equal to the original error. In cases of irregular terrain it would appear to be more accurate to use only a portion of the indicated correction. With the limited experience to date, however, it is difficult to specify a percentage.

### Miscellaneous Tests

The Beacon air-core uplink antenna and H-P 302A Wave Analyzer were used to check null locations and field intensities for comparison with the location receiver values. As at the previous site, no null location changes were indicated, but again the nulls were better defined using this equipment.



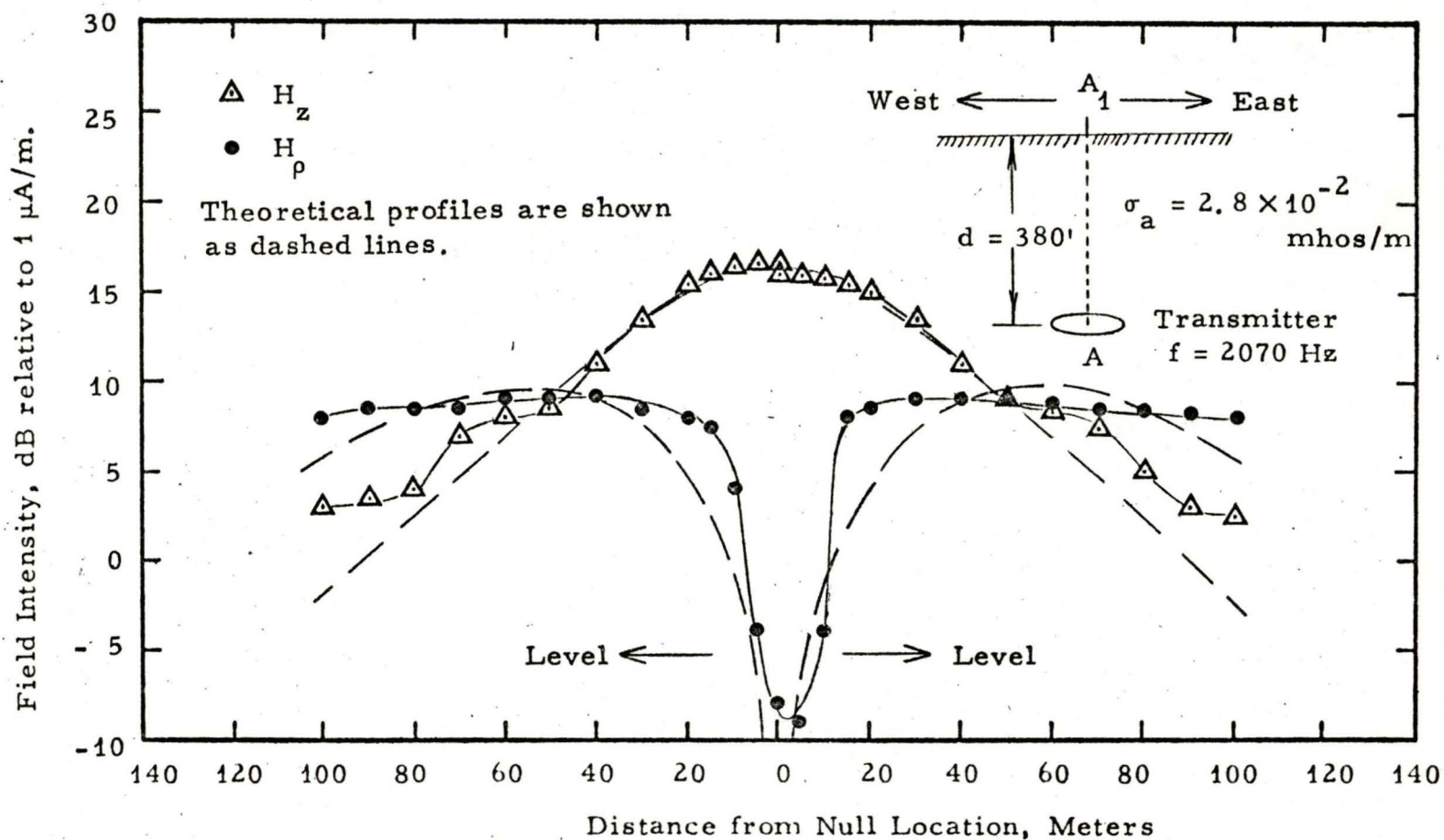


Figure 5-11. Field Intensity Profile above Vertical Magnetic Dipole at Putnam Mine, Elmwood, West Virginia. (East-West Profile Location A)

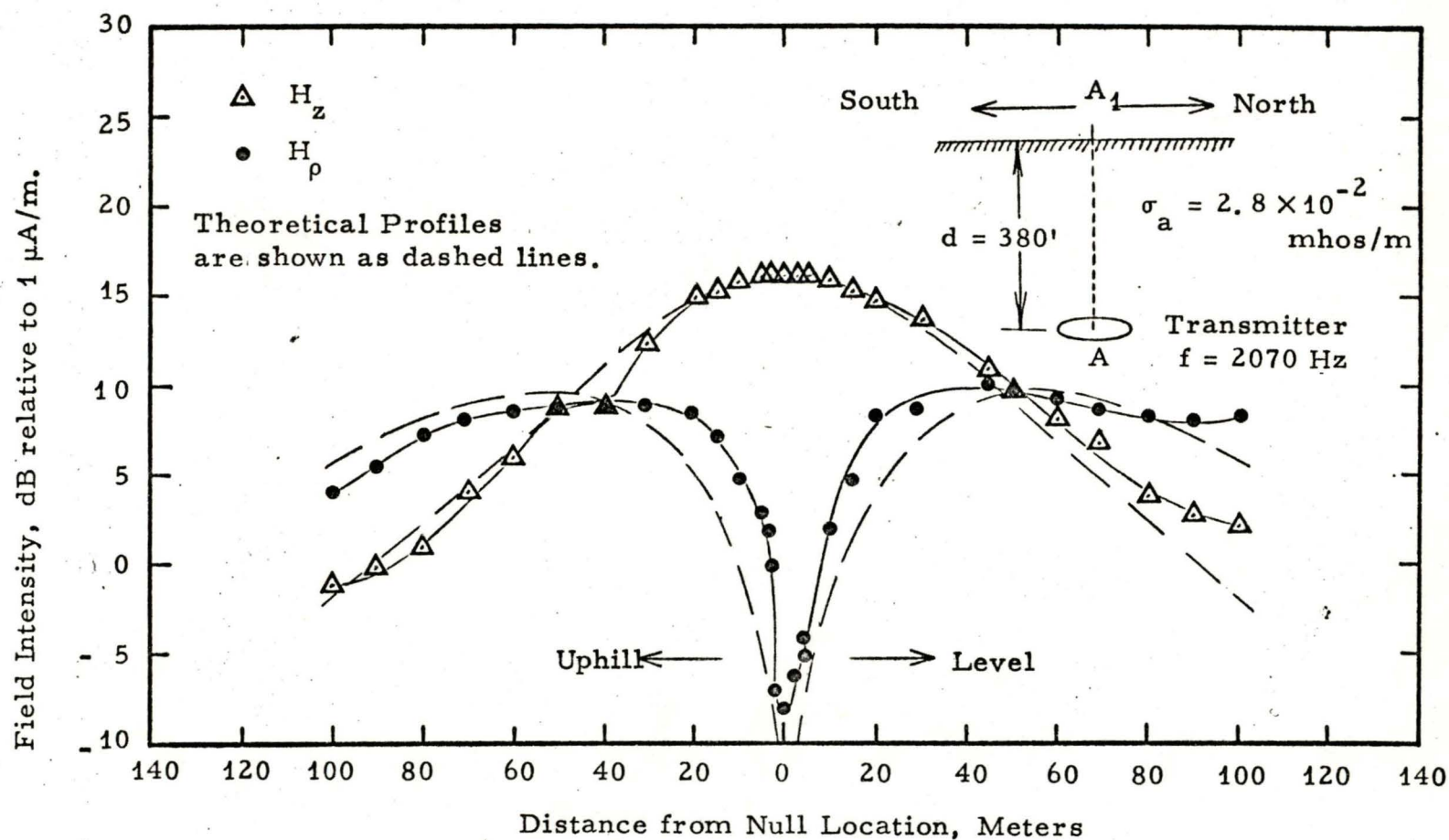


Figure 5-12. Field Intensity Profile above Vertical Magnetic Dipole at Putnam Mine, Elmwood, West Virginia. (North-South Profile Location A).



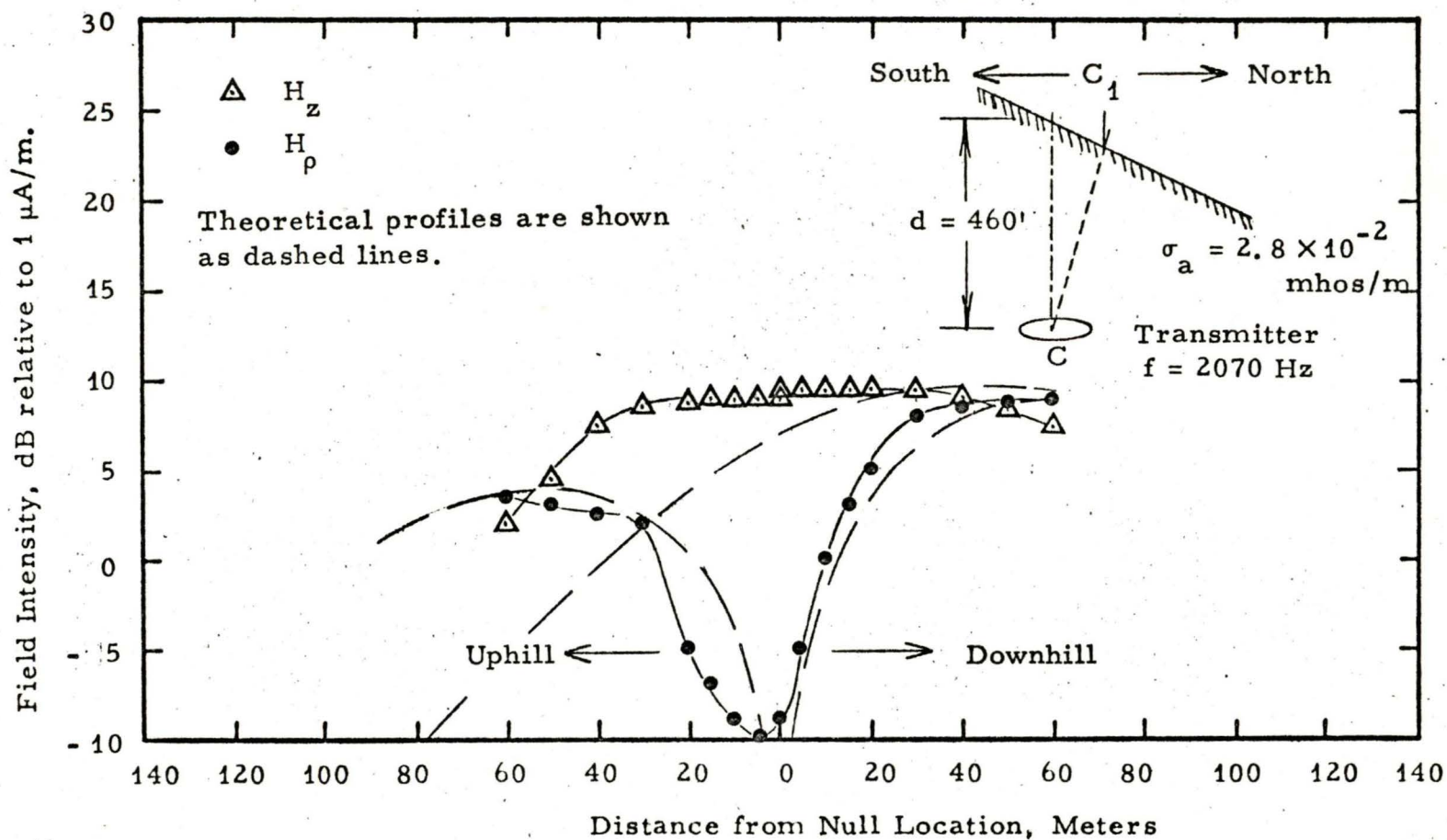


Figure 5-13. Field Intensity Profile above Vertical Magnetic Dipole at Putnam Mine, Elmwood, West Virginia (North-South Profile, Location C)

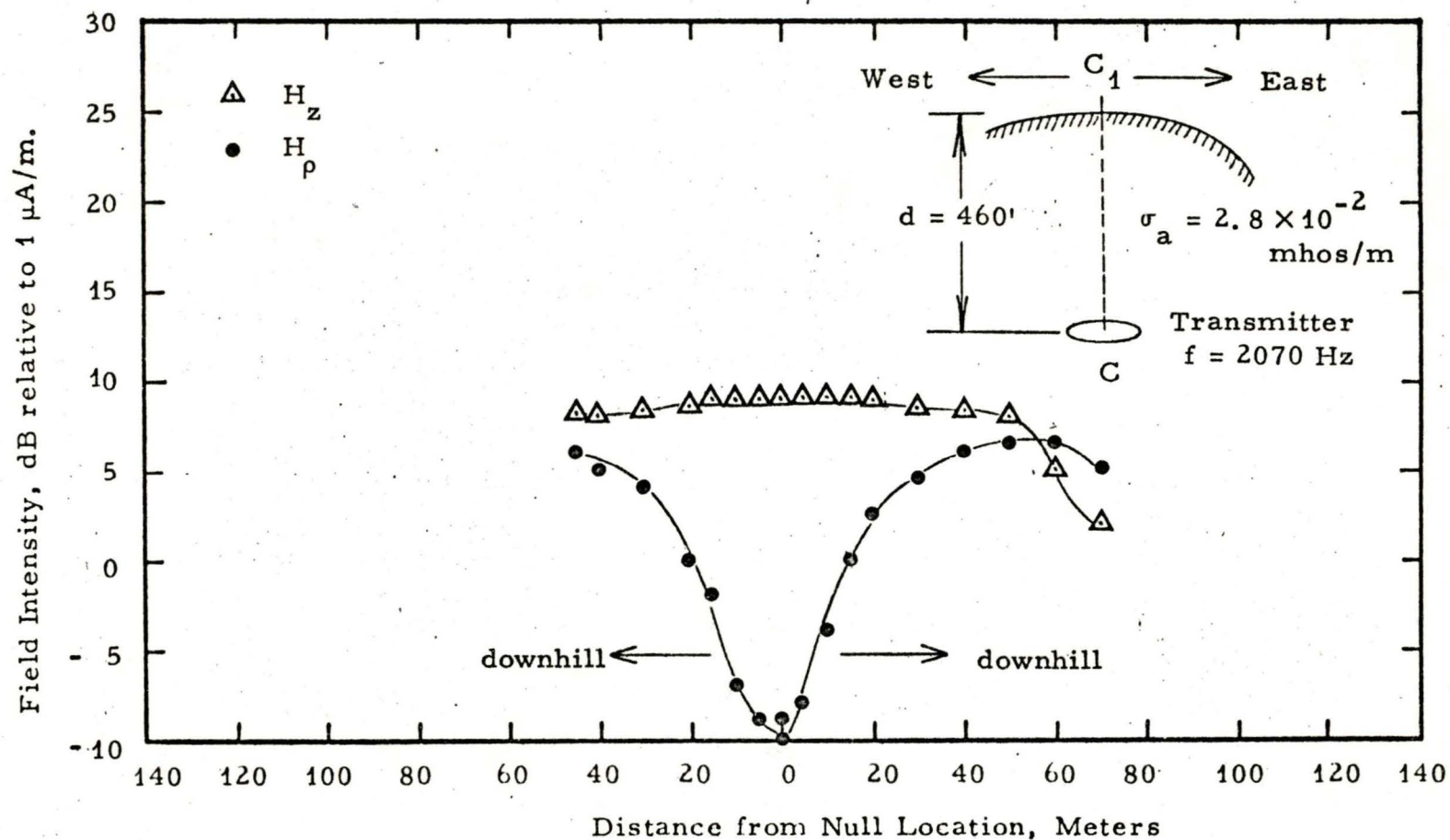


Figure 5-14. Field Intensity Profile above Vertical Magnetic Dipole at Putnam Mine, Elmwood, West Virginia. (East-West Profile, Location C)



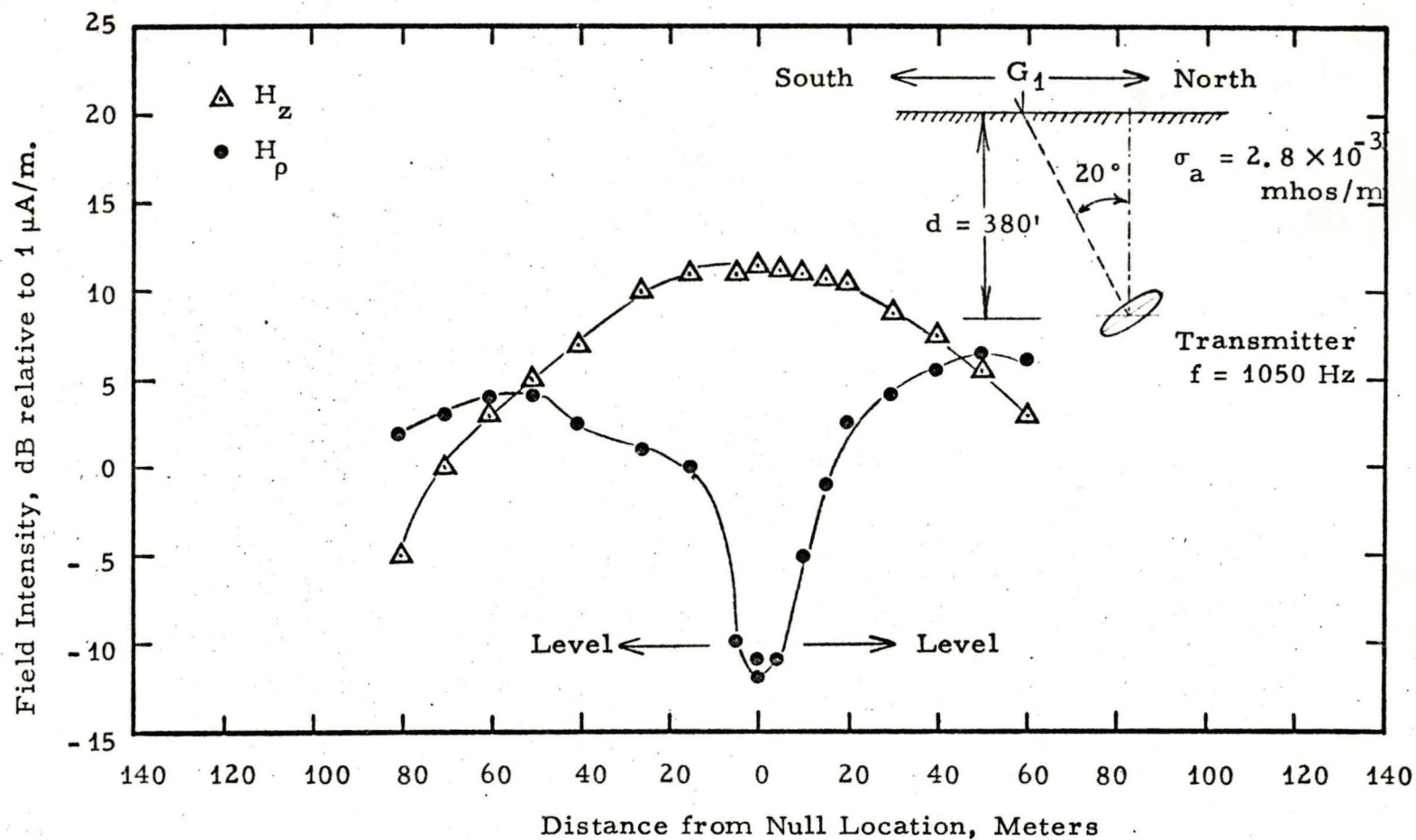


Figure 5-15. Field Intensity Profile above a Vertical Magnetic Dipole at Putnam Mine, Elmwood, West Virginia (North-South Profile, Location G)

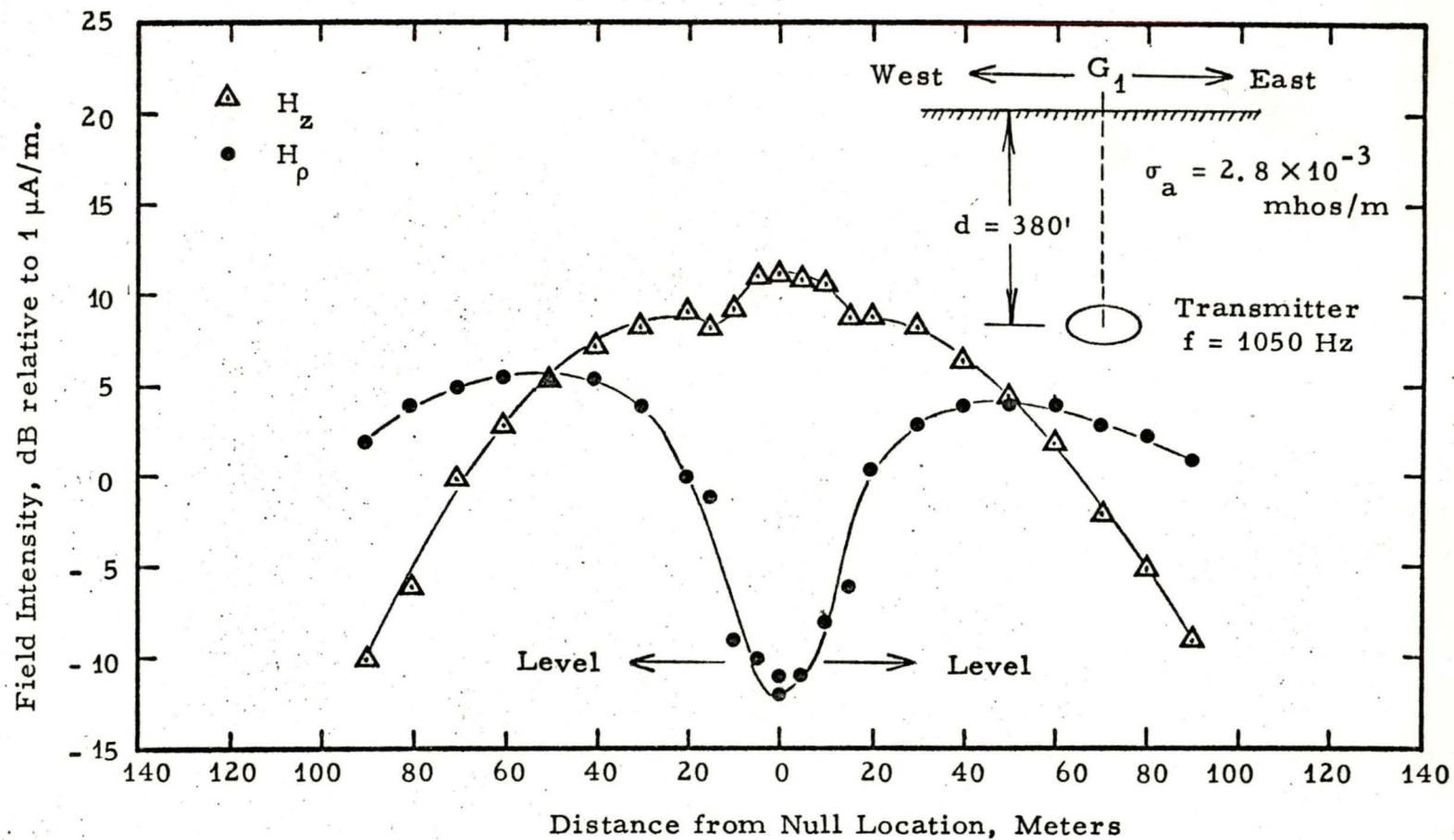


Figure 5-16. Field Intensity Profile above a Vertical Magnetic Dipole at Putnam Mine, Elmwood, West Virginia (East-West Profile, Location G)



### 5.1.3 Robena #4 Mine (U. S. Steel)

The Robena #4 Mine is part of the Robena Mine Complex located along the Pittsburgh coal seam in Greene County, Pennsylvania. All of the experimental work done by Westinghouse in January 1973 was done in the general vicinity of the Blaker shaft which is located just south of Fordyce, Pennsylvania. The average seam thickness in this mine is about 84". The entire mine complex has a daily coal production of about 15,000 tons and access to the mine is obtained via 12 shaft entries and one slope entry. The overburden thickness at this mine varies from about 650 ft to 1000 ft in the areas where Westinghouse personnel were performing their tests. A map showing the test area is shown in Figure 5-17.

#### Test Objectives

The primary objective of the tests performed at the Robena #4 mine was to evaluate the performance of the EM continuous wave location system in various overburden depths up to a maximum depth of 1000 feet. Prior to performing these tests, some modifications in the manpack transmitter were implemented to make it capable of driving a low impedance antenna wound around a coal pillar.

A reasonably long battery life was obtained by reducing the duty cycle of the tone transmission from 90% to approximately 10%. The tone burst interval of from 1 to 2 seconds was retained from the original design. In addition to the surface field measurements made with this equipment, a test was conducted to determine the feasibility of using a helicopter to aid in quick reconnaissance surveys of underground EM transmissions.

Figure 5-17. Robena Mine No. 4 Mine Map



### Ground Conductivity Measurements

A ground conductivity survey with dipole spacings ranging from one meter to 400 meters was run commencing at the streambed located in the lower right corner of the map of Figure 5-17 and expanding east perpendicular to the road. The results of the conductivity sounding show an essentially homogeneous overburden with an average conductivity down to the mine depth of  $1.1 \times 10^{-2}$  mhos/m. A plot of the conductivity sounding is shown in Figure 5-18.

### Signal Propagation Tests (Surface)

The initial deployment of manpack transmitters in the mine are indicated by the small circles labeled G and F on the mine map and correspond to the 3030 Hz transmitter and 2010 Hz transmitter respectively. The antennas used for these transmissions were single manpack antennas arranged in a single turn configuration at two intersections as shown on the map. Based on the known depth of overburden at this location and the measured conductivity, the expected field strength would have been on the order of  $0.378 \mu\text{A/m}$  and  $0.525 \mu\text{A/m}$  for the 3030 Hz and 2010 Hz transmission respectively. Under quiet surface noise conditions, it should have been possible to receive these transmissions. However, the surface location for this test turned out to be located just 200 ft. from a 3 wire power line, and attempts to receive either of these transmissions proved unsuccessful. The following day, the 2010 and 3030 Hz transmitters were removed and a fully charged 2070 Hz transmitter was deployed driving a 350 ft. length of #10 wire wound around a pillar in a one turn loop as shown by the location A on the map. Meanwhile, a 1050 Hz transmitter with single manpack antenna was located in a different portion of the mine as indicated by the small circle marked H on the map. Results of these tests showed the 2070 Hz transmission with the increased transmitter moment to be readily detectable in spite of its close proximity to the 3 phase power line. Accurate measurements of field strength were impossible with the modified equipment because of the short duty cycle of the tone burst and the heavy damping of the output meters. However,

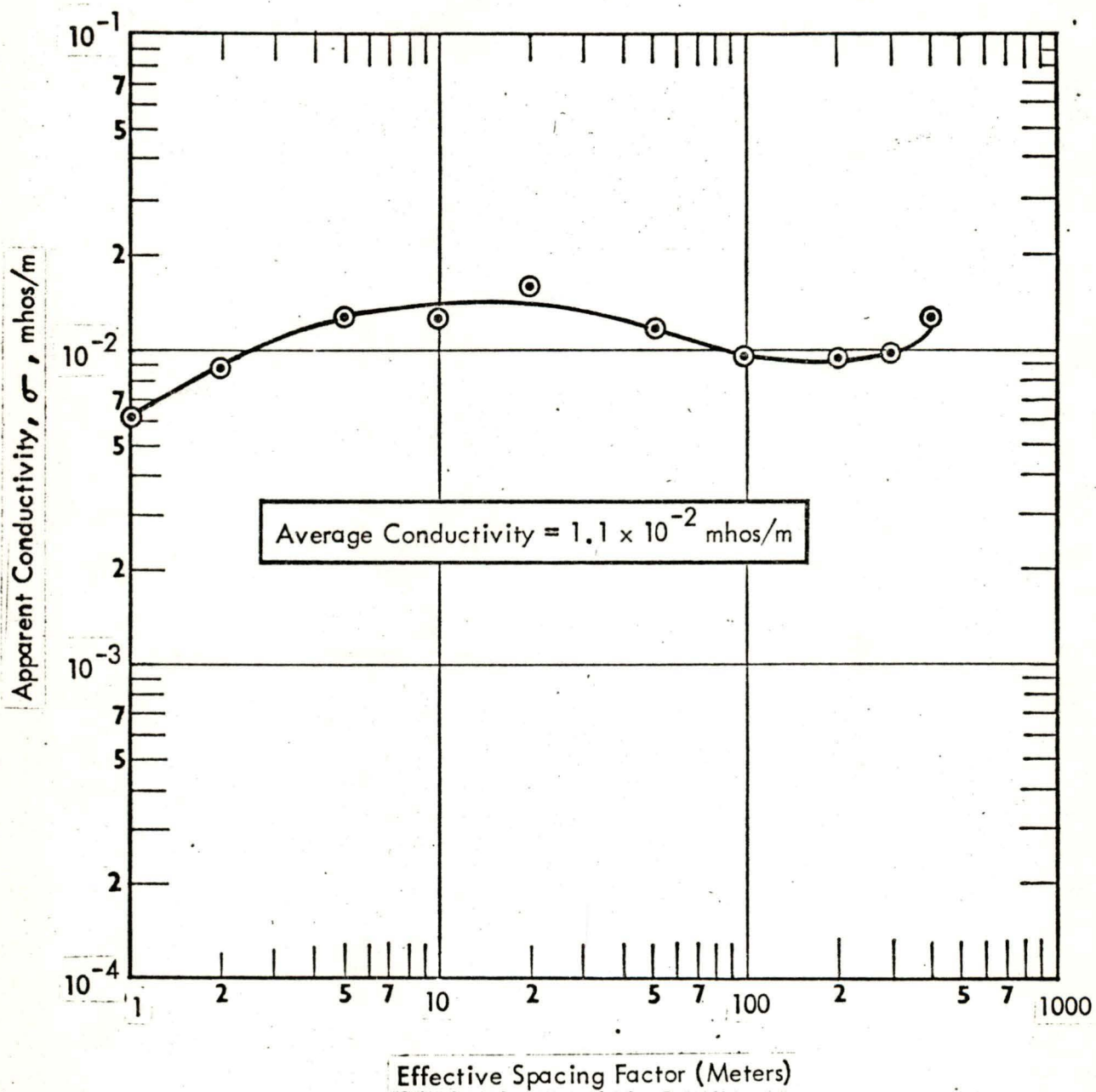


Figure 5-18. Robena Mine No. 4 Conductivity Sounding



we did measure the maximum horizontal range of detection where the signal was still distinguishable from the noise. This turned out to be 1125 ft. for the 2070 transmission at Location A.

Attempts that were made to detect the single manpack transmission at Location H were unsuccessful. From these tests, it can be concluded that a single manpack transmitting antenna deployed in a mine intersection does not produce a sufficient current moment to be readily detected at the Robena Mine #4.

The following day, the 350 ft. #10 wire antenna was deployed in the same general vicinity as the unsuccessful test at Location H. Also an array of 4 manpack transmitting antennas connected in series was deployed around a coal pillar adjacent to the No. 10 wire antenna. These latter 2 locations are identified on the map as B and C. Both of these transmissions were easily identified on the surface and surface fixes were obtained using both the Westinghouse receivers C 836A and C 842A.

The C 842A fixed tuned receiver was, at times, troubled by oscillations brought on by feedback between the electromagnetic earphones and the receiving loop antenna. Further tests using crystal earphones eliminated this problem. The error in surface fix for the 3030 Hz transmission was 53 feet. Part of this offset could be attributed to a fenceline located directly over the actual projection of the underground transmitting dipole. Of all the measurements made at the Robena Mine, this proved to be the greatest offset between surveyed and electromagnetic position.

The following day (Friday) two transmitters were deployed in the deepest section of the mine as shown by Locations D and E on the map. The actual overburden depth at these locations was estimated at 990 ft. from the mine topo map. The transmitters were permitted to run continuously throughout the weekend, while surface measurements were made on both Saturday and Sunday

to determine effective life of the transmitter. On Monday morning after 72 hours of continuous operation, these transmitters were still producing detectable signals at the surface. Figure 5-19 shows oscillograph photographs of tape recordings made on the C836A Receiver IF output after 53 hours of continuous transmitter operation.

A summary of the surface measurements made at the Robena #4 mine is given in Table 5-3. It is observed in this table that applying slope corrections based on continuous hill slopes in most of the cases made the location error worse than that of the uncorrected location. In extremely deep mines such as Robena #4 it is unlikely that the measured local slope at a particular surface location will continue down to the mine level. Consequently, in making such an assumption when using the slope correction curves, it often produces a greater offset than what is experienced by ignoring the slope in a locally hilly situation.

### Noise

The noise spectra shown in Figures 5-20 through 5-28 were obtained from cassette tape recordings obtained at the field site using a Wollensak Model 4300 tape recorder. These recordings were transferred to a closed loop cassette and played back into a narrowband (10 Hz) Hewlett-Packard Wave Analyzer, Model 3590A and recorded on an X-Y plotter. Because of variable gain settings used on the field tape recorder it was difficult to obtain exact gain repeatability; thus the absolute calibration of these noise records is assumed to be accurate within a tolerance of about  $\pm 3$  dB. The records are useful, however, in making noise comparisons from site to site and for determining the general frequency content at each site.

Figure 5-20 shows the vertical magnetic field noise spectrum obtained at a point 30 feet from the compressor at the Robena Mine. Notice the multiple harmonics of the 60 Hz power frequency extending out to frequencies of 2 kHz. Figures 5-21 and 5-22 show the vertical magnetic

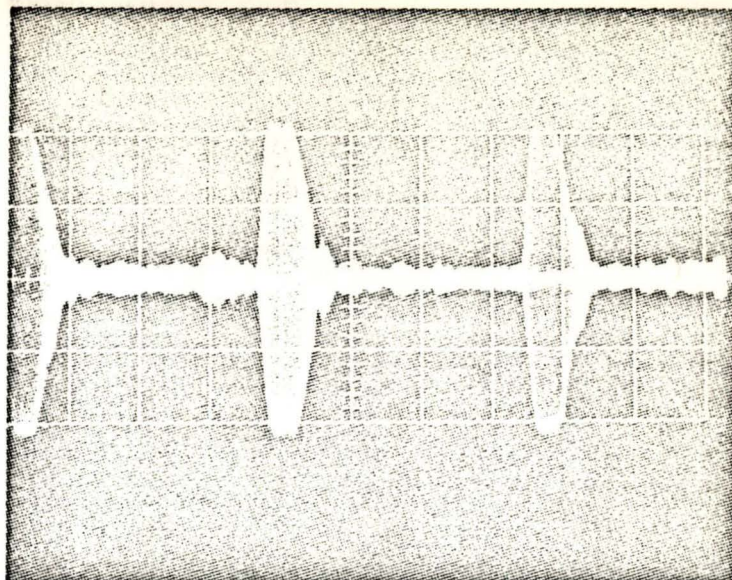


TABLE 5-3  
Results of Robena Mine Tests

<u>Location</u>	<u>f</u>	<u>Transmitting Antenna</u>	<u>Overburden</u>	<u>Slope</u>	<u>Field Strength</u> *	<u>Uncorrected Location Error</u>	<u>Horizontal Detection Range</u>	<u>Corrected Location Error</u>
A	2070	#10 Wire	800 ft.	16°	-5dB/μA/m	18 ft.	1125 ft.	27 ft.
B	2010	4 Manpack Antennas	725 ft.	0 - 13°	-14dB/μA/m	27 ft.	390 ft.	27' - 3'
C	3030	#10 Wire	725 ft.	0 - 13°	-3dB/μA/m	50 ft.	890 ft.	50' - 26'
D	1050	4 Manpack Antennas	990 ft.	16°	-26dB/μA/m	8 ft.	360 ft.	67'
E	2070	#10 Wire	990 ft.	16°	-15dB/μA/m	17 ft.	800 ft.	58'

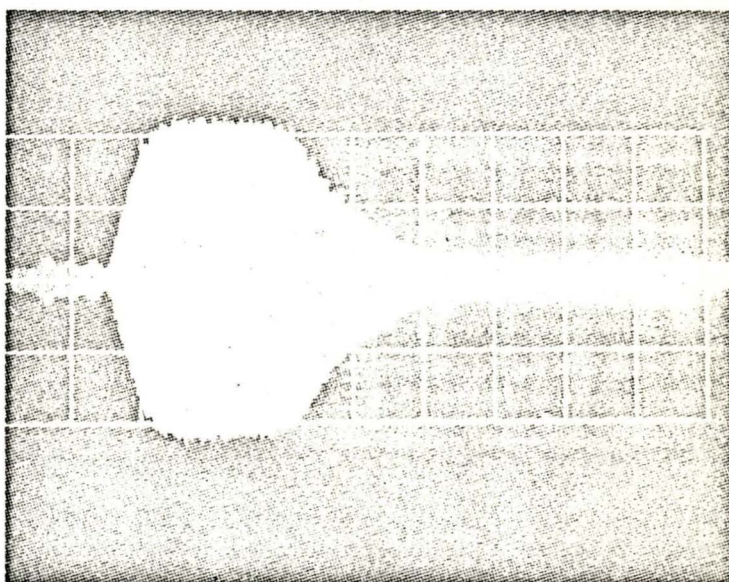
\* Represents relative field strength indication on the output meter. For pulsed signals, this meter indication is about 20dB low.

<u>Undetectable Signals</u>					<u>Comments</u>
F	2010	Single Manpack Antenna	800 ft.	16°	Power Line within 200 ft.
G	3030	" " "	800 ft.	16°	
H	1050	" " "	725 ft.	13°	Power Cables and metal Pipes Running up both Sides of Entry.



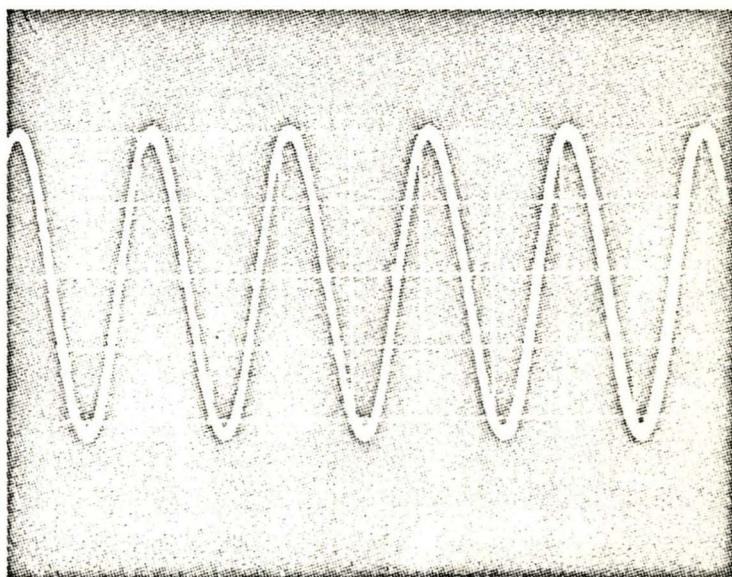
1 volt/cm

0.5 seconds/cm



1 volt/cm

0.1 seconds/cm



1 volt/cm

0.1 milliseconds/cm

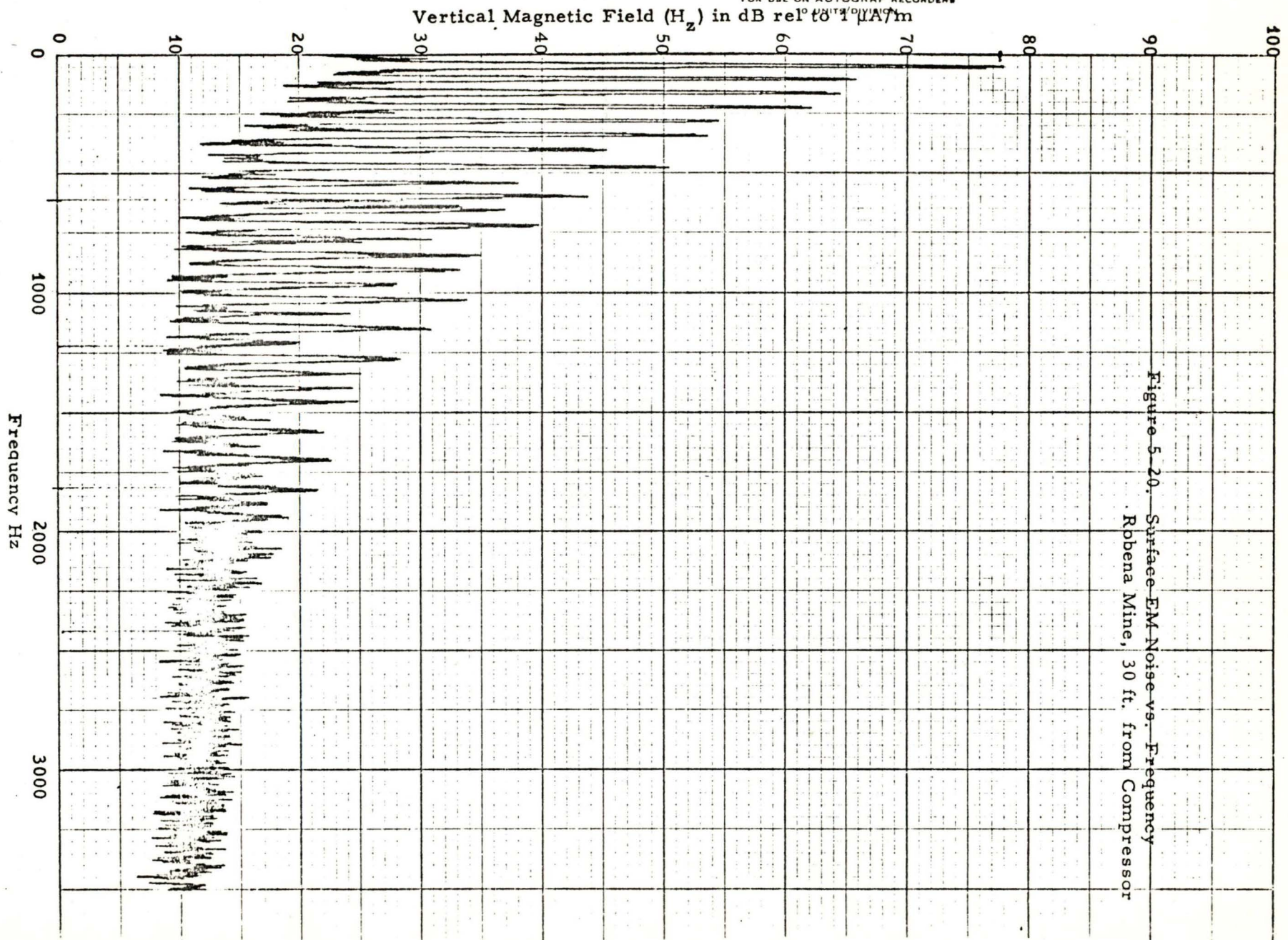
Figure 5-19. Oscilloscope photographs of receiver IF output after 53 hours of continuous transmitter operation.

frequency = 2010 Hz

overburden = 990 ft.

conductivity =  $1.1 \times 10^{-2}$   
mhos/m

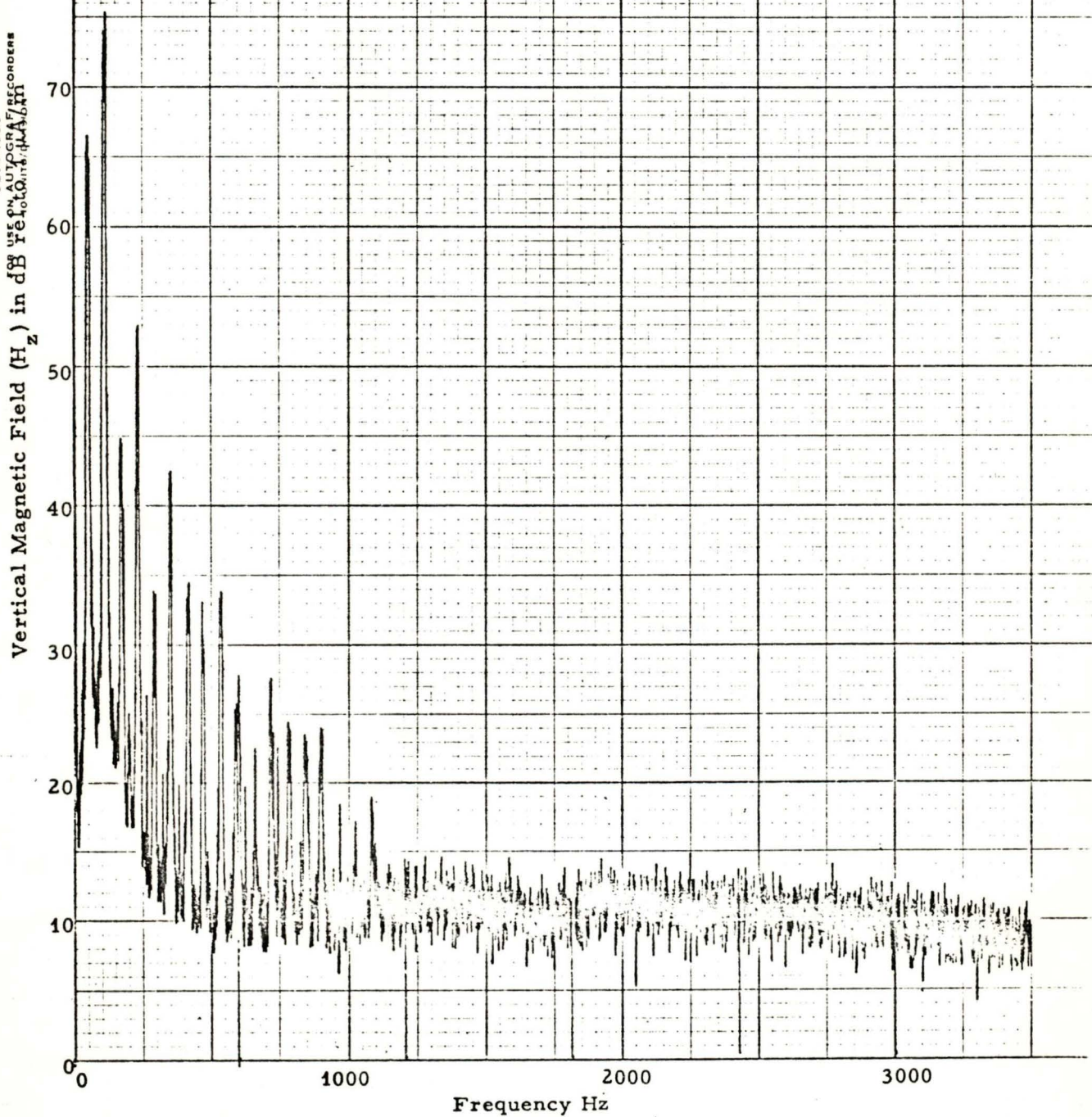






Vertical Magnetic Field ( $H_z$ ) in dB re  $10^{-12}$  W/m<sup>2</sup> at 100 kHz

Figure 5-24. Surface EM Noise vs. Frequency  
Location D & E, (Mine Operating)

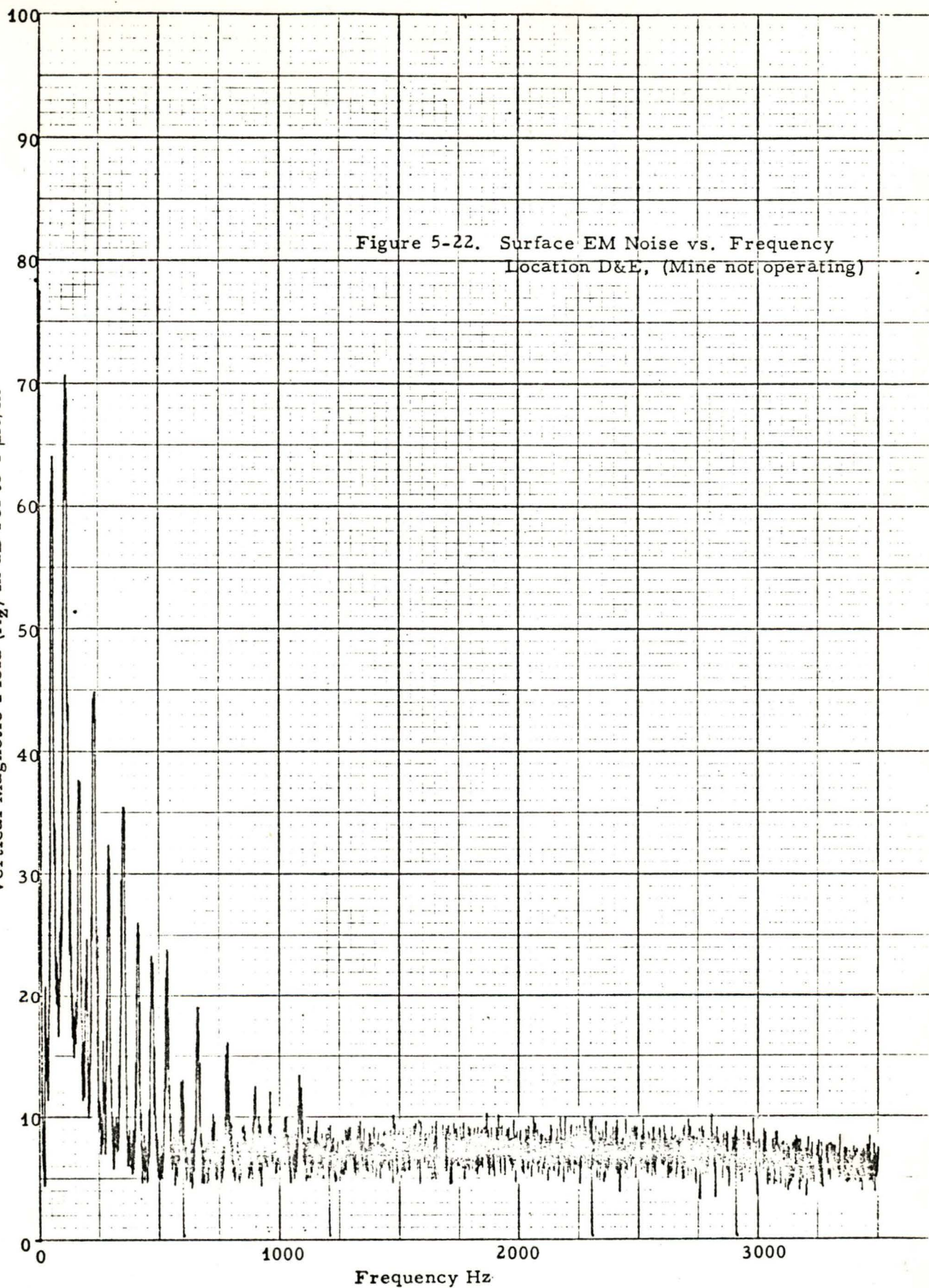




HEWLETT-PACKARD/MOSELEY DIVISION

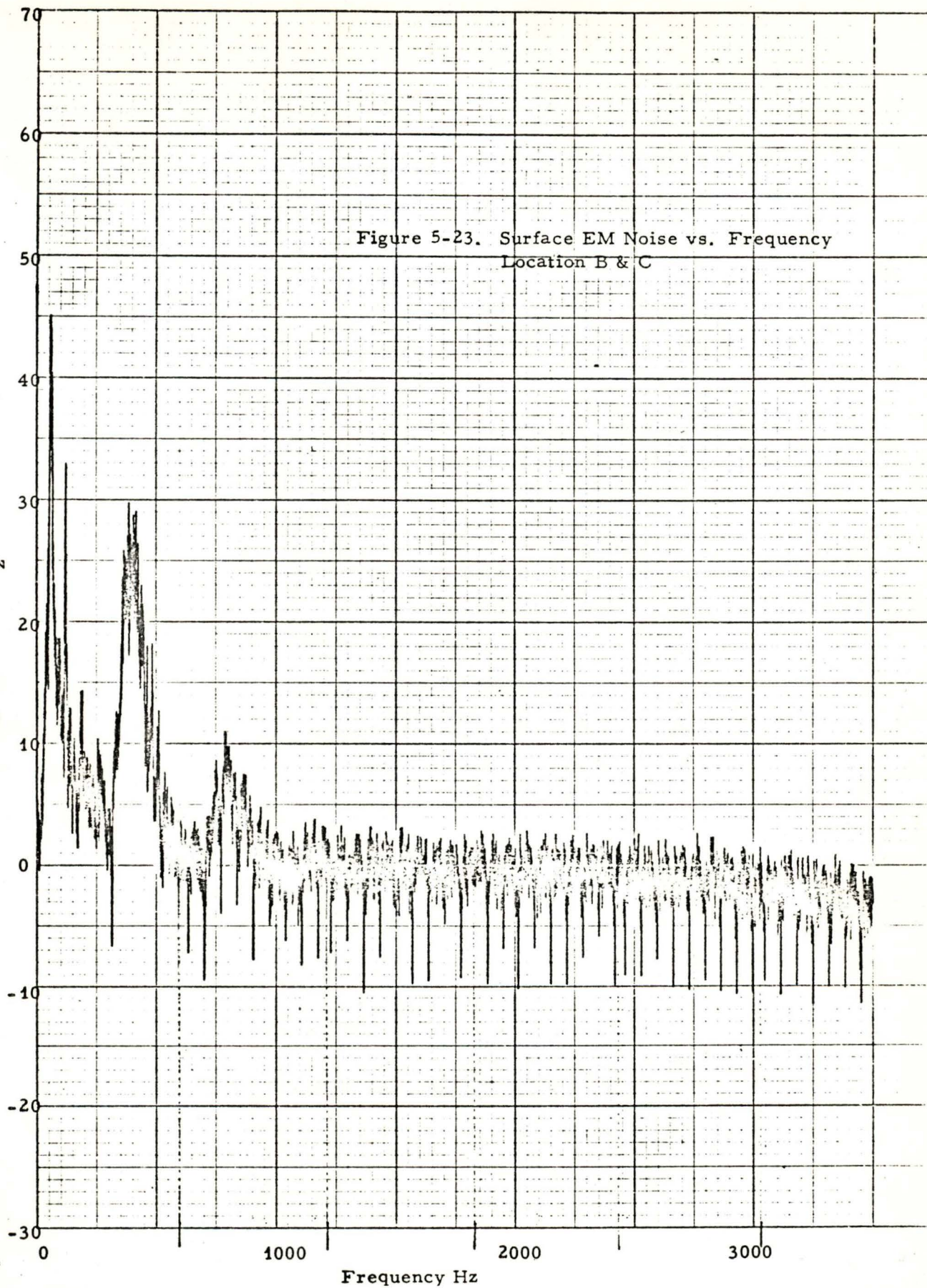
9270-1005  
FOR USE ON AUTOGRAPH RECORDERS

Vertical Magnetic Field ( $H_z$ ) in dB rel to  $1 \mu A/m$





Vertical Magnetic Field ( $H_z$ ) in  $\mu\text{B}$  for  $100 \text{ dB}$  READING





Horizontal Magnetic Field ( $H_p$ ) in dB  $\mu A/m$

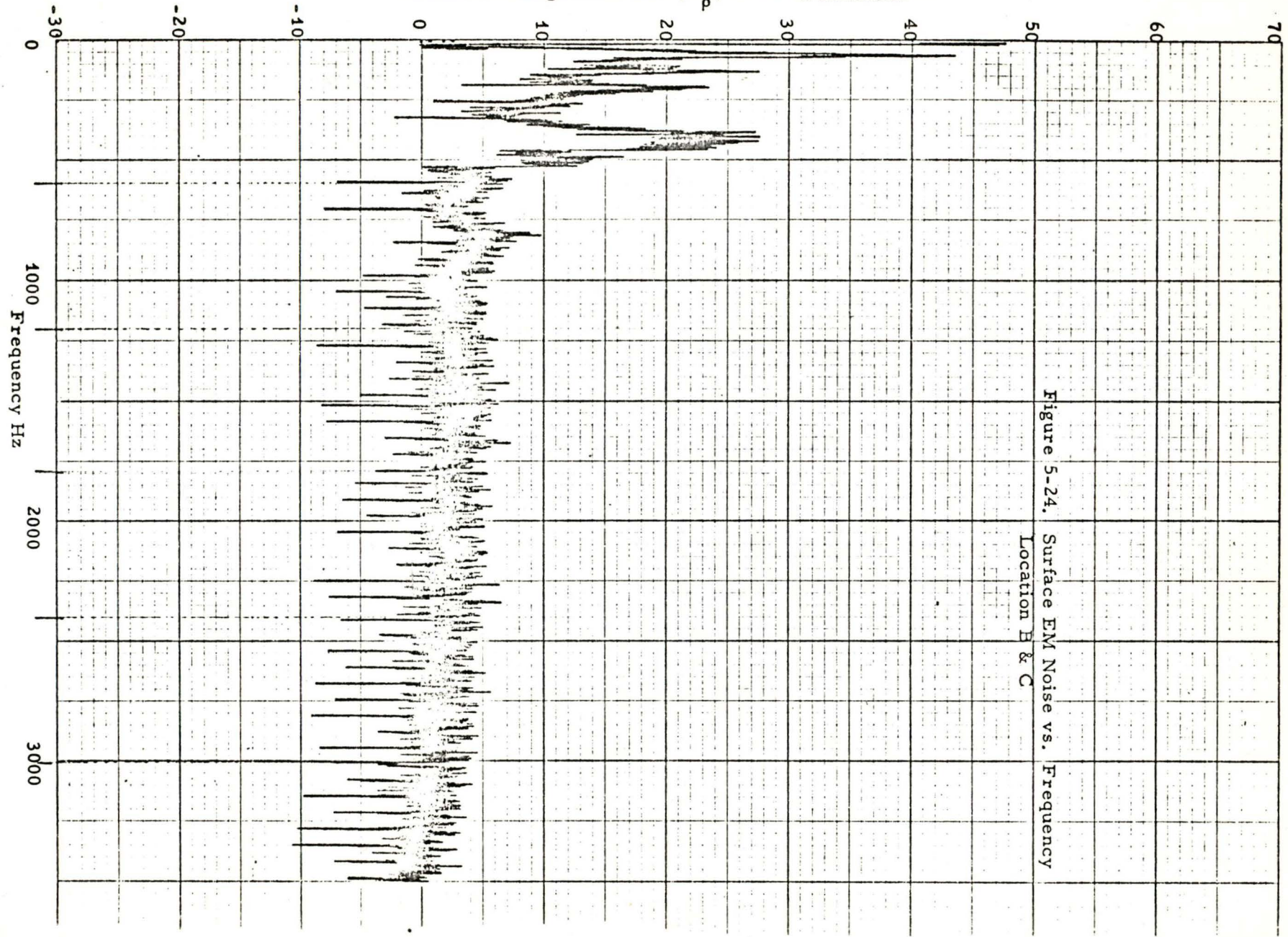
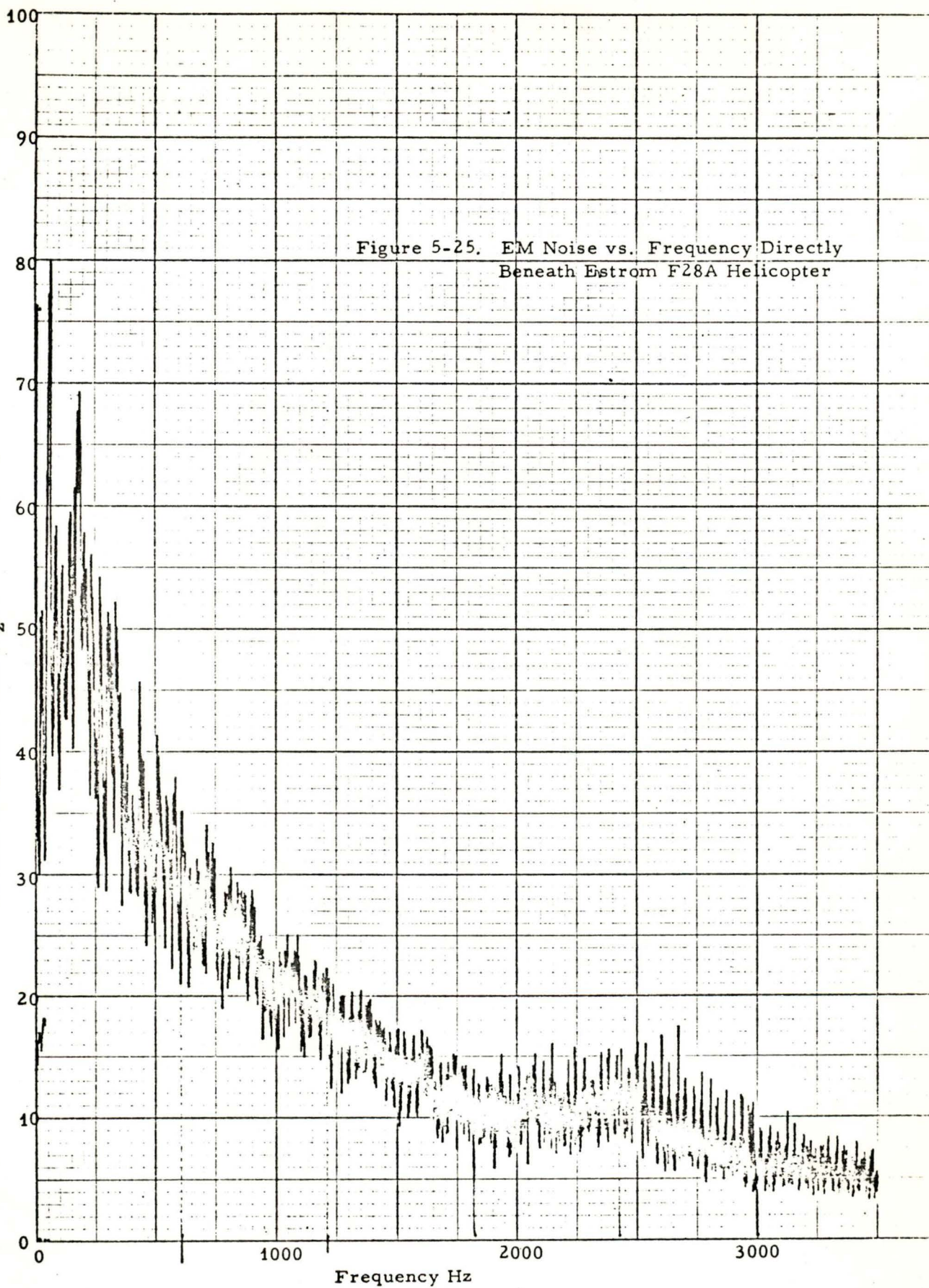


Figure 5-24. Surface EM Noise vs. Frequency  
Location B & C



HEWLETT-PACKARD/MOSELEY DIVISION  
9270-1005  
FOR USE ON AUTOCYCLE RECORDERS

Vertical Magnetic Field ( $H_z$ ) in dB rel to 1  $\mu$ W/m





HEWLETT-PACKARD/MOSELEY DIVISION

9270-1005

FOR USE ON AUTOGRAPH RECORDERS  
10 UNITS/DIVISION

Vertical Magnetic Field ( $H_z$ )

db relative to 1 A/m

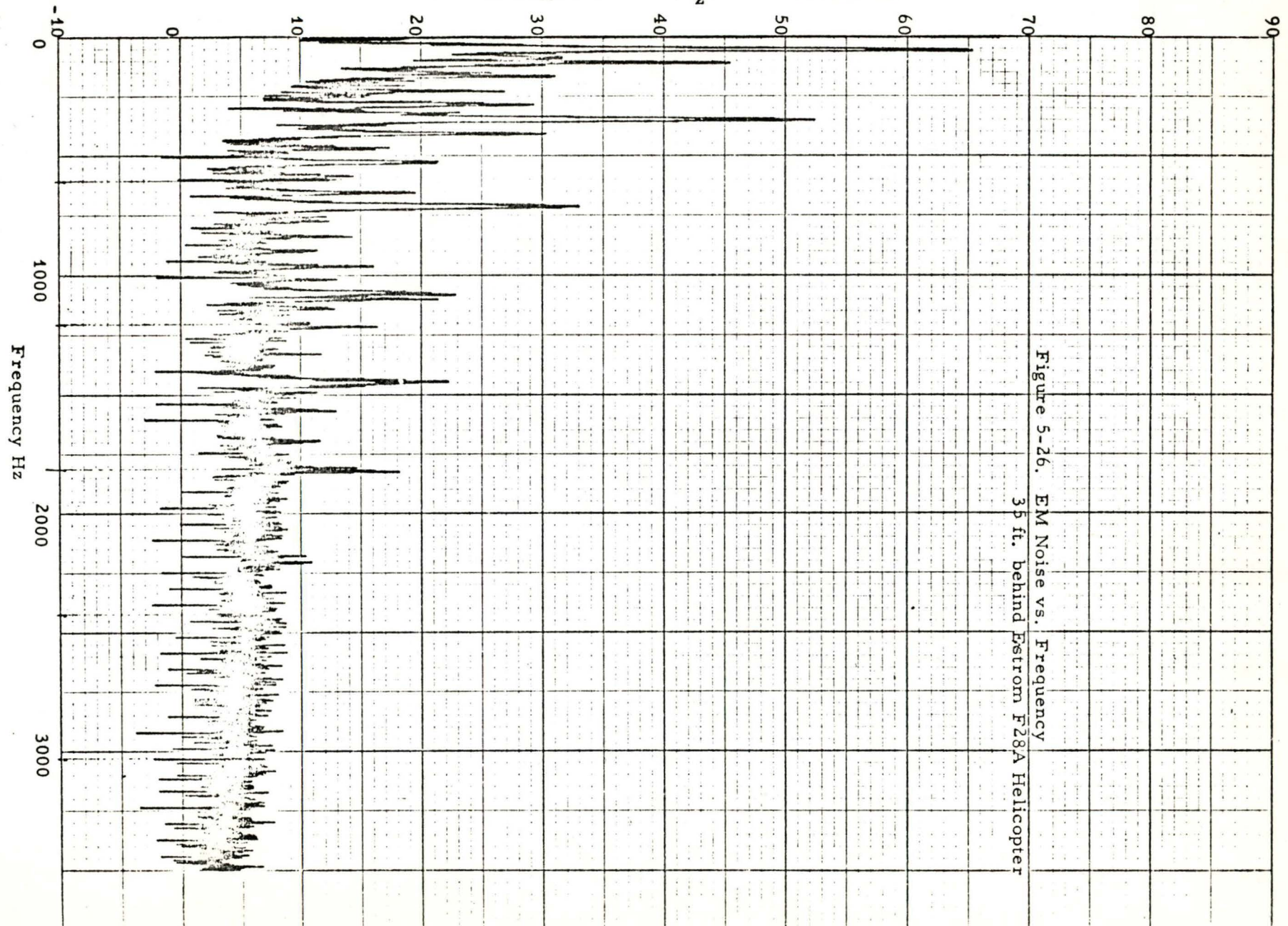


Figure 5-26. EM Noise vs. Frequency  
35 ft. behind Estrom F28A Helicopter



HEWLETT-PACKARD/MOSELEY DIVISION  
9270-1005

Vertical Magnetic Field ( $H_z$ ) in dB re 10  $\mu A/m$   
FOR USE ON AUTOGRAPH RECORDERS  
CONVERSION DIVISION

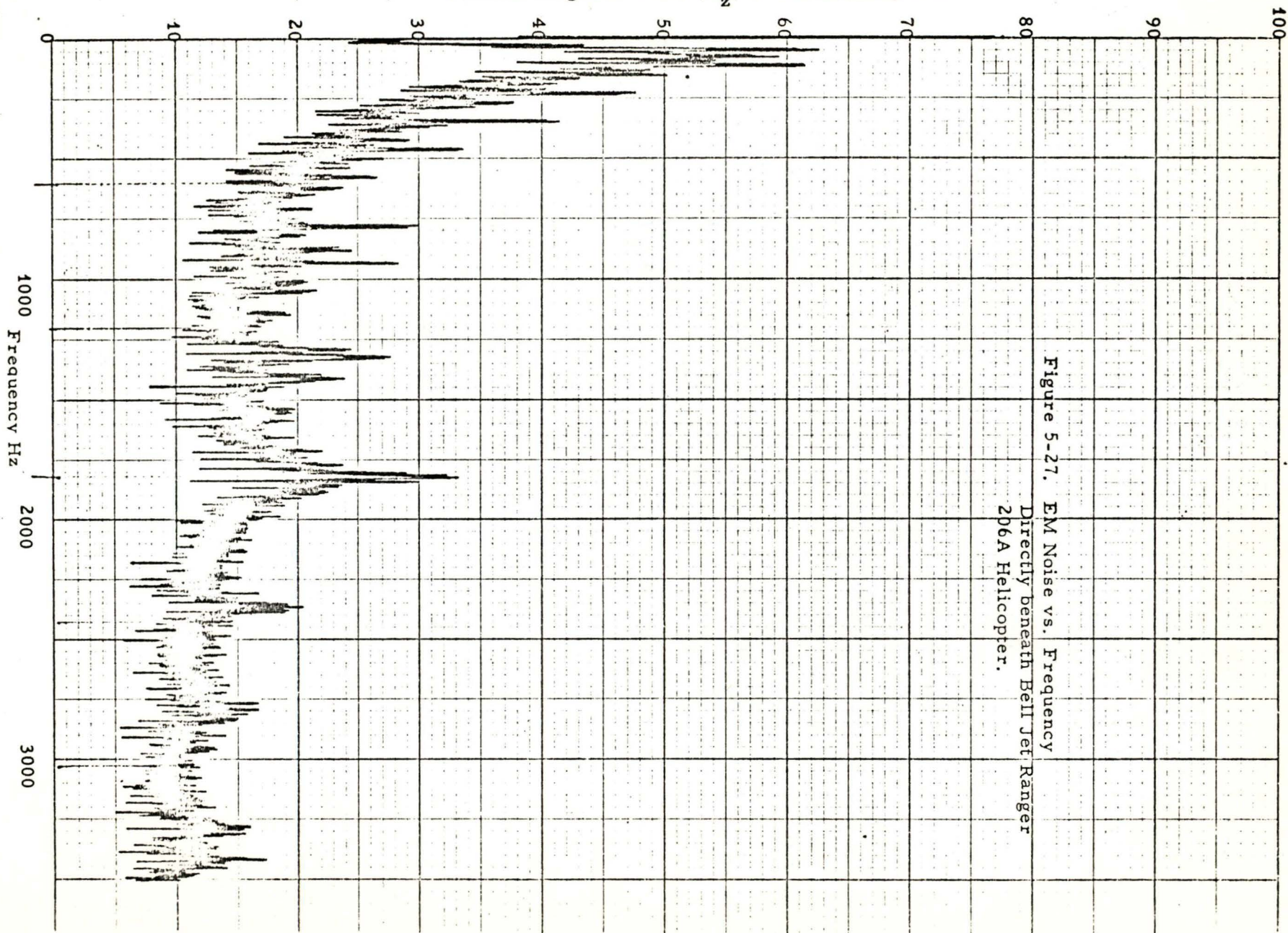


Figure 5-27. EM Noise vs. Frequency  
Directly beneath Bell Jet Ranger  
206A Helicopter.



HEWLETT-PACKARD/MOSELEY DIVISION  
9270-1003  
FOR USE ON AUTOGRAPH RECORDERS  
10 UNITS/DIVISION

db relative to 1 A/m

Vertical Magnetic Field ( $H_z$ )

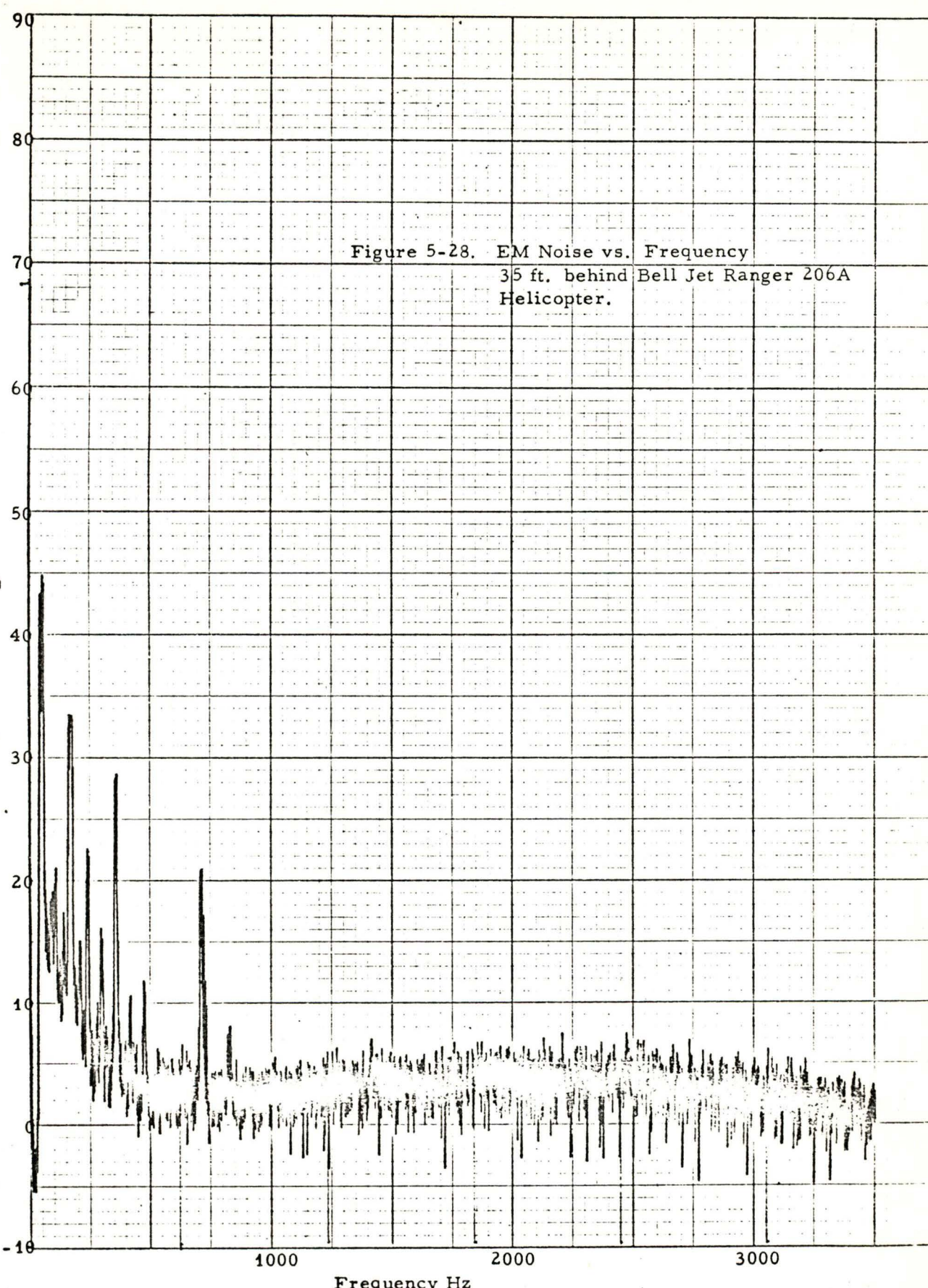


Figure 5-28. EM Noise vs. Frequency  
35 ft. behind Bell Jet Ranger 206A  
Helicopter.

field measured in the vicinity of locations D and E for both an operating mine and a non-operating mine. The general background noise as well as the harmonic peaks between 500 Hz and 1000 Hz are noticeably reduced when the mine is not operating. Since the Robena Mine is a dc mine with all its ac to dc conversion taking place at the surface, the drop in measured noise is undoubtedly due to the lighter load being placed on the nearby power lines while the mine is not operating.

Figures 5-23 and 5-24 show the noise spectrum measured at locations B and C. At this location there appears to be a high noise component in the vicinity of 420 Hz (7th harmonic), although the general background noise was less than on any of the other sites measured.

Noise generated by the two helicopters used in the reconnaissance testing is shown in Figures 5-25 through 5-28. Both the Enstrom F28A with a four cycle reciprocating gasoline engine and Bell Jet Ranger 206A with a turbine engine proved to be too noisy for a receiving antenna mounted on the skids of the aircraft. However at a distance of 35 feet away from the aircraft, the noise was substantially reduced, especially for the Bell Jet Ranger. Comparing Figures 5-26 with 5-28 shows that significant noise harmonics are present out to about 1800 Hz for the Enstrom F28A while the highest significant harmonic produced by the Bell Jet Ranger is about 800 Hz. This explains why the reception of signals was easier with the Bell Jet Ranger than the Enstrom F28A.

#### Helicopter Tests

The 2010 Hz and 3030 Hz transmitters were deployed at locations B and C in the mine to test for the feasibility of receiving these signals by helicopter. Surface measurements were repeated and results were consistent with those obtained previously for the same transmitting locations. High winds forced a postponement of any helicopter testing until the following day.

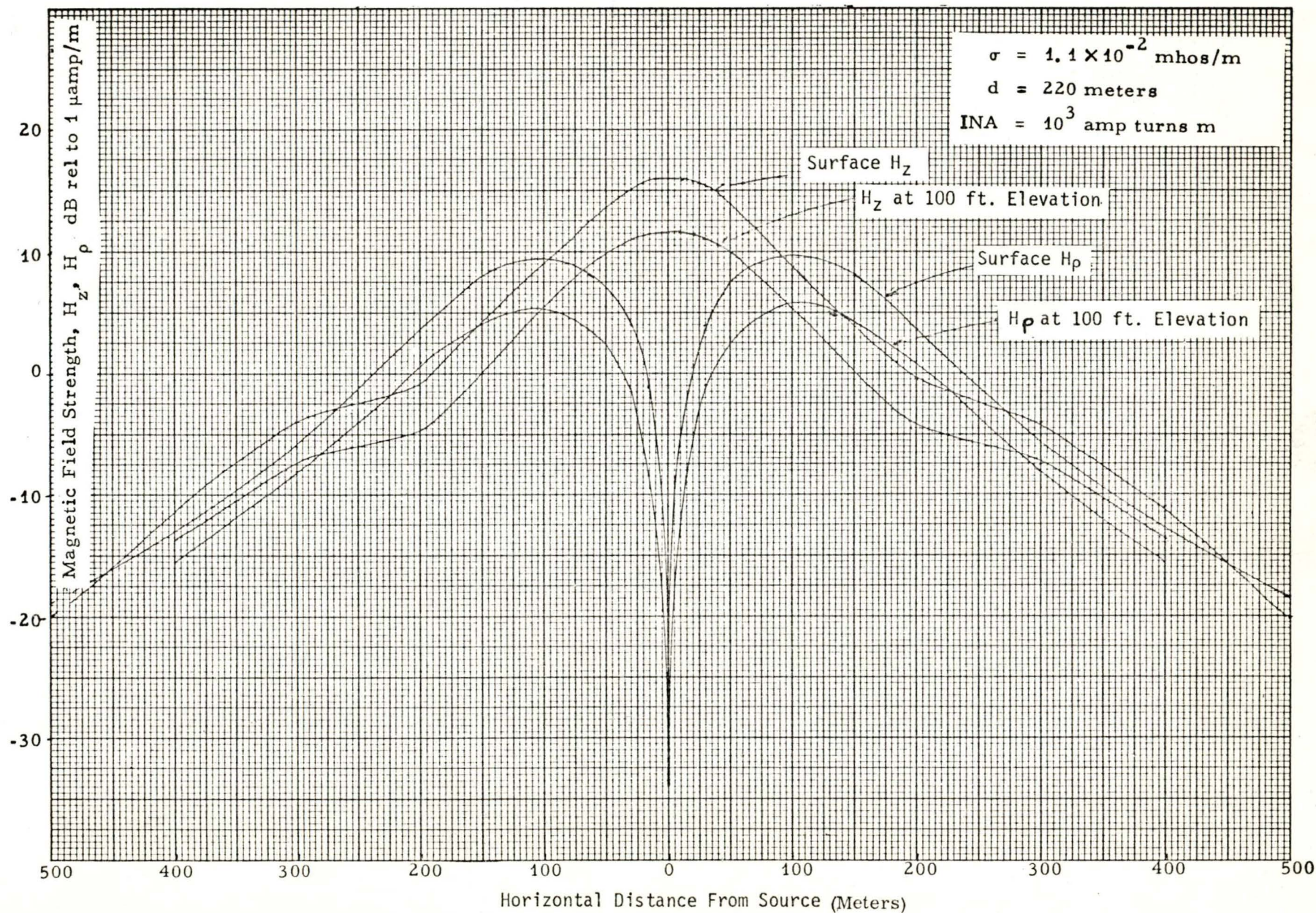


A theoretical profile of the expected fields over the Robena Mine is shown in Figure 5-29. This was computed for a transmitter source depth of 221 meters and elevations of 0 and 100 ft. At this mine, the decrease in field strength at 100 ft is only about 5 dB relative to surface fields.

The first aircraft used in the test was an Enstrom F28A with a 4-cylinder reciprocating engine leased from Keystone Aeronautics, Inc., McConnellsville, Pennsylvania. The initial attempt at receiving the EM signal was made with a wideband air core loop and preamp fastened to the skids of the aircraft and cabled to the C 836A receiver in the aircraft. Background noise levels were observed to increase 60 dB when the engines and the power alternators were fired up, making signal reception impossible. The manpack locator C 842A and the EM Location receiver C 836A with ferrite antennas were also tried with the antennas placed in the plexiglass bubble inside the aircraft. Again, the signals from the subsurface transmitters were readily detectable on both systems provided that the helicopter engines remained off. In actual operation though, high levels of helicopter noise precluded any measurements being made with antennas inside or close to the aircraft. We then determined that signals could be received if the receiving antenna was separated by cable at least 20 ft. from the aircraft on the ground with the aircraft engines fired up. On taking off, however, the signal was lost in the noise since apparently the noise levels produced beneath the aircraft in flight were greater than those experienced with the aircraft on the ground with the receiving antenna located a comparable distance away from it.



Figure 5-29. Theoretical Field Profiles for Airborne Fields Over Robena Mine.





With the ferrite loop tethered 35 feet beneath the aircraft and using the C 836A receiver, signals were marginally detectable in the immediate vicinity of the surface location at an altitude of 100 ft. Some of the background noise was apparently produced by physical motion of the antenna package at the end of the tether since it was observed to quiet down when the aircraft went into a hovering routine. It was concluded that the system performance using the Enstrom F28A helicopter as a vehicle was only marginal at best, and would not have been adequate to detect the transmitting source had its location been completely unknown. Consequently, we made arrangements for the pilot to return in the afternoon with a Bell Jet Ranger 206A with an Allison 250 turbine engine.

The tests run with the Bell Jet Ranger 206A were similar to, but more successful than, those run in the morning with the Enstrom F28A. As before, it was impossible to receive signals with the loops mounted within or close to the aircraft. However, with the ferrite loop tethered 35 ft. beneath the aircraft, it was possible to clearly detect the signal over a lateral radius of approximately 500 ft. from the surface location, and at an altitude of 125 feet. The receiving antenna orientation for these tests was approximately  $45^{\circ}$  from horizontal. Several flights were made through the zone of coverage at a speed of 25 mph and each time the signal became distinctly audible inside the zone of coverage. Later the wideband air core loop and preamp was tethered below the aircraft and it too, produced clearly detectable signals with about the same lateral range as obtained with the ferrite loops. The aircraft was raised to increasingly higher altitudes above the ground with the signal becoming undetectable at an altitude of 250 ft.

One difficulty noted with our variable tuned receiver (C836-A) was that the tuning control tended to vibrate out of tune while the aircraft was in motion. This difficulty would be eliminated using fixed tuned receivers. With the tethered wideband antenna and preamp that was successfully demonstrated in these tests,

it should be possible to build a multichannel receiving system for use inside the aircraft with a multichannel strip chart readout for post flight analysis of receiver records. Such records correlated with real time flight location could greatly facilitate early detection and location of trapped miners.

Operational considerations for helicopter reconnaissance of EM fields at the Robena #4 Mine were developed as follows. The Robena #4 complex covers roughly an area of 4 X 2 miles. If we assume that a miner may be trapped anywhere in this mine and may be transmitting uplink signals on a 2-second pulse interval, the following rules could be followed to provide complete reconnaissance coverage of the mine.

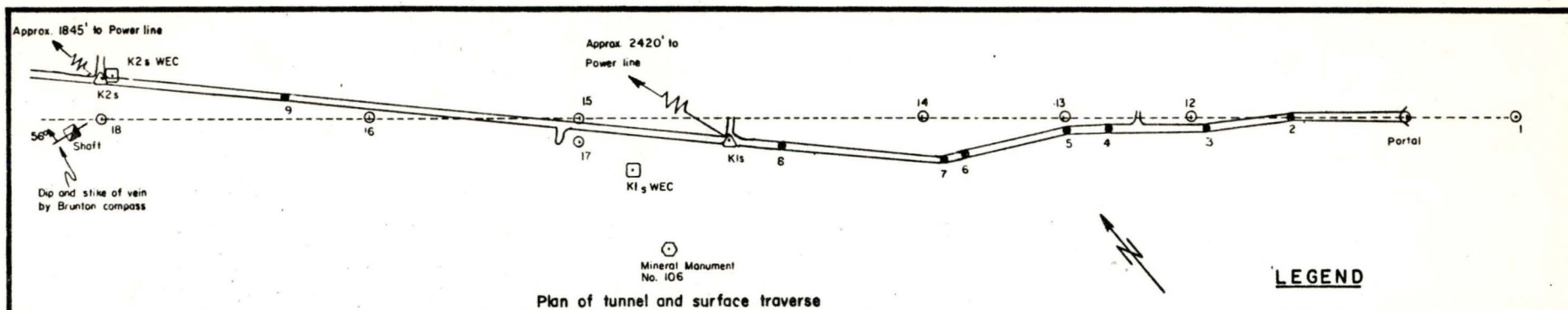
- (a) Each flight line should be 800 feet wide to allow for sufficient overlap of adjacent lanes.
- (b) Ground speed velocity should be no greater than 50 ft/sec (35 mph) so that at least 20 pulses of the signal could be heard before passing out of its zone of coverage.
- (c) For 200,000 line ft. to be flown at 50 ft/sec it would require 4,000 seconds (slightly greater than 1 hour) to scan the entire mine.

## 5.2 Hardrock Mines

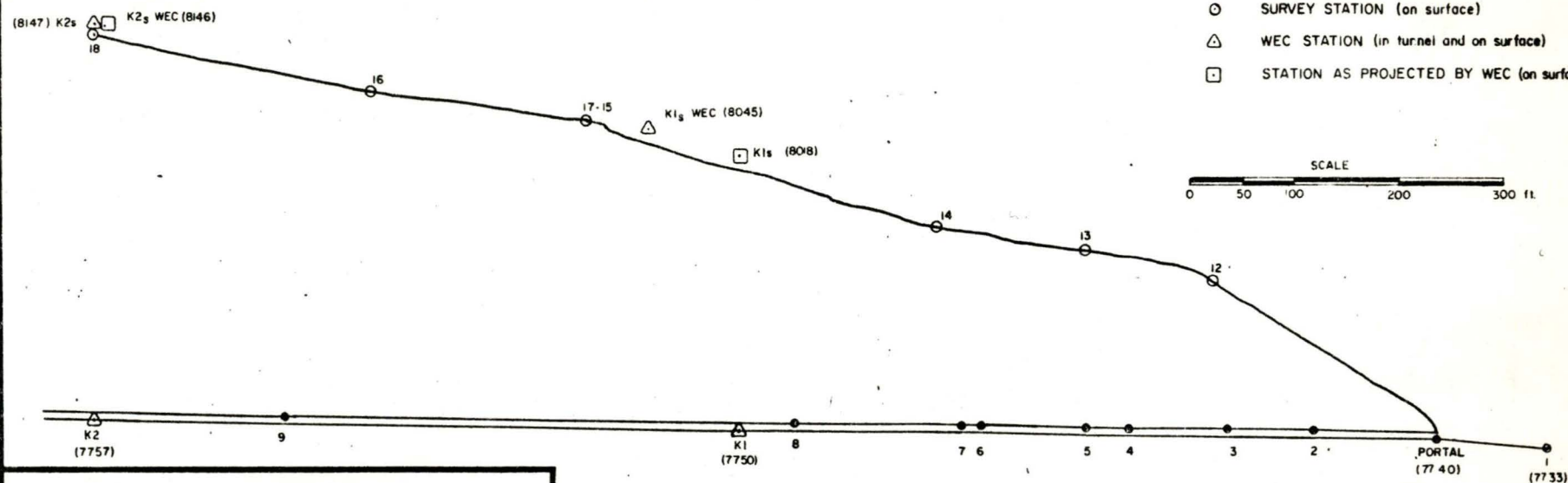
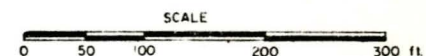
### U. S. Tunnel, Idaho Springs, Colorado

One hardrock mine was visited during the subject test program: the U. S. Tunnel No. 1 at Idaho Springs, Colorado. This mine consists of a single tunnel approximately 1350 ft. long. A survey map of the area and a terrain profile is shown in Figure 5-30. The measurements made at this mine were of a preliminary nature and were intended more to be used as an equipment shake-down before proceeding to the Eastern Coal Mines described in the previous sections of this report. The surface fix at station K25 through 389 feet of





- LEGEND**
- SURVEY STATION (underground)
  - SURVEY STATION (on surface)
  - △ WEC STATION (in tunnel and on surface)
  - STATION AS PROJECTED BY WEC (on surface)



# TRANSIT - TAPE SURVEY

## of the U. S. TUNNEL

Sec 3, T4S, R73W  
CLEAR CREEK CO., COLORADO

for WESTINGHOUSE ELECTRIC CORP.  
(GEORESEARCH LABORATORY)

FIGURE 5-30

K. W. NICKERSON & ASSOCIATES  
712 12th. St.  
Golden, Colorado 80401

Survey by: K. W. Nickerson December, 1972

overburden was obtained using the newly developed Westinghouse receiver Model C 836A and produced a location only 15 ft. away from the surveyed location as obtained by a surveying company (K. W. Nickerson & Associates).

One other surface fix was obtained at a shallower portion of the mine using the Westinghouse miniature field intensity meter as a receiver. This receiver which was built on an earlier program did not have sufficient sensitivity to define a precise null location. As a result, the surface location could not be precisely defined by a sharp null. The location at this point was determined as the center of a fairly wide null area of about 100 ft. diameter. This proved to be about 100 ft. off the actual surveyed location. The field intensity meter was not used for further measurements on this program.

Conductivity measurements were made directly above the tunnel between points K1<sub>s</sub> and K2<sub>s</sub>. The resulting conductivity sounding is shown in Figure 5-31. The average conductivity for this region was  $3.4 \times 10^{-3}$  mhos/m.

The location measurements were made at a point about 1000 feet from the power line running down the road (Colorado Highway 103) and about 1800 feet from a power line crossing the hill to the north. The resulting noise spectra for the vertical magnetic field is shown in Figure 5-32. Noise plots of this nature are primarily useful for evaluating the noise peaks occurring within a given band. The noise floor shown on the plot may be somewhat misleading in that the out of band rejection of the data processor is not as great as a typical narrow band receiver of the same 3 dB bandwidth. Consequently, the noise floor shown on these plots are undoubtedly raised by the contribution of noise peaks occurring outside of the measured bandwidth.



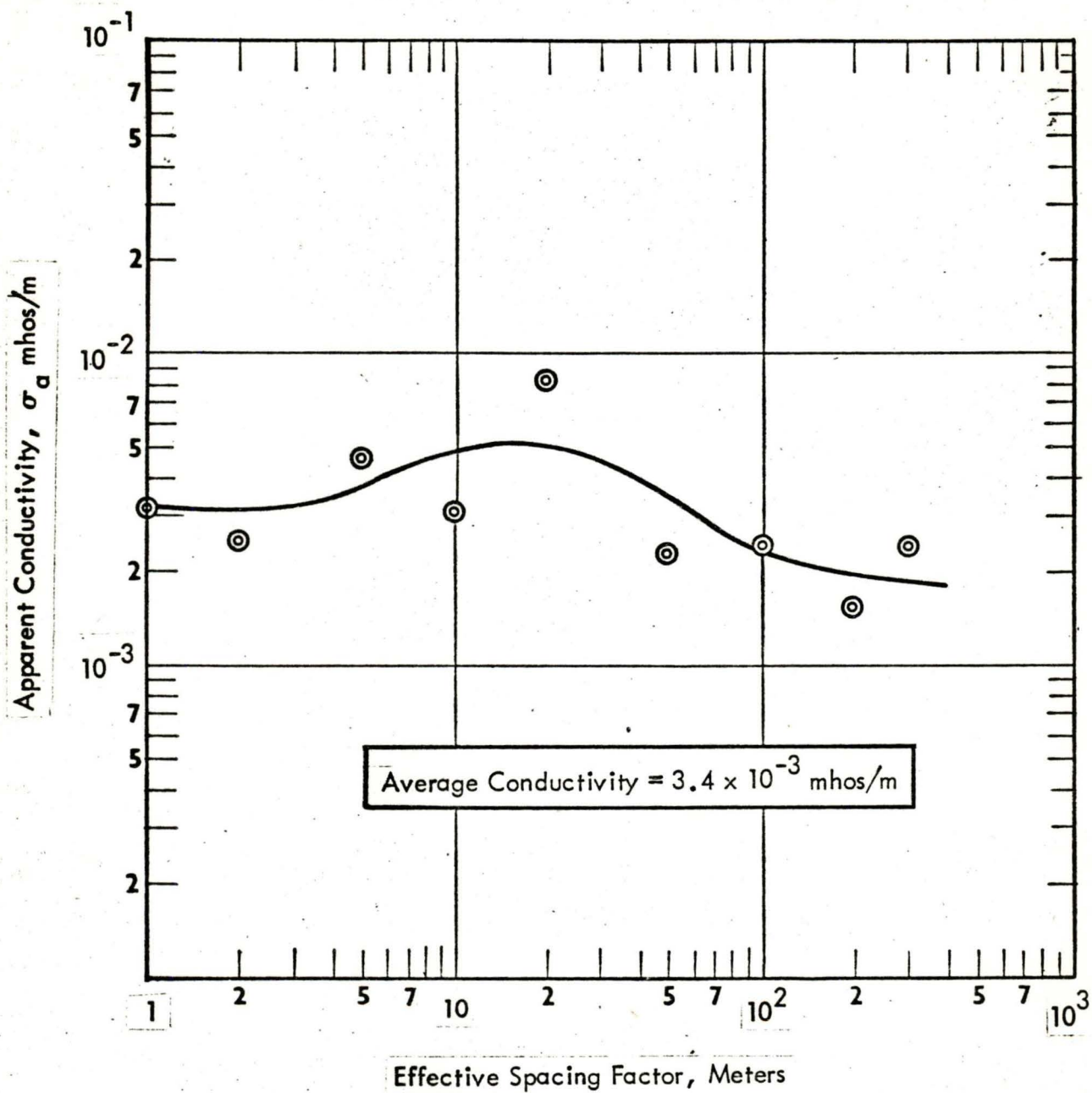
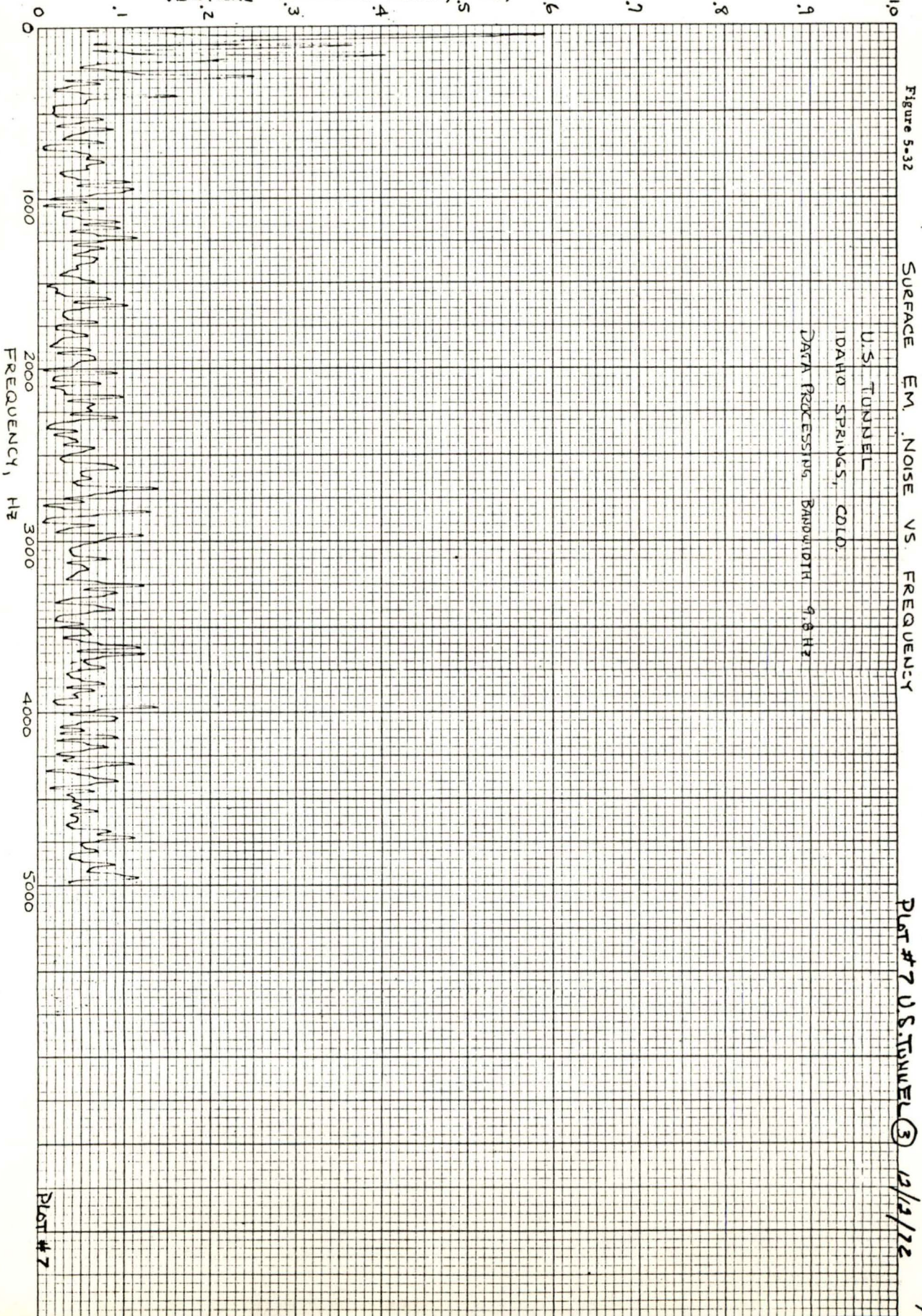


Figure 5-31 Earth Conductivity Sounding, U.S. Tunnel, Idaho Springs, Colorado



K&E 10 X 10 TO THE INCH 47 0780  
10 X 15 INCHES  
KEUFFEL & ESSER CO. MADE IN U.S.A.  
VERTICAL MAGNETIC FIELD,  $\mu$ Hz,  $\text{mG/m}$





## 6.0 MINE LOCATION SYSTEM CHARACTERIZATION

The multiple access trade-off curve (MATC) shown in Figure 6-1 has been developed for evaluating the performance of various configurations of the mine location systems. The curves may be used to determine the location system parameters required to meet a given set of performance conditions. For example, if the mine depth, overburden conductivity and noise environment are known, the curves can be used to determine the antenna size, weight, and battery life as a function of operating frequencies. Inversely, if the system parameters are specified, the curves can determine the operational depths at which signals may be detected as a function of overburden characteristics and noise.

Certain basic assumptions were used to derive these curves. They are:

1. A square loop configuration is employed for the transmit antenna and a coaxially oriented loop antenna is used for reception.
2. The antenna resistance equals the dc wire resistance.
3. The antenna current waveform is an on-off single ended square wave, so the peak current is twice the average current. (Later tests have clearly shown the feasibility of using transformerless push-pull transmitters, See Section 7)
4. Battery life estimates are based on a 20 percent duty cycle.

The use of the curves can be demonstrated by example. A dotted line is shown on the curves to indicate the performance of one system configuration tested at the Robena Mine. The transmitter consisted of a tuning fork oscillator driving a switching transistor in the antenna lead and connected to a 4-volt miner's lamp battery. The switching source resistance,  $R_s$ , was 0.53 ohms. The antenna was 360 feet of #19 copper wire installed as a single turn loop around a pillar of coal in the mine. The results shown on



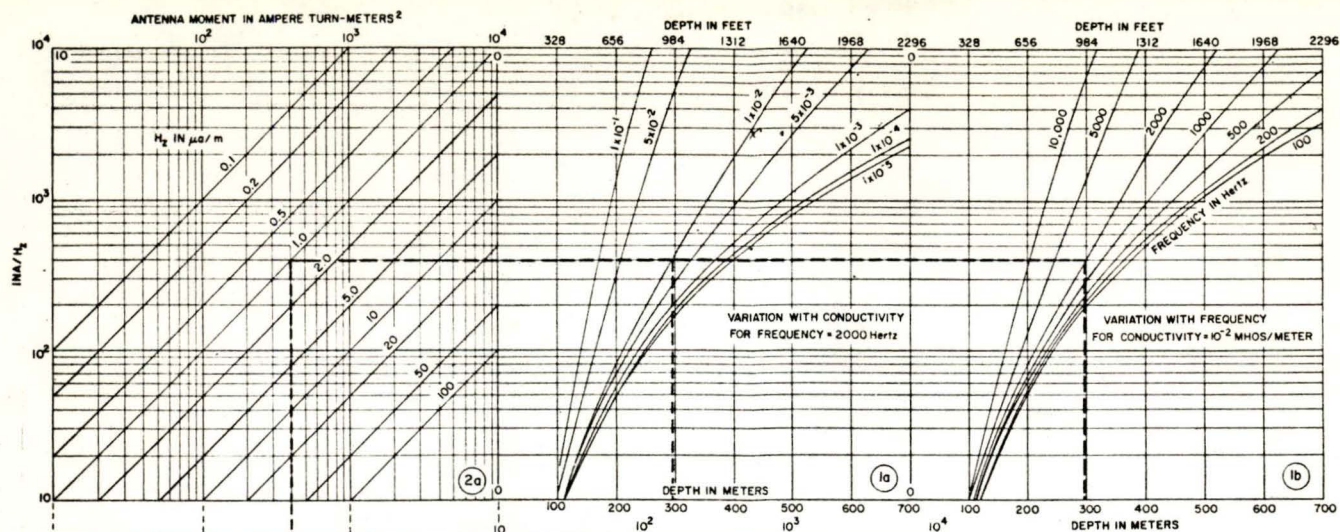
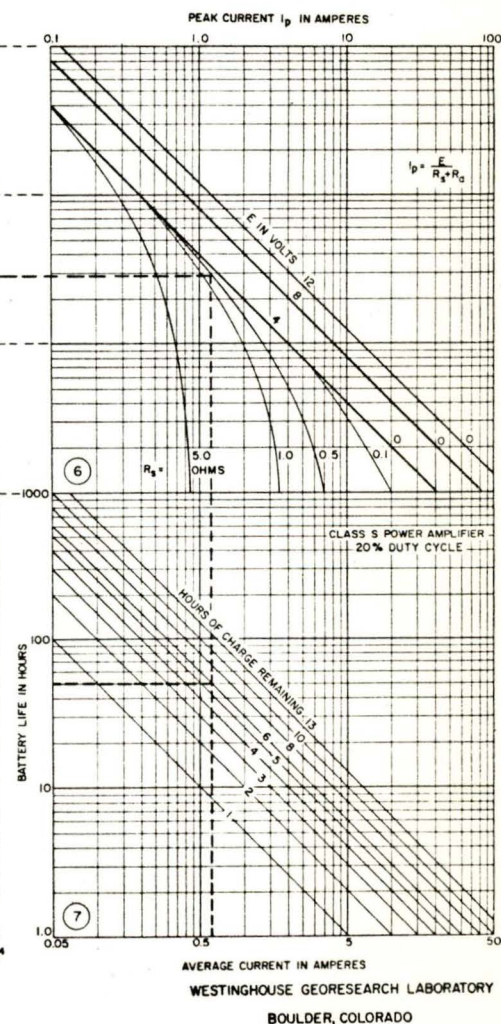
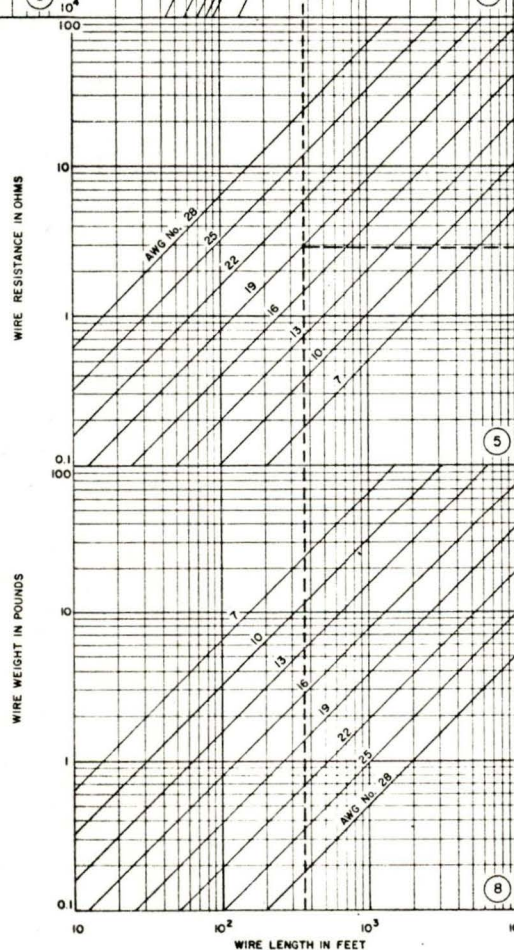
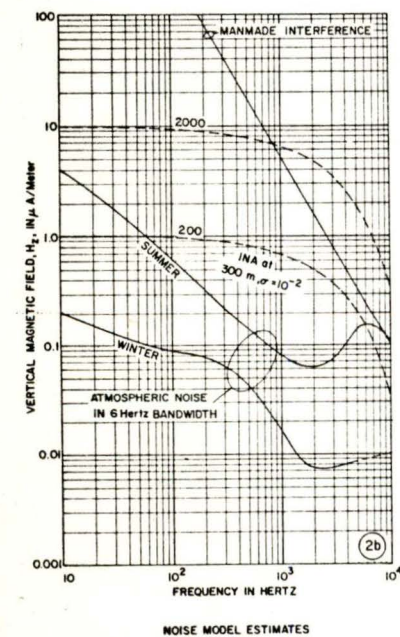
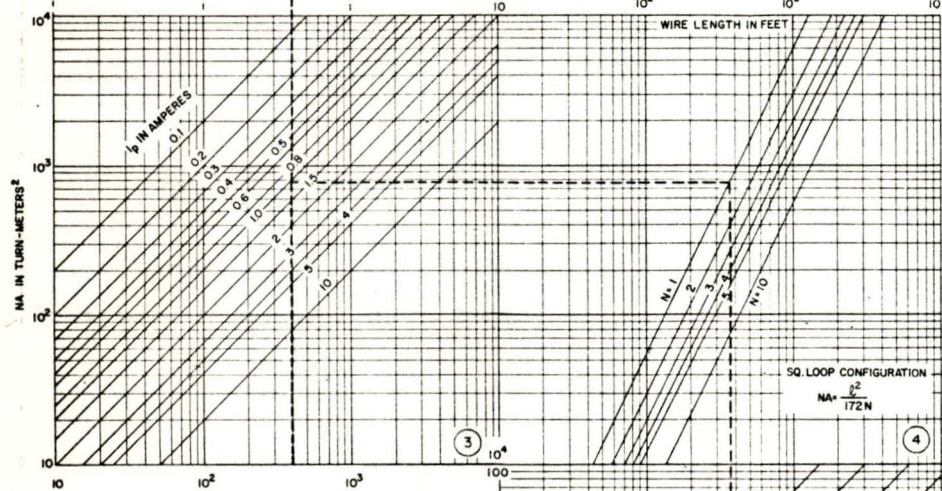


Figure 6-1  
MULTIPLE ACCESS TRADE-OFF CURVES  
FOR  
MINE LOCATION SYSTEM CHARACTERIZATION





the MATC are for 2000 Hz and an overburden effective conductivity of  $10^{-2}$  mhos/meter. The surface receiver consisted of a 15-inch diameter tuned antenna, matching circuitry, 5 Hz bandwidth filter, audio amplifier and ear phones for audible signal detection.

For these system parameters, the MATC yields the following:

Curve 8: Antenna weight = 1.4 lbs.

Curve 5: Antenna resistance = 2.8 ohms.

Curve 6: Peak current = 1.2 amperes.

Curve 7: Battery Life = 50 hours (assuming 6-hour charge remaining)

Curve 4: Area - turns = 750 turn-meters<sup>2</sup>.

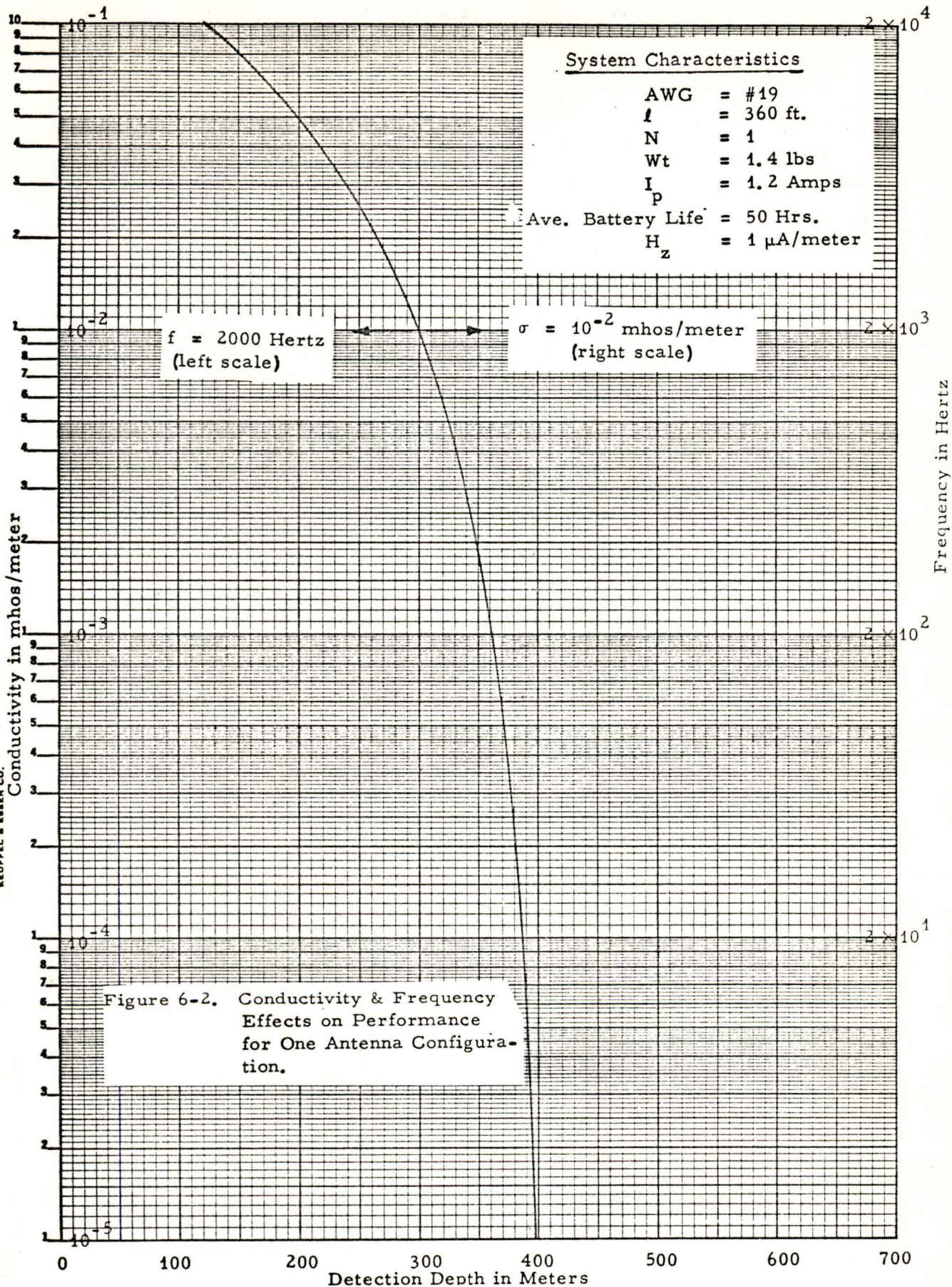
Curve 3: Antenna Moment = 400 ampere-turn-meters<sup>2</sup>.  
(Note: The peak current selected must be identical to value given by Curve 6).

Curve 2a:  $INA/H_z = 400$  amp-turn-meters<sup>2</sup> for a  $1 \mu A$ /meter field. The actual  $H_z$  required depends on the noise and the signal-to-noise ratio required for detection/location purposes.

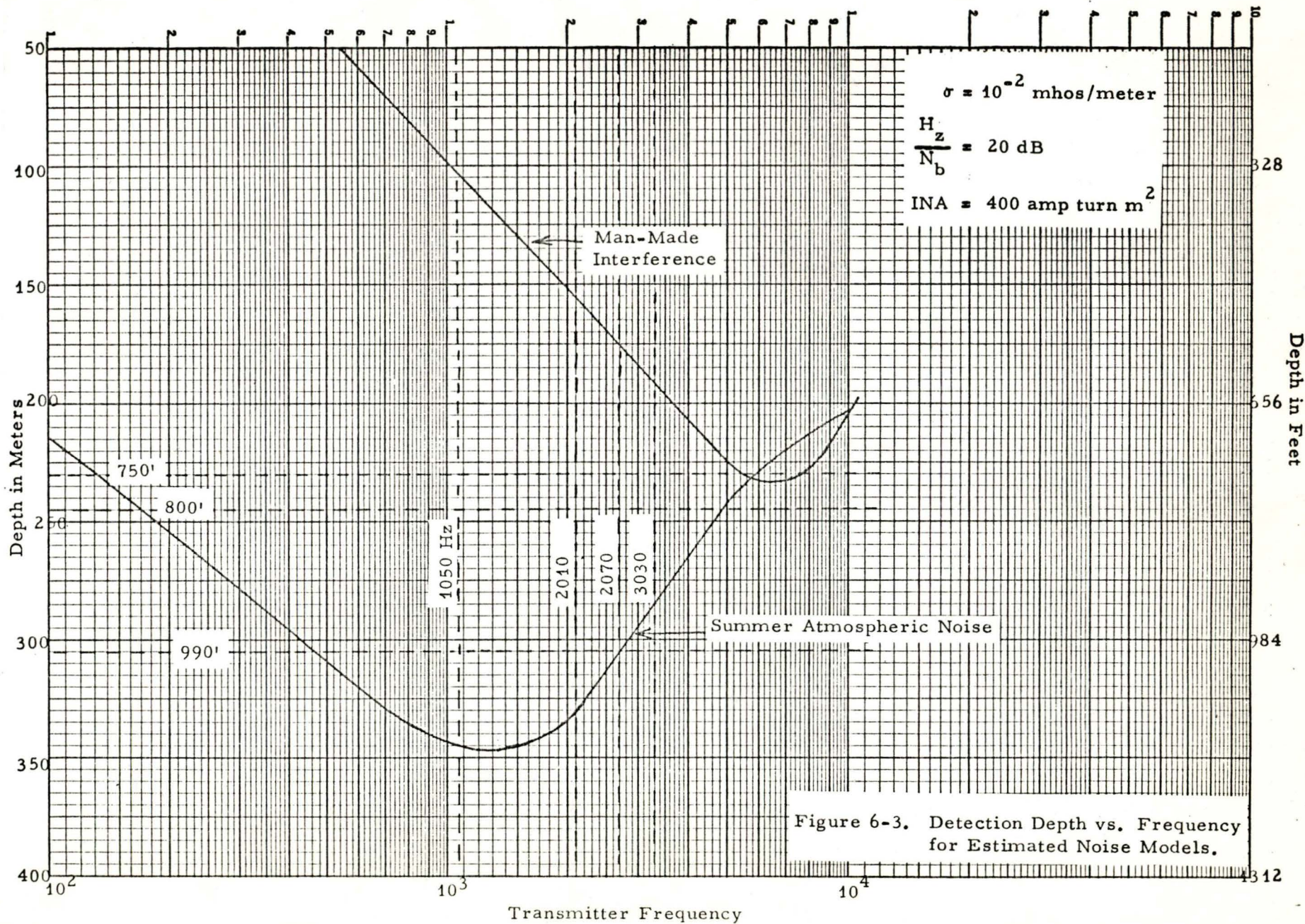
Curve 1a, b: These curves have been used to plot detection depth vs. frequency for a constant conductivity and depth vs. conductivity for a constant frequency in Figure 6-2. Values given assume that a signal level,  $H_z = 1 \mu A$ /meter is required.

Curve 2b: This separate curve may be used to estimate required  $H_z$  based on expected noise environment. Atmospheric noise values shown are for an effective noise bandwidth of 6 Hz. Figure 6-3 shows a plot of depth vs. frequency obtained using these noise models for  $\sigma = 10^{-2}$  mhos/meter and assuming the signal required was 10 times the noise in a 6 Hz bandwidth, i. e., ( $H_z/N_b = 20$  dB). The horizontal and vertical dashed lines indicate the depth and transmission frequencies used at Robena.











The man-made interference shown on Curve 2b is based on some preliminary spectral noise data obtained by NBS at the Mid-continent Mine in Colorado. A 200 ampere arc welding unit was operating 200 feet away. The noise spectrum peaked at 60 Hz and contained several harmonics of 60 Hz which decreased at the higher frequencies. Atmospheric noise levels were obtained from noise models derived from data measured at Boulder, Colorado. These noise models are for the vertical magnetic field which was found to be 5 dB less than the horizontal magnetic field.

The mine location systems which have been field tested were designed to operate at frequencies midway between harmonics of 60 Hz in the 1 to 3 kHz band. With a narrowband receiver ( $< 10$  Hz) the atmospheric noise limitation can only be approached. The two receivers used in the field test program had an effective noise bandwidth of about 6 Hz and 10 Hz.

The signal-to-noise ratios observed with these receivers at Robena indicated the noise was less than  $1 \mu\text{A}/\text{meter}$  at the three different locations where measurements were obtained. At Robena and at two other test mines in West Virginia it was observed that operating frequencies of 2010, 2070, and 3030 Hz yielded higher signal-to-noise ratios than 1050 Hz. This is attributed to the increasing man-made interference at the lower frequency.

The MATC can be used to indicate various trade-offs and to characterize the system. Three other examples are given in Figures 6-4, 6-5, and 6-6.

Figure 6-4 shows the field strength obtained as a function of depth for the three different single turn, square-loop antenna configurations used at Robena. This Figure is for an operating frequency of 2 kHz and  $\sigma = 10^{-2}$  mhos/meter. Signals generated with the 90' antenna were undetectable at 230 meters ( $\approx 750'$ ) because of the noise. The other antennas produced detectable signals at 1000 foot depths.



**K-E** SEMI-LOGARITHMIC 46 5493  
 3 CYCLES X 70 DIVISIONS  
 KEUFFEL & ESSER CO.

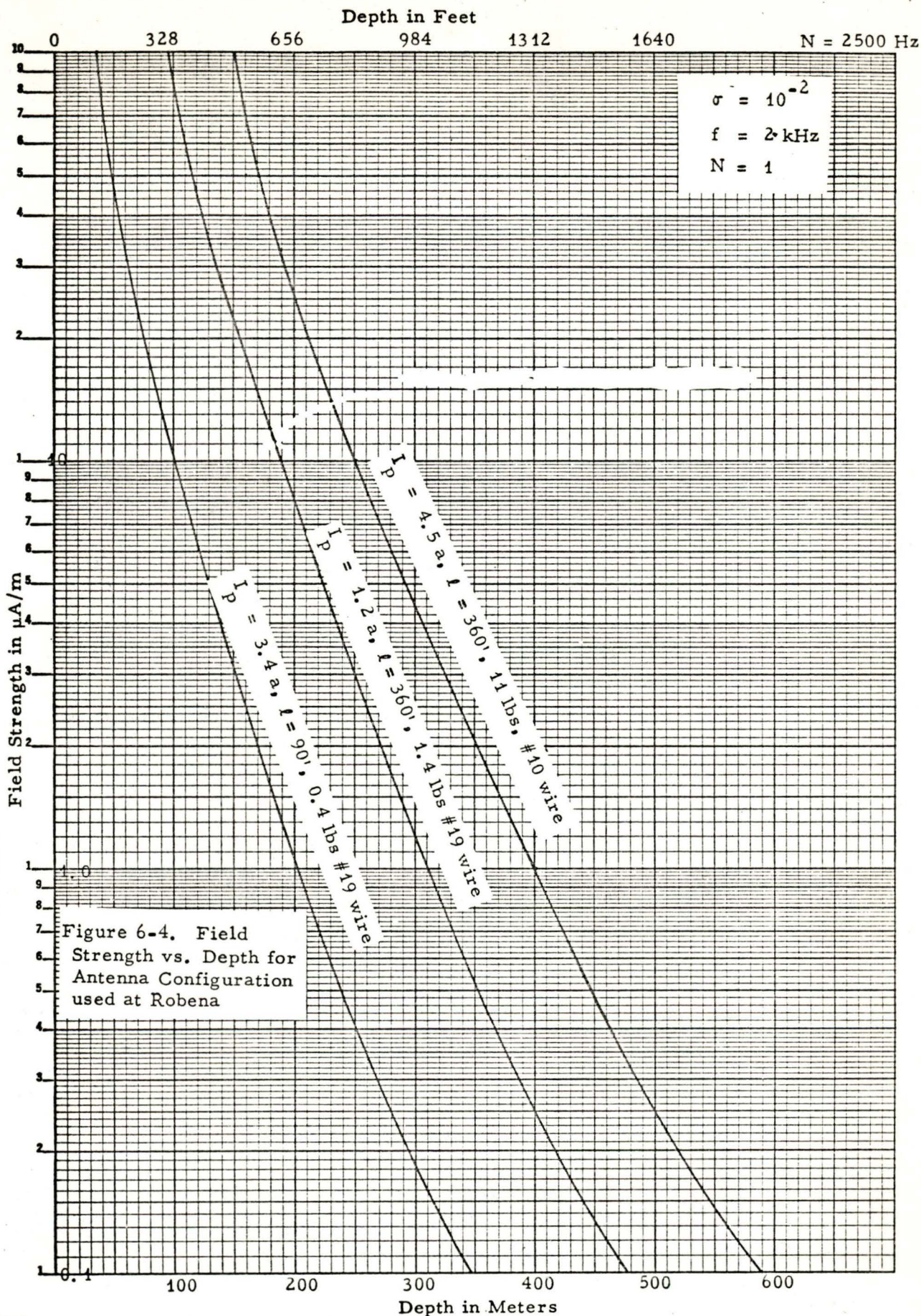




Figure 6-5 compares the performance of different loops, a single turn of #19 wire and two turns of #22 wire in terms of battery life and depth for a  $1 \mu\text{A}/\text{meter}$  field. These results can be obtained using one or more of the antennas fabricated for test. Each antenna packaged contained two #22 wires 90 feet long which could be connected in parallel to yield the equivalent of one #19 wire 90 feet long. Each antenna package could also be connected in series with another to produce a larger moment.

Figure 6-6 indicates the trade-off between antenna weight and battery life for several single turn antenna configurations required to yield a given field strength at a 1000 foot depth and for  $\sigma = 10^{-2}$ . It indicates that a factor of 10 increase in field strength requires that the antenna weight also be increased by a factor of ten for a constant battery life.

It was shown in Figure 6-4 that 360 feet of #19 wire carrying 1.2 amperes of peak current would generate a  $1 \mu\text{A}/\text{meter}$  field on the surface from a depth of 300 meters ( $\approx 1000$  feet) and  $\sigma = 10^{-2}$  mhos/meter at a frequency of 2 kHz. This  $1 \mu\text{A}/\text{meter}$  signal field was detectable at Robena because the noise in the detection bandwidth was sufficiently low.

The system was well within the intrinsically safe limits. In a higher noise environment, however, the signals may not be detectable. It is useful to examine the performance which could be achieved as the intrinsic safety limits are approached.

One method would be to use two miners' lamp batteries in series to provide an 8-volt source. With a 0.5 ohm source impedance, a 10 ampere peak current could be generated in a single turn loop using 360 feet of #9 wire. The MATC shows the field generated for the same condition as before (1000 feet,  $10^{-2}$  mhos/meter, 2 kHz) is now  $10 \mu\text{A}/\text{meter}$ , a 20 dB improvement in field strength. Similar results can be achieved using a 4 volt battery and reducing the source resistance from 0.5 ohms to 0.1 ohms. In either



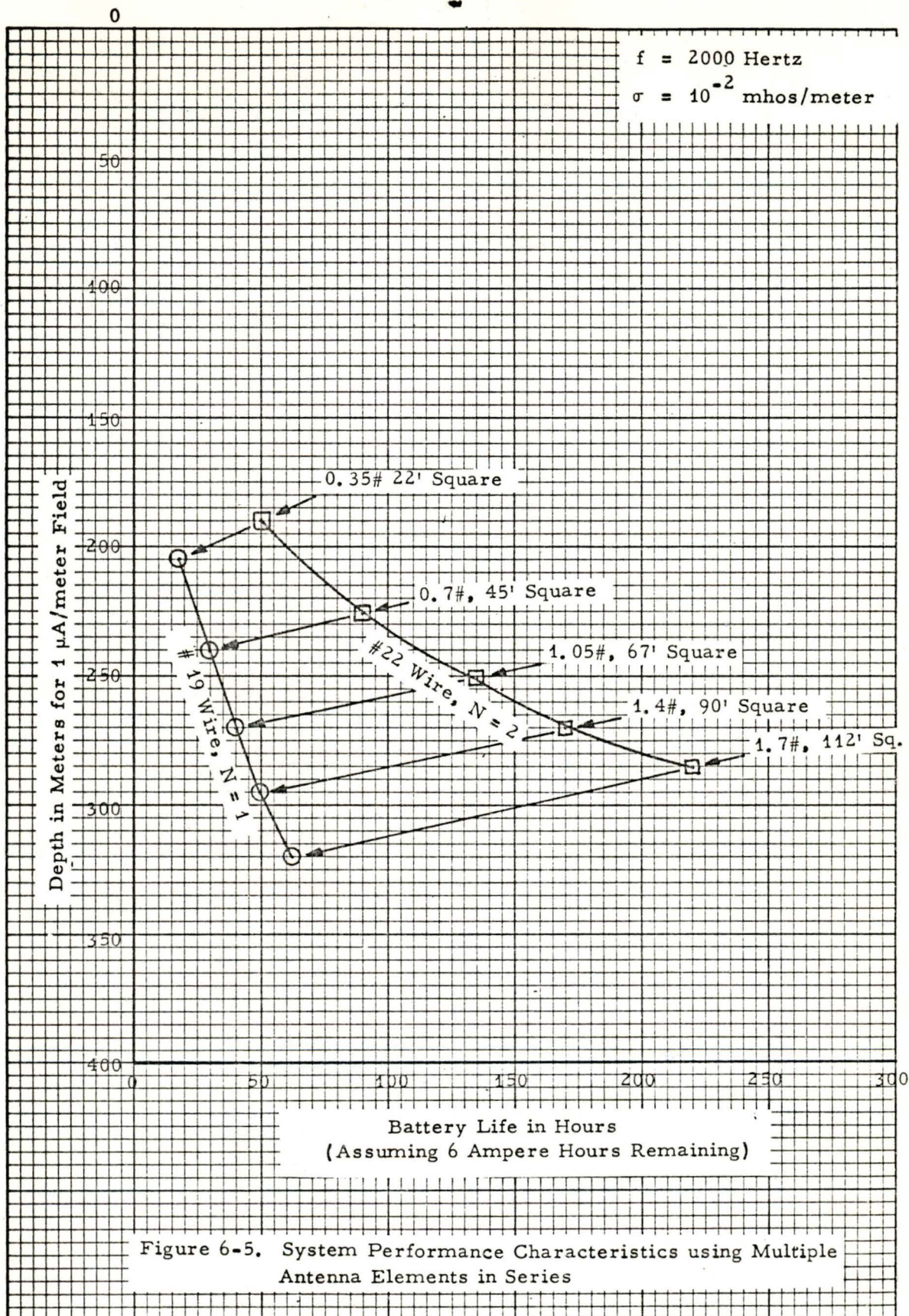
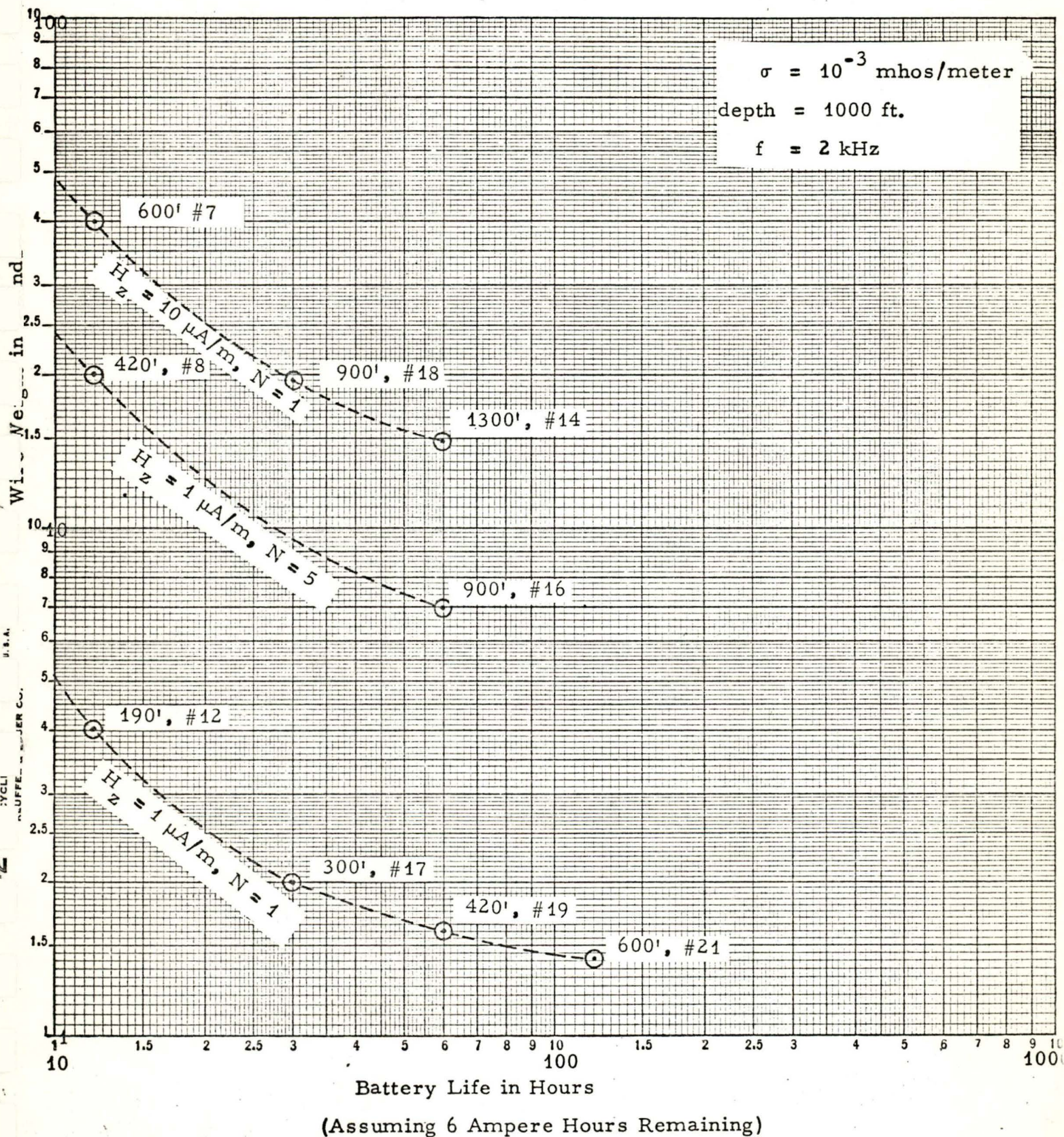




Figure 6-6. Wire Weight vs. Battery Life for Different Antenna Configurations.





case the systems are intrinsically safe; however, the antenna wire weight has increased by a factor of 10 (1.4 pounds to 14 pounds) and the battery life decreased by almost a factor of 10 (50 hours to 6 hours, assuming that on the average a 6 ampere-hour charge remains on the battery).

## 7.0 ALTERNATE LOCATION SYSTEM CONFIGURATION

### Alternate Transmitter Configuration

At the conclusion of the field tests at Robena Mine, it was mutually agreed upon between Westinghouse and Bureau of Mines that further transmitter development would be of more benefit to Bureau of Mines than completion of hardrock mine tests. Consequently the remaining funds were spent on increasing the power and efficiency of the manpack transmitter.

Results of the intrinsic safety tests at BuMines Approval and Testing Lab in Pittsburgh showed that the manpack transmitter in its present configuration was operating well below the limits of intrinsic safety. Moreover, the Robena tests showed that a stronger signal strength on the surface would have greatly facilitated the location process at that mine. Consequently an effort was put forth to make maximum possible use of the miner's battery to maximize transmitter current moment.

### Transmitter Development

The primary transmitter modification resulting from this effort was the incorporation of a full wave switching circuit to replace the existing half-wave circuit. Several methods of driving a full wave switching circuit from a single dc voltage source were considered. Those which required drive transformers or push pull output transformers were discarded in favor of the circuit described below for the following reasons.

1. Transformers impose further restrictions on intrinsic safety.
2. Transformers take up additional space and weight.
3. Transformers contribute to overall power inefficiency.



Figure 7-1 is a simplified diagram of the circuit developed on this program. Switches 1 and 2 are MJE 1090 PNP transistors and switches 3 and 4 are MJE 1100 NPN transistors forming two complementary pairs. The output antenna can be series tuned directly without requiring an output transformer (this was not possible using the existing half wave transmitter since the tuning capacitor quickly became charged in one direction and drove the output transistor to cutoff. The drive for the MJE 1090 PNP transistors is obtained from inverted NPN 2N4400 transistors referenced to B+ instead of ground. These transistors were found to switch as efficiently as the conventionally driven MJE 1100's. Although the addition of the 2nd transistor in the current path doubled the total turned on series impedance of the output circuit, the output current was significantly increased as a result of the 100% duty cycle of the battery. The only thing preventing a doubling of the output current was the fact that the load resistance in this case was quite low (0.35 ohms) and the increased switch impedance significantly limited the current to something less than the double current value.

#### Transmitter Performance

Several different transmitter configurations were tested in the laboratory before arriving at the final configuration labelled No. 5 in Table 7-1. Some of these configurations utilize output transformers connected in a push-pull arrangement while others, including the final circuit, involved direct coupling to the load. The load resistance for each of these tests consisted of 350 ft. of #10 AWG insulated wire deployed outdoors in the form of a horizontal circular single turn loop. The inductance of this loop is approximately 200  $\mu$ H and the dc resistance is roughly 0.35 ohms with an additional 0.1 ohm resistor for current monitoring. Based on the results shown in Table 7-1, the circuit providing the highest level of output power and current moment into a 350 ft #10 wire loop is the full wave solid state switching amplifier employing double MJE 1100 and MJE 1090 Darlington transistors as the switching elements.

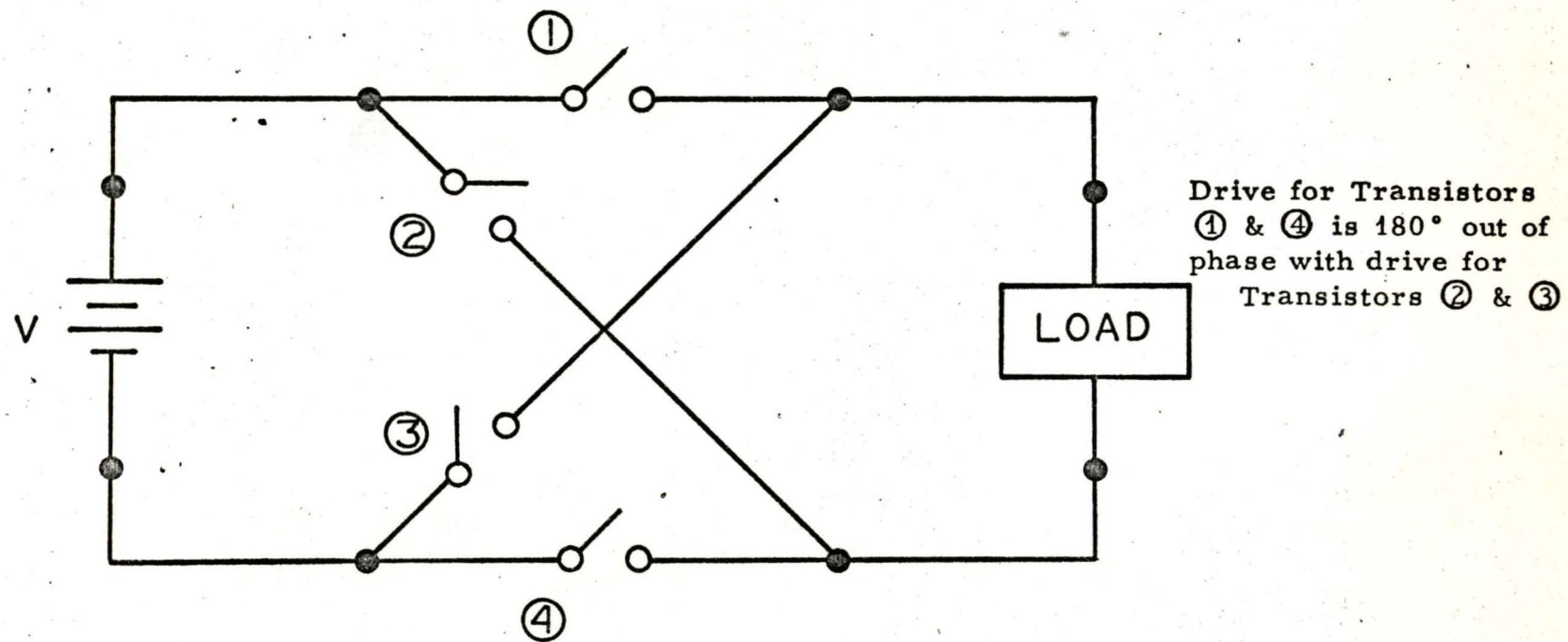


Figure 7-1. Full Wave Switching Arrangement.



TABLE 7-1

Performance of Several 2500 Hz Solid State Switching Amplifiers  
into Inductive Load of 200  $\mu$ H, 0.45 $\Omega$

<u>Circuit</u>	$V_{dc}$ volts	$I_{dc}$ amps	Power In watts	$I_{out}$ amps	$R_L$ ohms	Power Out watts	Efficiency %
1. Full Wave Bridge Series Tuned Single Power Transistors	4	1.6	6.4	2	.45	1.76	27.5
2. Full Wave Bridge Parallel Tuned Single Power Transistors	4	1.2	4.8	1.65	.45	1.19	24.9
3. Push Pull Bridge Series Tuned Transformer Coupled	4	2.4	9.6	2.5	.45	2.75	28.6
4. Push Pull Bridge Parallel Tuned Transformer Coupled	4	1.4	5.6	1.6	.45	1.12	20.1
5. Full Wave Bridge Series Tuned Double Power Transistors	4	2.5	10.0	2.95	.45	3.82	38.2

With a 4 volt dc supply such as the miners lamp battery, the rms current measured into a tuned inductive load of 200  $\mu$ henries and 0.45 ohms is about 3 amperes. Figure 7-2 shows the boundary line for intrinsically safe conditions for resistive loads as a function of current and voltage [ 5 ]. This figure shows that a 4 volt system delivering 3 amperes to a resistive load is well within the limits of intrinsic safety. This system is currently planned for an intrinsic safety test at the Approval and Testing Department, U.S. Bureau of Mines, Pittsburgh, Pennsylvania sometime late in March 1973. Prior to this test, a laboratory exercise was conducted to determine the switching amplifiers capability of handling power levels at increased supply voltages which would exceed intrinsically safe conditions.

Table 7-2 gives the results of this exercise. The data points obtained for a resistive load of 0.4 ohms are also plotted on Figure 7-2 and show the system to become unsafe at a supply voltage of 9 volts. (For inductive loads, tuning is required and intrinsic safety limits change depending on the frequency of operation and the AC voltage drop across the tuning elements.) Table 7-2 also shows that the total path resistance including the switches, the power supply source resistance and the 0.4 ohm load is exactly 1 ohm at 4 volts but decreases as power supply voltage increases. This is due to the improved efficiency (lower turn on resistance) of the switches with higher collector voltages. At a supply voltage of 12 volts, the equivalent switch resistance is 0.2 ohms while at 4 volts the resistance is 0.3 ohms.

These tests demonstrate the feasibility of increasing the current moment of the existing manpack location transmitter by doubling the solid state switches to provide a full wave switching configuration. Further increases in moment can be obtained by increasing the source voltage of the transmitter.

#### Alternate Receiver Configuration

The manpack locator Model C842A was modified slightly to provide additional bandpass filtering in the operational amplifier stages. The existing circuit provides for bandpass filtering in 2 places; (1) capacitive tuning at the loop antenna terminals, and (2) tuning fork filter. Additional selectivity in



TABLE 7-2

## Performance of 2500 Hz Switching Amplifier

Supply Voltage (Volts)	0.9 Ohm Resistive Load			0.4 Ohm Resistive Load			
	Power Supply Current	Load Voltage (P-P)	Load Current (P-P)	Power Supply Current	Load Voltage (P-P)	Load Current (P-P)	Load Current (RMS)
4	2.2A	4 V	4.45A	3.45A	3.2V	8 A	4 A
5	3.0A	5.6V	6.23A	5.0 A	4.3V	10.74A	5.37A
6	3.9A	7 V	7.78A	6.3A	5.4V	13.5 A	6.75A
7	4.8A	8.4 V	9.34A	6.7 A	6.6V	16.5A	8.25A
8	5.8A	10.4 V	11.58A	9.2A	8.0V	20 A	10 A
9	6.75A	12.2V	13.56A	10 A	8.7V	21.76A	10.85A
10	7.75A	14 V	15.58A	11.95A	10.4V	26 A	13 A
11	8.5 A	15.3V	17.0 A	13.2 A	11.4V	28.4 A	14.2 A
12	9.4A	16.7V	18.57A	14.8 A	12.2V	30.5 A	15.25A

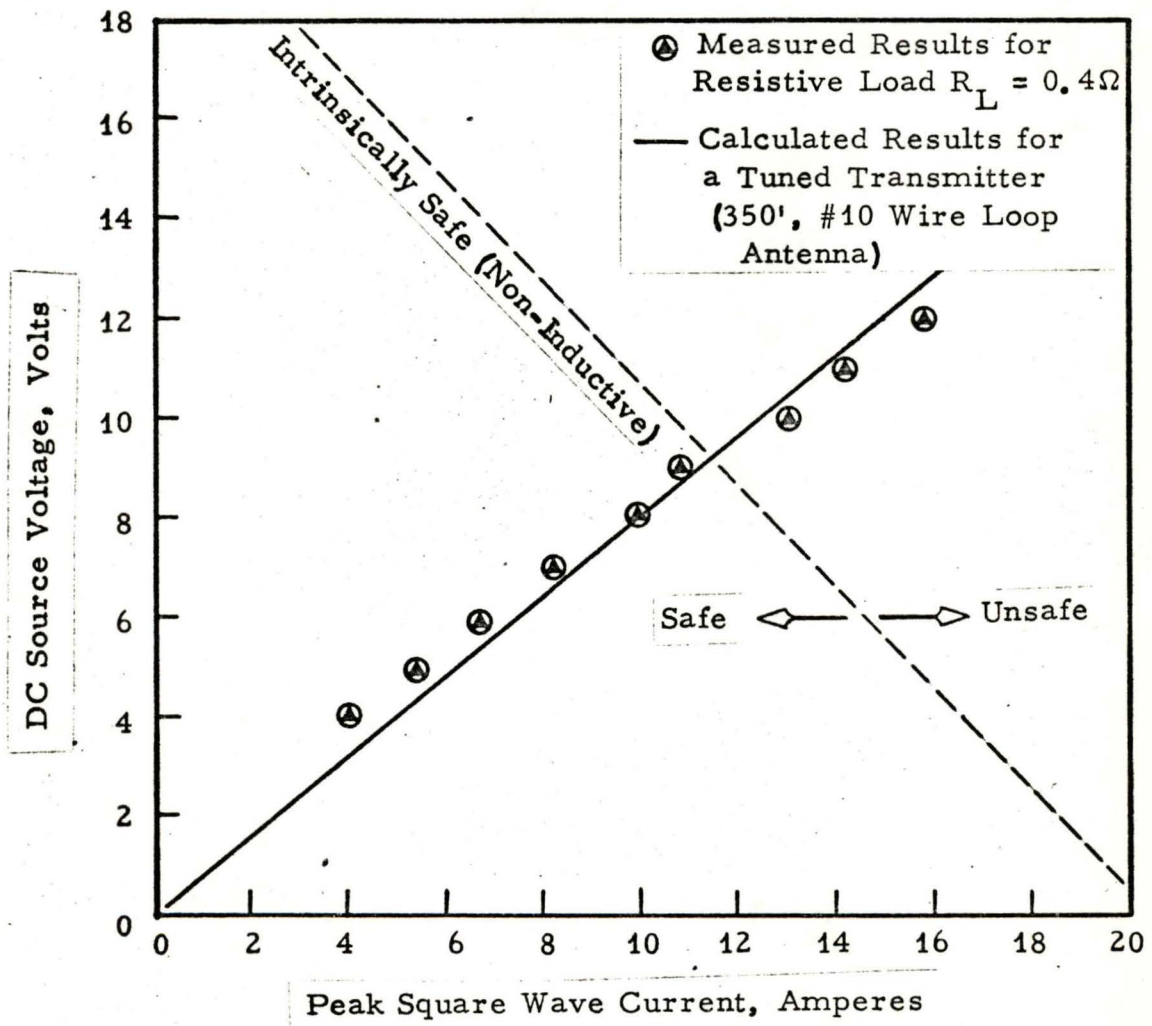


Figure 7-2. Current vs. Supply Voltage for a Full Wave Switching Amplifier into a 0.4 Ohm Resistive Load



the existing receiver circuit is provided by highpass filtering in the front end and lowpass filtering in the final stages of amplification. Although this receiver performed satisfactorily in the field, a steady background hiss was noticeable in the headphones at all times. This annoying hiss has been eliminated by replacing each of the highpass and lowpass amplifiers by bandpass amplifiers tuned to the operating frequency. The modified system now contains four bandpass amplifiers with a  $Q$  of 10 each, one tuning fork filter and a tuned loop antenna. The three dB bandwidth of the receiver remains virtually unchanged due to the controlling influence of the tuning fork filter; however, with the additional bandpass filtering, the roll-off characteristics are much sharper and the out of band rejection is greater than previously obtained with the existing circuit.

## 8.0 IMPROVED LOCATION SYSTEM SPECIFICATIONS

The following is a list of optimized system specifications based on current knowledge of mining parameters and rescue system priorities.

### Transmitter

Power Source -	Miners Lamp Battery (4 volts) or external 6 volt supply
Current Output -	4 amperes rms at 4 volts 6.3 amperes rms at 6 volts
Frequency Range -	One selected frequency between 300 Hz and 3000 Hz. (At least 20 Hz removed from the nearest 60 Hz harmonic).
Frequency Stability -	$\pm 2$ Hz for $-20^{\circ}\text{C}$ to $+60^{\circ}\text{C}$
Amplifier -	Full wave solid state switching amplifier.
Antenna -	Approximately 350 ft of #10 wire formed in a circular loop.
Transmitter Duty Cycle -	10% (200 milliseconds on, 2 seconds off).
Battery Life -	50 hrs on 4 volt miners battery 20 hrs on 6 volt gel cell (20 amp/hrs).
Packaging -	$4 \times 2 \times 1\frac{1}{2}$ chassis
Weight -	$\frac{1}{2}$ pound (excluding antenna and battery)

### Receiver (Surface Manpack Locator)

Full Scale Sensitivity -	1 volt rms output for $1 \mu\text{A/m}$ field.
Frequency -	One selected frequency between 300 Hz and 3000 Hz (at least 20 Hz removed from the nearest 60 Hz harmonic).
Temperature Range -	$-20^{\circ}\text{C}$ to $+60^{\circ}\text{C}$
Temperature Coefficient -	$\pm 35$ ppm/ $^{\circ}\text{C}$



### Receiver (continued)

Bandwidth -	0.2% of operating frequency
Selectivity -	Four bandpass amplifiers ( $Q = 10$ ), Tuning Fork Filter and Antenna Tuning.
Output -	Crystal Headphones
Size -	3 5/8" $\times$ 4 5/8" $\times$ 2"
Weight -	2 1/4 pounds
Battery -	Two 6 volt gel cells (40 hrs. between charge)
Antenna -	500 turn 15" diameter shielded air core loop or 1" diameter ferrite loop stick with reduced sensitivity

### Receiver (Multichannel Helicopter Receiver)

Full Scale Sensitivity -	1 volt rms output for 1 $\mu$ A/m field
Frequency -	Up to 6 selected frequencies between 300 Hz and 3000 Hz (at least 20 Hz removed from the nearest 60 Hz harmonic)
Temperature Range -	-20° C to +60° C
Temperature Coefficient -	$\pm$ 35 ppm/° C
Bandwidth -	0.2% of the operating frequency for each channel.
Selectivity -	Each channel - Four bandpass amplifiers ( $Q \approx 10$ ), Tuning Fork Filter and Antenna Tuning.
Output -	Headphones Flashing Light Indicators Oscillographic Recorder (Optional)
Size -	3 3/4" $\times$ 19" $\times$ 10"
Battery -	Six 6 volt gel cells (20 hrs between charge)
Antenna -	Transformer coupled wideband air core loop and preamp - with flat response from 1000 Hz to 3000 Hz. 500 turns, 24" $\times$ 24" shielded loop.

## 9.0

## CONCLUSIONS AND RECOMMENDATIONS

The following conclusions are drawn from the results presented in this report:

1. In order to penetrate a 1000 ft  $10^{-2}$  mhos/meter mine with practical EM rescue signals in a typical noise environment, it is necessary to have a current moment in the mine of at least 1000 amp turns  $m^2$ . This current moment could not be obtained with the original 90 ft ribbon antenna cable but later was obtained with a 350 ft length of #10 wire deployed around a coal pillar as a single turn loop antenna.
2. The 90 ft manpack transmitting antenna provided sufficient signals at all of the mines visited with the exception of Robena where the overburden depth was 1000 ft. Consequently, it can be estimated that for mines 500 ft or less and with conductivities  $10^{-2}$  or less, the existing system is sufficient for mine rescue EM detection in typical EM noise environments.
3. At the mines visited, signals transmitted near 2 to 3 kHz were more readily detected than those near 1 kHz. This is due mainly to the sharp decrease in both man-made noise and atmospheric noise between 2 to 3 kHz.
4. For most of the location tests described herein, the position detected by EM methods proved accurate within about 20 ft prior to applying hill slope corrections. In irregular terrain, the hill slope model loses some of its validity and the corrections made on this data tended to overcorrect the data resulting in no significant improvement and in some cases degradation in position accuracy.



5. Close proximity of two or more manpack transmitters (within 35 ft) operating at different frequencies does not alter the position determined for each transmitter independently. This demonstrates the feasibility of a multifrequency rescue network with many transmitters assigned to different mine personnel employed in the same mine.
6. Helicopter reconnaissance of coal mines for EM rescue signals is feasible provided that the receiving antenna be lowered from the craft to avoid the high electrical noise levels generated by the helicopter engines and power circuits. This usually requires about 30 to 35 feet of tethering cable. Jet turbo prop helicopters produce less electrical noise than do the reciprocating gas engine helicopters, and are more suitable for reconnaissance of low frequency EM signals over a mine.
7. Battery life for a manpack transmitter can be greatly extended by using intermittent CW transmissions operating at a 10-20% duty cycle. Null detection is not noticeably degraded for on-off times of 200 ms and 2 seconds respectively. Furthermore the periodic tone burst characteristic of the interrupted transmission makes it easier to identify on the surface and eliminates confusion with powerline interference.
8. Multiple access trade-off curves can be derived for a given transmitter with known characteristics. These curves are useful in determining what type of antenna would be required to give adequate signal penetration through a given mine overburden or conversely whether a given antenna configuration would perform satisfactorily over a given range of mine conditions.

More theoretical analysis of field anomalies should be undertaken so that the field party may be aware of errors that may exist due to these anomalies. For practical EM location work, these anomalies consist primarily of (1) terrain irregularities, and (2) surface conductors such as pipelines, power and phone lines and other metal objects near the surface. So far a theoretical model has been developed to account for anomalies due to sloping terrain with a continuous slope extending down to the mine level. Results have shown that this model is not valid for the deeper mines where the local slopes on the surface extend to only a fraction of the total overburden depth. More theoretical investigation is needed on such features as valleys (i. e. two opposing slopes intersecting along a line). Also more theoretical work is needed to determine the scattering effects of long metallic objects near the receiving location. This type of work will not necessarily delay the construction and implementation of useful hardware but will merely provide information that could significantly enhance the interpretation of results obtained with such hardware.

Finally, it should be determined that the EM location transmitters can be safely operated in the presence of permissible explosives as they might be arrayed in normal mining operations. Preliminary investigations by Westinghouse on Contract #H0101262 [1] indicate that this will be possible, but total assurance should be made.



9. An improvement in transmitter current moment can be obtained from a given battery source by using a full wave push pull switching amplifier and tuning the antenna. Test results show that 4 amps rms could be delivered to a 0.4 ohm resistivity load from a single 4 volt miners battery using the full wave amplifier. Some power is lost in the additional bank of switching transistors required for full wave operation. However, an overall increase in rms output current from 1.5 amps to 3.8 amps into a 350 ft. #10 wire loop was realized by adding the full wave switching capability.
10. The test results contained herein are in agreement\* with the theoretical work done by Dr. J. M. Wait who has been briefed several times on program progress.

#### Recommendation and Equipment Comparison

The results of these tests continue to show the feasibility of a practical EM Trapped Miner Location System. Follow-on efforts should be oriented towards developing and producing usable hardware that will be acceptable by the mining industry and will effectively accomplish the task of trapped miner location. The results of this study continue to show that no one system can be optimized for all mining conditions. Consequently, in the hardware development and production phase of these systems, it is recommended that two or possibly three classes of systems be identified so that some degree of freedom can be offered to the customer in selecting the optimum portability/power combination most suitable for his particular mine.

More testing should be performed using a helicopter to fully evaluate multichannel receiver concepts for quick reconnaissance surveys over a mine. A multichannel receiver should be developed and fabricated for these tests. Along with the recommended helicopter tests, further testing is needed with the portable EM location receivers to build up a performance data bank for a greater variety of mine conditions. At each mine, there should be one or more simulated mine rescue exercises where the surface field party has no prior knowledge of the whereabouts of the subsurface transmitters.

---

\* Private communication - C. Sturgill and Dr. J. M. Wait on 9/12/73.

In the three tables below a comparison summary is presented which includes the three basic EM location systems (Pulse, Half Wave CW and Full Wave CW) with different antennas and two conditions of conductivity ( $10^{-2}$  mho/meter and  $10^{-3}$  mho/meter). Maximum off-set ranges for different mine depths are also shown. An attempt to extrapolate the maximum range values to the case of helicopter deployment of the receiver was unsuccessful due to lack of noise signature information on helicopters. The most that can be said for such a deployment at the present time is that operation to at least 250 feet is possible, with some selectivity in helicopter configuration.

The effect of reducing the conductivity from  $10^{-2}$  mhos/meter to  $10^{-3}$  mhos/meter will increase the depths at which all systems in the Maximum Range Performance table will operate. The resultant change can be estimated from a consideration of the expression for the magnitude of the  $H_z$  component of the magnetic field, i.e.,

$$H_z = \frac{INA |G|}{2\pi Z^3} \quad (\text{Reference Figure 2-1, page 4})$$

The horizontal axis of the reference figure (figure 2-1) is scaled in units of  $(Z/\delta)$ , where the skin depth varies as a function of frequency, and conductivity. A decrease in conductivity results in an increase in  $\delta$ , which in turn reduces the quantity  $(Z/\delta)$ . This has the effect of increasing the value of  $|G|$ , and hence, the level of the signal  $H_z$ . At 2000 Hertz and  $10^{-2}$  mhos/meter,  $\delta = 110$  meters, approximately. At the same frequency and  $10^{-3}$  mhos/meter,  $\delta = 330$  meters, approximately. Corresponding values for  $\delta$  at 500 Hertz are 220 meters and 700 meters approximately. At depths of 1500 feet or less i.e.,  $Z/\delta < 5$ , which are of interest here, an increase in the value of  $\delta$  by a factor of three will result in a factor of



## LOCATION SYSTEM COMPARISON

System Design Feature	Pulse 100 Ft. Antenna	CW				Comments
		Half Wave 90 Ft. Antenna	Half Wave 360 Ft. Antenna	Full Wave 90 Ft. Antenna	Full Wave 360 Ft. Antenna	
Operating Frequency	500 Hz.	2000 Hz.	2000 Hz.	2000 Hz.	2000 Hz.	CW system capable of other operating frequencies
Transmitter Weight (Including Antenna)	2.0 lbs.	1.5 lbs.	13.0 lbs.	2.0 lbs.	13.0 lbs.	Transmitter weight small compared to antenna weight
Receiver Weight	15.5 lbs.	24 lbs. or 2.25 lbs.	24 lbs. or 2.25 lbs.	24 lbs. or 2.25 lbs.	24 lbs. or 2.25 lbs.	Two receivers built for CW system
System Weight	17.5 lbs.	25.5 lbs. or 3.75 lbs.	37 lbs. or 15.25 lbs.	26 lbs. or 4.25 lbs.	37 lbs. or 15.25 lbs.	Heavy Receiver handles multiple frequencies
Transmitter Battery	4 Volts	4 Volts	4 Volts	4 Volts	4 Volts	Miner's Lamp battery
Receiver Battery	NiCad (24 cells @ 1.2V Rechargeable	12V Rechargeable	12V Rechargeable	12V Rechargeable	12V Rechargeable	Commercially available
Intrinsically Safe (Transmitter)	Yes	Yes	Yes	Yes	Yes	Documented by tests
Intrinsically Safe (Receiver)	No	No	No	No	No	Equipment not actually tested
Battery Life: a. Transmitter	33 Hrs.	8.8 Hrs.	8.8 Hrs.	24 Hrs.	24 Hrs.	Fully Charged batteries assumed 40 hours applies to small version
b. Receiver	10 Hrs.	10 Hrs.	40 Hrs.	40 Hrs.	40 Hrs.	

MUN IGE FOR E  
[OFF-SET DISTANCE VS MINE DEPTH (FT)]

System Mine Depth	Pulse 100 Ft. Antenna	CW				Comments
		Half Wave 90 Ft. Antenna	Half Wave 360 Ft. Antenna	Full Wave 90 Ft. Antenna	Full Wave 360 Ft. Antenna	
400	1550	500	1620	1350	1700	Assumptions: $\sigma = 10^{-2}$ mho/m Rcvr Sensitiv $.1\mu$ Amp/me Noise: Summer Atmospheric Only S/N = 10 dB f reliable detection
700	1450	Inoperative	1500	1210	1610	
1000	1230	Inoperative	1350	310	1425	
1500	550	Inoperative	730	Inoperative	900	

110

NOTE: The presence of local man-made electrical noise will reduce above off-set distances.

In the case of the pulse system, for example, and a local noise level of 10 dB relative to  $1\mu$  amp/meter, with a mine depth of 460 feet, the maximum off-set would be 1200 feet, approximately.



approximately ten increase in the value of  $|G|$ . This analysis also points out the advantage of utilizing the lower frequencies, provided all other factors in comparing two different frequencies are equal.

The above increase in  $|G|$  due to reduced conductivity ( $10^{-2}$  to  $10^{-3}$  mhos/meter) extends the maximum range of the various systems as follows:

<u>System</u>	<u>Maximum Range Increase (Ft.)</u>
Pulse	600
1/2 Wave (90 Ft. Ant.)	330
1/2 Wave (360 Ft. Ant.)	820
Full Wave (90 Ft. Ant.)	500
Full Wave (360 Ft. Ant.)	1200

These values were used to calculate the new maximum off-set distances shown in the table below.

## [OFF-SET DISTANCE VS MINE DEPTH (FT)]

System Mine Depth	Pulse 100 Ft. Antenna	CW				Comments
		Half Wave 90 Ft. Antenna	Half Wave 360 Ft. Antenna	Full Wave 90 Ft. Antenna	Full Wave 360 Ft. Antenna	
400	2150	880	2430	1810	2910	Assumptions: $\sigma = 10^{-3}$ mho/met Rcvr Sensitivity .1 Amp/meter Noise: Summer Atmospheric Only S/N = 10 dB for reliable detection
700	2080	650	2310	1750	2855	
1000	1850	20	2250	1710	2780	
1500	1050	Inoperative	1930	1150	2480	



## REFERENCES

- [1] Westinghouse Final Report, CMR & SS, Vol. II, September, 1971.
- [2] Wait, J. R. and L. L. Campbell, The Fields of an Oscillating Magnetic Dipole Immersed in a Semi-Infinite Conducting Medium, JGR, Vol. 58, No. 2, June 1953.
- [3] Sinha, A. K. and P. K. Bhattacharya, Vertical Magnetic Dipole Buried Inside a Homogeneous Earth, Radio Science, Vol. 1 (New Series), No. 3, March 1966.
- [4] Bensema, W. D., Coal Mine ELF Electromagnetic Noise Measurements, NBS Report
- [5] Wolfe, R., Private Communication, 1970.

## PART II - PULSE SYSTEM

### 1.0 INTRODUCTION AND SUMMARY

#### 1.1 BASIC PHENOMENON

The idea of a pulse location system for locating trapped miners was conceived from the radar technology principle of converting low average power to high peak power by pulsing the available energy. Further studies (theoretical) were initiated at Westinghouse Electric Corporation to determine specific configurations based upon environmental and performance restraints such as overburden propagation effects, battery supply limitations, endurance requirements, weight and size limitations, explosion hazards (intrinsic safety) and other pertinent characteristics. Under this concept and with the sponsorship of the U.S. Bureau of Mines a system was designed, constructed and tested over the period 7/1/72 to 1/14/73, the results of which are summarized below and covered in detail in succeeding paragraphs.

#### 1.2 SUMMARY

The equipment was tested at two mines (Section 4.1) and proved to have detection accuracies of 10 feet or better in mines to 400 feet in depth. One measurement exceeded 10 feet but it was the first measurement made and the terrain was very irregular, so it was discarded in view of the excellent results achieved. Other features revealed by the test program included:

- 1) Endurance - In two instances satisfactory surface signals were received after 24 hours of continuous transmitter operation in the mine. These signals had sharp directional indications at a 300 ft offset from the transmitter.
- 2) Coverage - Sharp directional signals were received from the buried transmitter (400 ft) at a distance of 1200 ft offset.



- 3)      Weights - Transmitter - .5 lbs.  
          Transmitter Ant. - 1.5 lbs.  
          Receiver           - 13.5 lbs.  
          Receiver Ant.     - 3.8 lbs.
- 4)      Intrinsic safety. Both transmitter and receiver  
          were intrinsically safe, the former by actual  
          laboratory tests and the latter by circuit review  
          and analysis.

## 2.0 THEORY

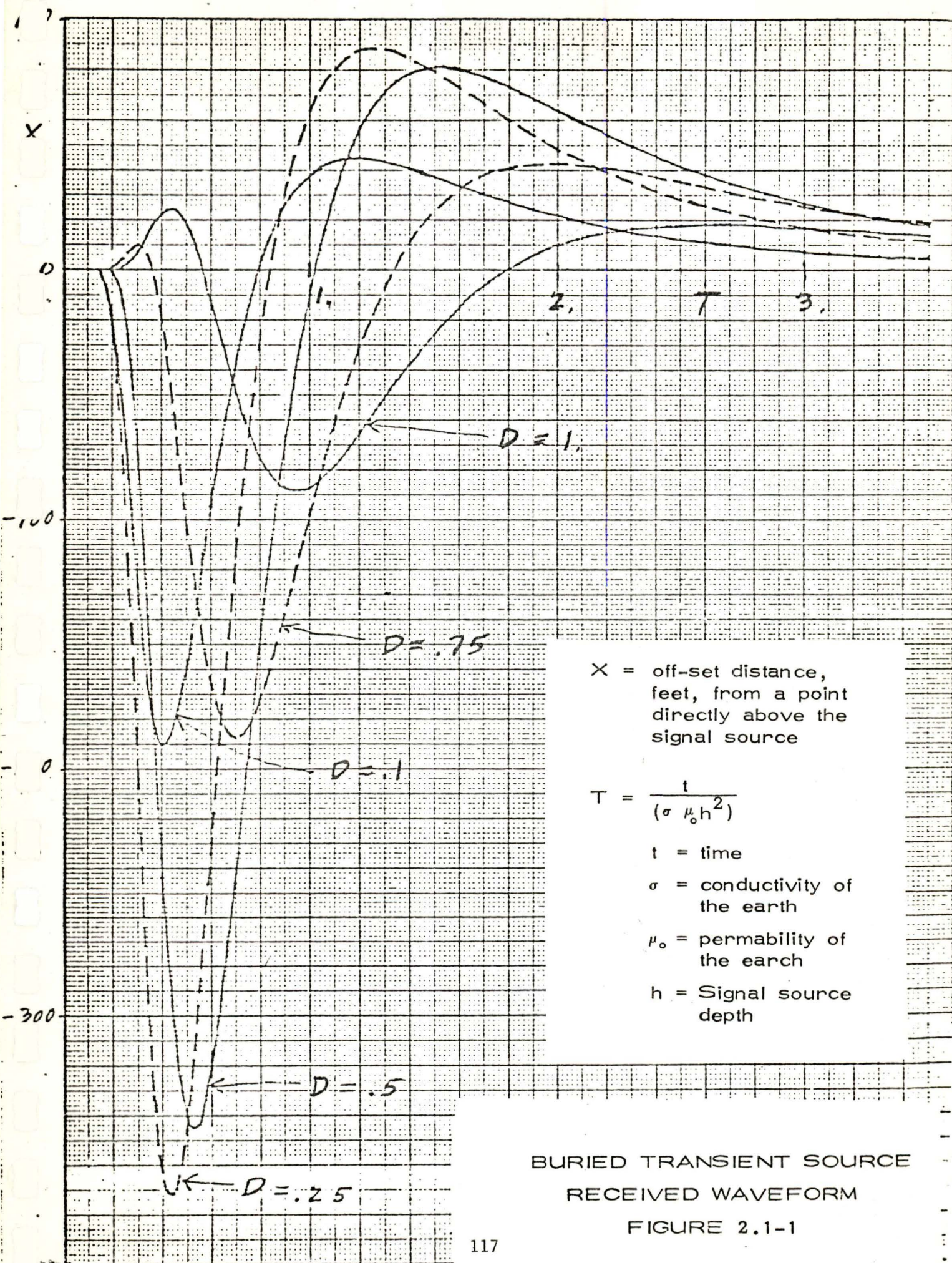
### 2.1 INTRODUCTION

The basic theory for the feasibility of the use of pulse techniques to locate trapped miners in the event of an emergency was developed in a series of papers by Dr. James R. Wait, et al, in the published literature and in reports to the U.S. Bureau of Mines. The initial paper<sup>1</sup> "Transient Signals from a Buried Magnetic Dipole" assumed a buried source excited by a unit impulse function of current. A subsequent paper<sup>2</sup> assumed a Step Function Excitation instead of an impulse function. A further paper<sup>3</sup> developed especially as a result of Westinghouse request dealt with the case where the excitation was exponential in nature as one would expect where a loop of wire with a finite inductance and resistance is involved.

#### 2.1.1 Background

In all of the above papers the authors clearly stated that the received waveform was dependent on  $D$ , a dimensionless quantity equal to the offset (horizontal distance from observer to a point directly over the miner) divided by the depth of the buried source. Thus wave shape discrimination appeared to be a possible criterion for miner location. Believing this to be the case, Westinghouse requested Dr. Hill at the Institute for Telecommunication Sciences, U.S. Department of Commerce, Boulder, Colorado, to exercise his computer program for an exponential buried source to develop wave shapes for closer spacings of offset values ( $D$ ). In the original paper<sup>3</sup> a spacing of .5 was used for  $D$ . The new computations (figure 2.1-1) were based on intervals of .25 for  $D$ . This is equivalent to 250 feet (1000 foot depth) or 75 feet (300 foot depth). From the curves, it was clear that adequate resolution and accuracy could not be achieved by use of wave shape discrimination alone. In addition, it appeared that a very precise knowledge of conductivity was required to accurately define the zero crossings of the curve. Thus, Westinghouse reluctantly abandoned the concept of wave shape







discrimination as a location technique and turned instead to the earlier concept of null detection established for a CW signal. This concept is equally applicable to the pulse techniques. The concept takes advantage of the fact that for a vertical magnetic dipole (sub-surface) the electromagnetic fields on the surface are characterized by the following:

(a) The Horizontal Magnetic Field experiences a sharp null directly above the source, while (b) the vertical magnetic field experiences a maximum directly overhead<sup>4</sup>.

## 2.2 ANALYSIS

Since the approach selected was the use of a vertical magnetic dipole as the transmitting antenna and the detection of a null in the surface horizontal magnetic field, the system design centered around the generation of a large magnetic moment and the use of a sensitive high gain receiver. The detection of very small signals in the presence of noise was of paramount importance.

### 2.2.1 Geometry

The situation can be represented by figure 2.2-1 where the loop L represents the vertical magnetic dipole. Since the loop is deployed on the mine floor in a circular or near circular configuration its axis is vertical. This defines the vertical magnetic dipole. On the surface the electromagnetic field can be divided into three components,  $H_x$ ,  $H_y$  and  $H_z$  as shown.  $H_z$  is the vertical component and  $H_x$  and  $H_y$  are horizontal orthogonal components as shown.  $h$  is the depth of the buried source. Directly over the source the vertical component  $H_z$  is a maximum, while the horizontal component (resultant of  $H_x$  and  $H_y$ ) goes to zero. To locate the buried source field strength profiles are obtained in two orthogonal directions measuring both components (see section 4, Experimental Results).



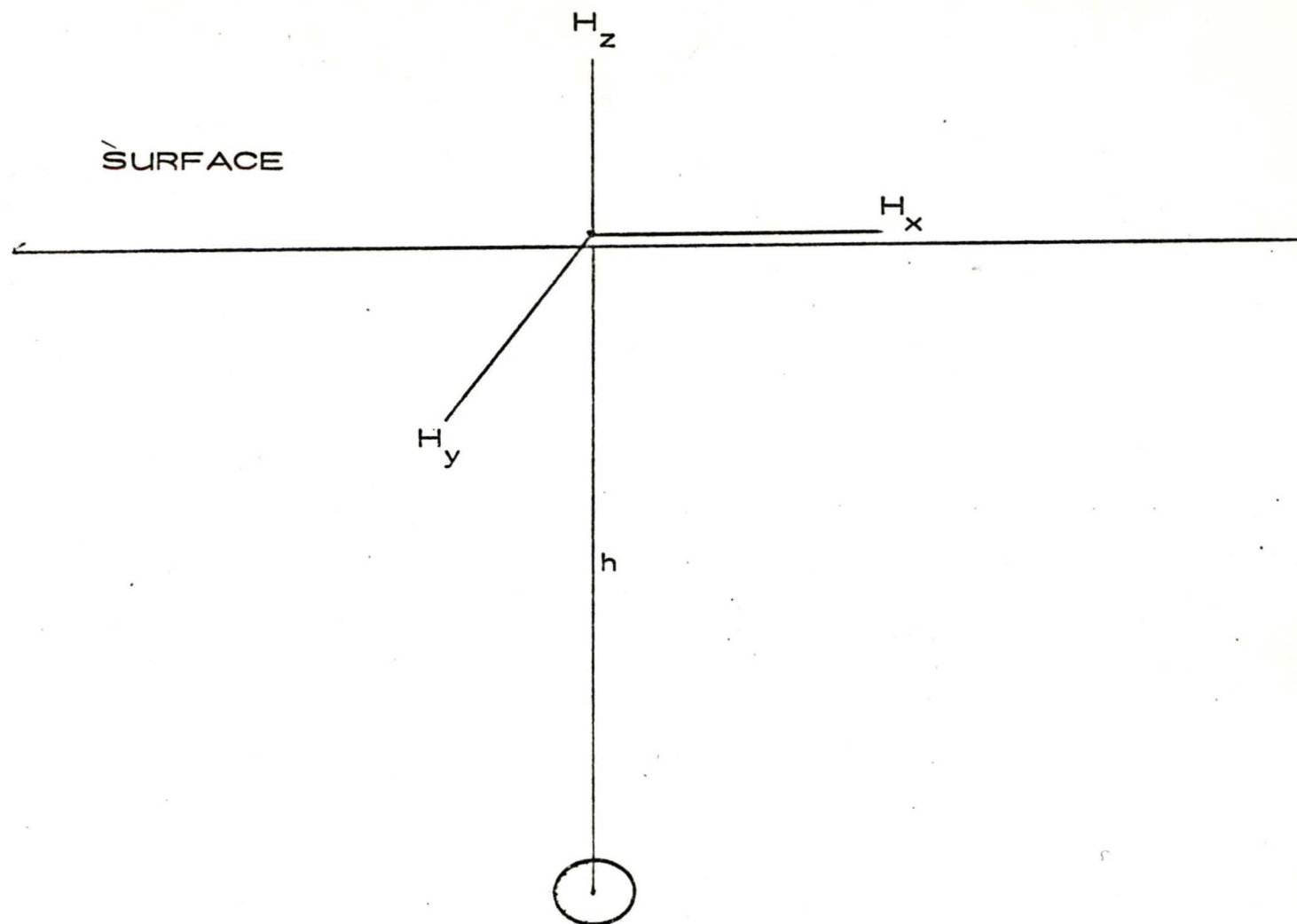


Figure 2.2-1. Geometry of Location System

### 2.2.2 Propagation Through The Earth

The propagation of transient electromagnetic signals through the earth has been analyzed extensively by Wait [1, 2, 3, 4]. In the design of hardware to operate in this environment useful relations [3, 7] include:

$$H = \frac{INA}{2\pi h^3} X_R \quad (1)$$

and

$$\delta = \frac{1}{(\pi \mu_o f \sigma)^{1/2}} \quad (2)$$

where

H = Horizontal magnetic field component ultimately measured in dB relative to one micro-amp per meter.

I = current, amperes

A = area enclosed by the transmitting antenna, meters<sup>2</sup>

h = transmitter depth, meters

$X_R$  = an attenuation factor due to the overburden.  $X_R$  is dimensionless and a function of other variables<sup>3</sup>, D and T.

$\delta$  = skin depth, or characteristic depth of penetration of the electromagnetic signal in a conducting medium in meters

$\mu_o$  = magnetic permeability of the overburden.

f = operating frequency, Hz.

$\sigma$  = effective, or average, conductivity of the overburden, mhos/meter

Relation (2) above suggests using the lower frequency spectrum, however, the choice of operating frequency is strongly related to local noise conditions. Experimental equipment developed under this contract operates in the vicinity of 500 Hz.



Values of  $X_R$ , a function of the dimensionless parameters  $D$  and  $T$ , are shown<sup>3</sup> in Figure 2.2.2 below, and

$$T = \frac{t}{\sigma \mu_0 h} \quad (3)$$

$$D = \frac{X}{h} \quad (4)$$

where

$t$  = time

$X$  = surface off-set distance of the receiver from  
a point directly above the transmitter

$\sigma \mu_0, h$  are as defined in (2) above.

The relations (1), (2), (3) and (4) above represent the fundamental relations on which the equipment was designed. In particular, Figure 2.2.2 is used in conjunction with (1) above to predict the signal strength at the receiver for various antenna configurations, antenna currents and transmitter depths. For hardware design purposes here a value of  $T = 0.5$  has been used since there will be little increase in the current for the various values of  $D$ . This corresponds to a "worst case" value of 0.2-0.4 for  $X_R$ . Test results achieved and discussed elsewhere in this report indicate that this is a satisfactory hardware design procedure.

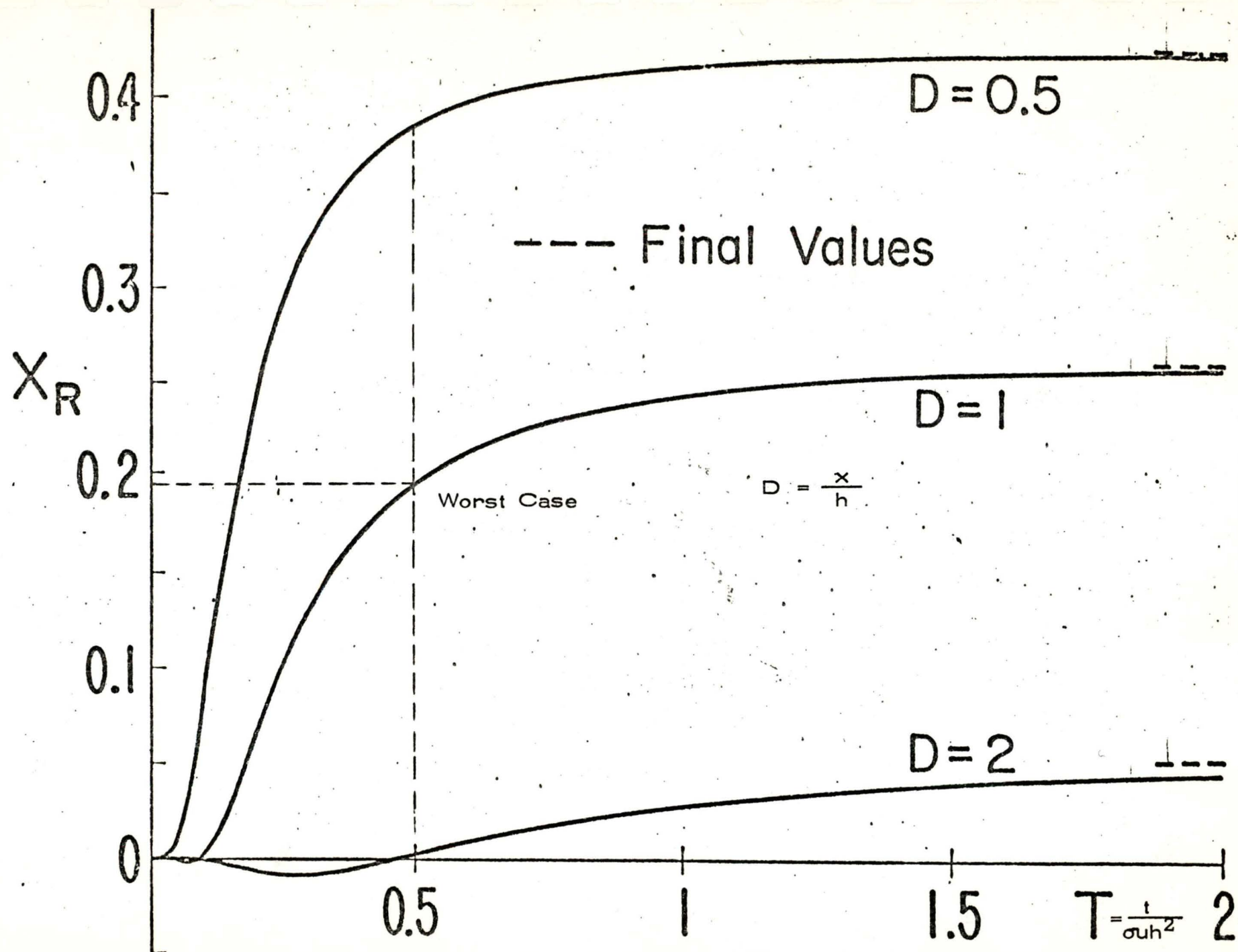


Figure 2.2-2. Propagation Factor



As an example, if we assume a required sensitivity of .1 ua/m (a realistic receiver capability) then we have

$$.1 \times 10^{-6} = \frac{1NA}{2\pi h^3} \quad .2 \quad (5)$$

Minimum required moment =  $1NA = 154$  for  $h = 366$  meters (1200 ft)

This type of information was the basis for designing the transmitting system.

### 2.2.3 Transmitter Design

The basic requirement for the generation of adequate signals in a pulse system is the establishment of a large magnetic moment. For the antenna a large loop is indicated (large A) consistent with physical constraints in the mine and resolution requirements of source location. A loop 100' in circumference was selected to give the largest area achievable in most mines and small enough to adequately locate a source within the circle. The requirement to minimize weight indicated that one turn of wire for the loop would have to do if the current could be high enough, 100 feet of #12 stranded copper wire was selected as the antenna ( $N=1$ ,  $A=75$  sq. meters). Thus the current  $I$  would have to be no less than 2 amperes to give a minimum moment of 154 (formula 5). No problem exists with reception of the vertical component since it is generally larger than the horizontal component in the areas of interest.

2.2.3.1 Since the antenna is a loop of wire, it has a finite inductance and resistance. The approach to generating a current pulse is based upon the charge and discharge of the inductance (loop) in an L-R circuit by application of a step voltage. The constraints are the voltage and the ampere-hour rating of the miners' battery and intrinsic safety requirements.

2.2.3.2 To maximize the received signal to noise ratio on the surface it was decided to limit the transmitter spectrum to 4 spectral lines (fundamental and 3 harmonics) and design the receiver with 4 comb

filters to respond to each frequency. This is in effect determined by the transmitting pulse width. Ten channels are possible (table 2.2.3-2 for identification purposes with associated pulse widths. A near triangular current waveform is generated by the charging of an L-R circuit by a 3 volt d.c. source (a 1 volt drop occurs in the switching circuitry). Thus

$i = \frac{E}{R} (1 - e^{-\frac{Rt}{L}})$  is the instantaneous current in the antenna circuit. With the following constants

$$E = 3$$

$$R = .16$$

$$L = 40 \text{ uh}$$

$$t = 250 \text{ us (the rise time for the 400 us pulse)}$$

we have:

$$i = 15.2 \text{ amperes (figure 2.2.3-2)}$$

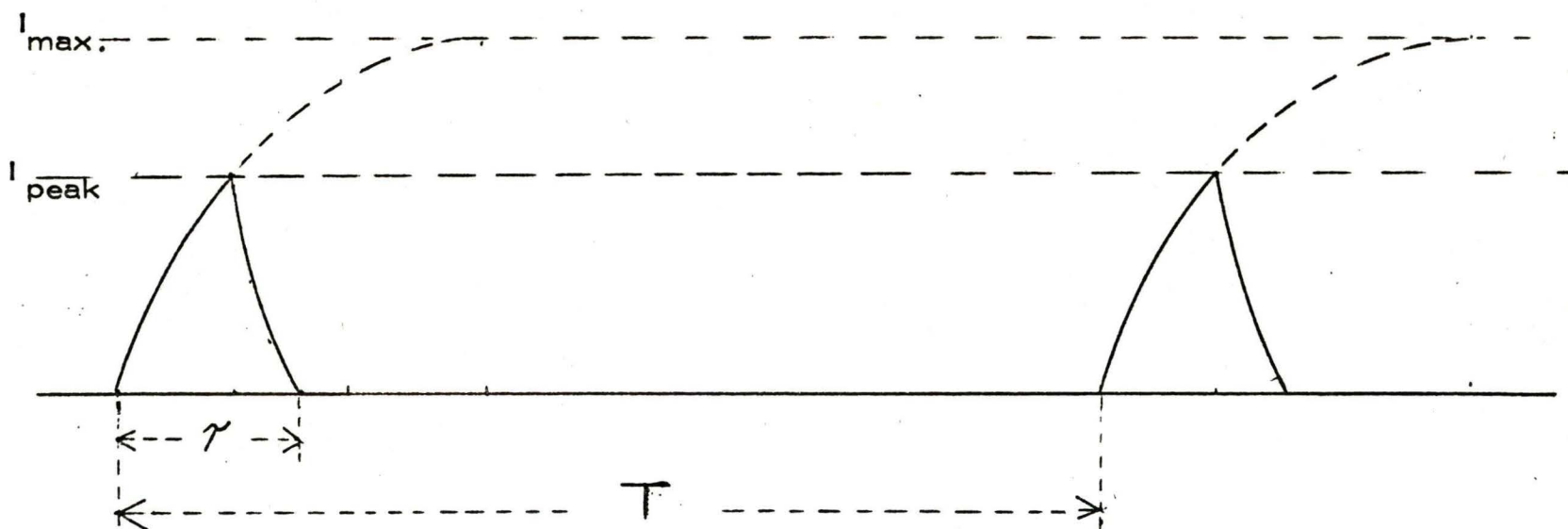
If we cut off the current rise time at 250 us then the peak current of the pulse ( $I_{\text{peak}}$ , figure 2.2.3-2) is 15.2 amperes. The discharge time constant is easily adjusted for 150 us giving a pulse width of 400 us. Similarly for the 330 us and 300 us pulses, the respective peak currents are 14 amperes and 13.3 amperes).

2.2.3.3 To compute the received field intensity from a pulse source whose peak amplitude is 1 amperes (assuming NA=75) we can use figure 2.2.3-3. Two values of current (10 and 15 amperes) are shown to bracket the range of currents proposed for all the required identification channels. From the graph we see that for a given required field intensity the depth of coverage increases by about 10% when the transmitter current increases from 10 amperes to 15 amperes. We also see that, for a buried source 1000 feet (366 meters) below the surface, the received field intensity is .9 ua/m versus 1.3 ua/m for the two currents.



TABLE 2.2.3-2

Pulse Recurrence Frequency (PRF)		Pulse Width (Microseconds)
I	470.5 Hz	400
II	510.5 Hz	400
III	550.5 Hz	400
IV	590.5 Hz	400
V	630.5 Hz	330
VI	670.5 Hz	330
VII	710.5 Hz	330
VIII	750.5 Hz	300
IX	790.5 Hz	300
X	830.1 Hz	300



PULSE WAVEFORM

Figure 2.2.3-2



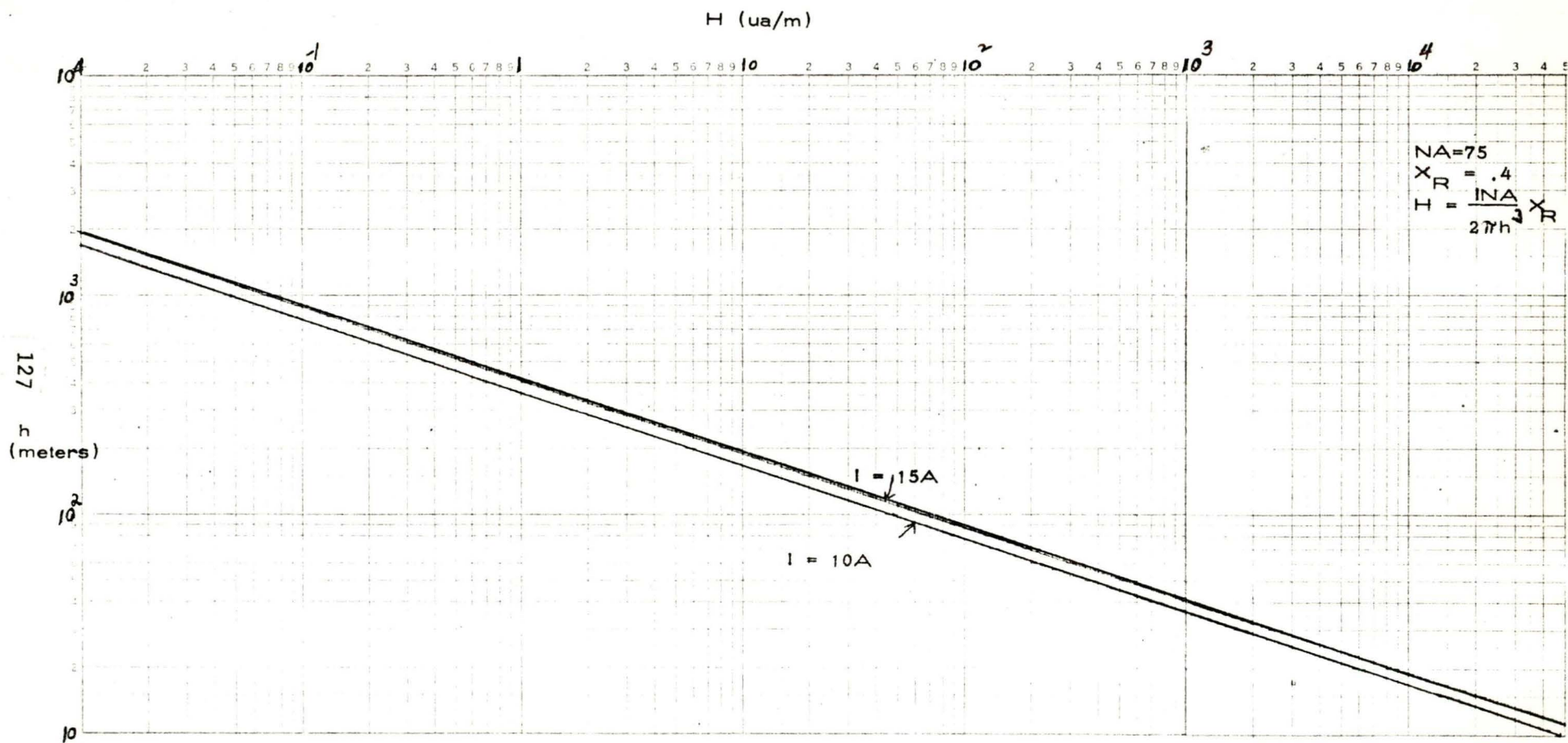


Figure 2.2.3-3. Received Field Intensity

#### 2.2.4 Receiver Design

The receiver for this system must be very sensitive ( $.1 \mu\text{a/m} - 2 \text{ dB NF}$ ) and have good filter characteristics for noise rejection. The front end is a high gain, high impedance operational amplifier ( $\mu\text{A-739C}$ ). This is followed by 4 BP filters (for a given prf) each centered around a harmonic of the fundamental prf. Any filter may be separately removed or inserted into the system by a manual switch selection system. The outputs of the filters are combined to provide an aural indication and a visual indication on a meter. The filter bandwidths are approximately 25 Hz at the 3 dB points. The receiving antenna consists of an air core loop 22" in diameter. To provide a  $.1 \mu\text{a/m}$  sensitivity the receiving loop would have to provide a  $.23 \mu\text{v}^*$  signal to the receiver input circuitry ( $f = 470.5 \text{ Hz}$ ). The actual required signal at the receiver input for a 10 dB signal to noise ratio at the output was measured at about 4.5 nanovolt.

#### 2.3 TERRAIN SLOPE CONSIDERATIONS

The preceding analysis assumes that there is no slope to the surface terrain and/or the plane of the transmitting loop. In practice the surface terrain may have appreciable slope or the mine floor may have a slope. In these cases, a correction factor would have to be applied to the measured location to determine the true location. Westinghouse has developed a computer program to provide the required correction curves (Reference 6). This program trigonometrically combines the solutions for a buried vertical magnetic dipole with those for a buried vertical magnetic dipole. The model has only solved the problem for a uniform slope, however, so it does not prove very useful for cases where the slope is continually changing or has abrupt discontinuities such as cliffs and ravines. In the Putnam mine tested (Section 4.2) there was no appreciable slope to the terrain, so no correction was needed. In the Island Creek mine (Section 4.1) the

---

\* Using  $E = 2 \pi f u_0 \text{ HAN}$  from Reference 6 (Fig. 4.5-2)



terrain was very rugged precluding the determination of a single value for the slope. The latter site did show a larger error than the former probably due to terrain irregularities.

## 2.4 NOISE EFFECTS

Considering the numbers of channels proposed for the system and the associated harmonic frequencies, the range of 470 to 3200 Hz was selected as the operating range of the pulse system. Higher frequencies would result in excessive attenuation through the overburden. The effect of noise in the audio frequency spectrum is to put a lower bound on signal levels that can be received. The noise generally is derived from three sources, atmospheric noise, man-made noise and internal receiver noise. The interference effects due to the various types of noise are minimized by use of selected frequencies within the audio band.

### 2.4.1 Internal Receiver Noise

At the audio frequency range low noise receivers are readily obtained. Sensitivities in the area of 1 nanovolt for a 10 db signal to noise ratio at the output are well within the state of the art. Coupled with a high gain antenna, one can achieve overall sensitivities of .1  $\mu\text{a}/\text{m}$  or better.

### 2.4.2 Atmospheric Noise

Atmospheric noise in the audio spectrum has been studied intensively in recent years in connection with long range and underground communications. Figure 2.4-2 (from Ref. 6) shows measured data for the horizontal magnetic field. The region of 500 to 3000 Hz indicates median noise signals are 30 db below 1  $\mu\text{a}/\text{m}$  in this area. This indicates a good choice of frequencies for the pulse location system. This data is borne out by other independent measurements (W.D. Bensema, NBS 10-739, "Coal Mine ELF Electromagnetic Noise Measurements").

#### 2.4.3 Man-Made Noise

Man-made noise from electrical machinery, power lines, vehicles, etc. can be troublesome. The frequencies selected for the pulse system as well as their harmonics do not conflict with commercial frequencies or their harmonics. Broad band noise is a problem; however, its effects are considerably reduced by suitable design and operational tactics. Bandpass filters which can be added or removed as required can help to alleviate this problem. In addition care can be used in surface measurements to minimize the interference which is usually directional in nature.

As noted earlier, detailed noise measurements were not made at the mines visited, and this section on noise is necessarily brief. Studies on mine noise have been completed by the Bureau of Mines under other contracts with A. D. Little, Inc., NBS, Colorado School of Mines and WGL. These studies collectively represent the most competent background information on noise.



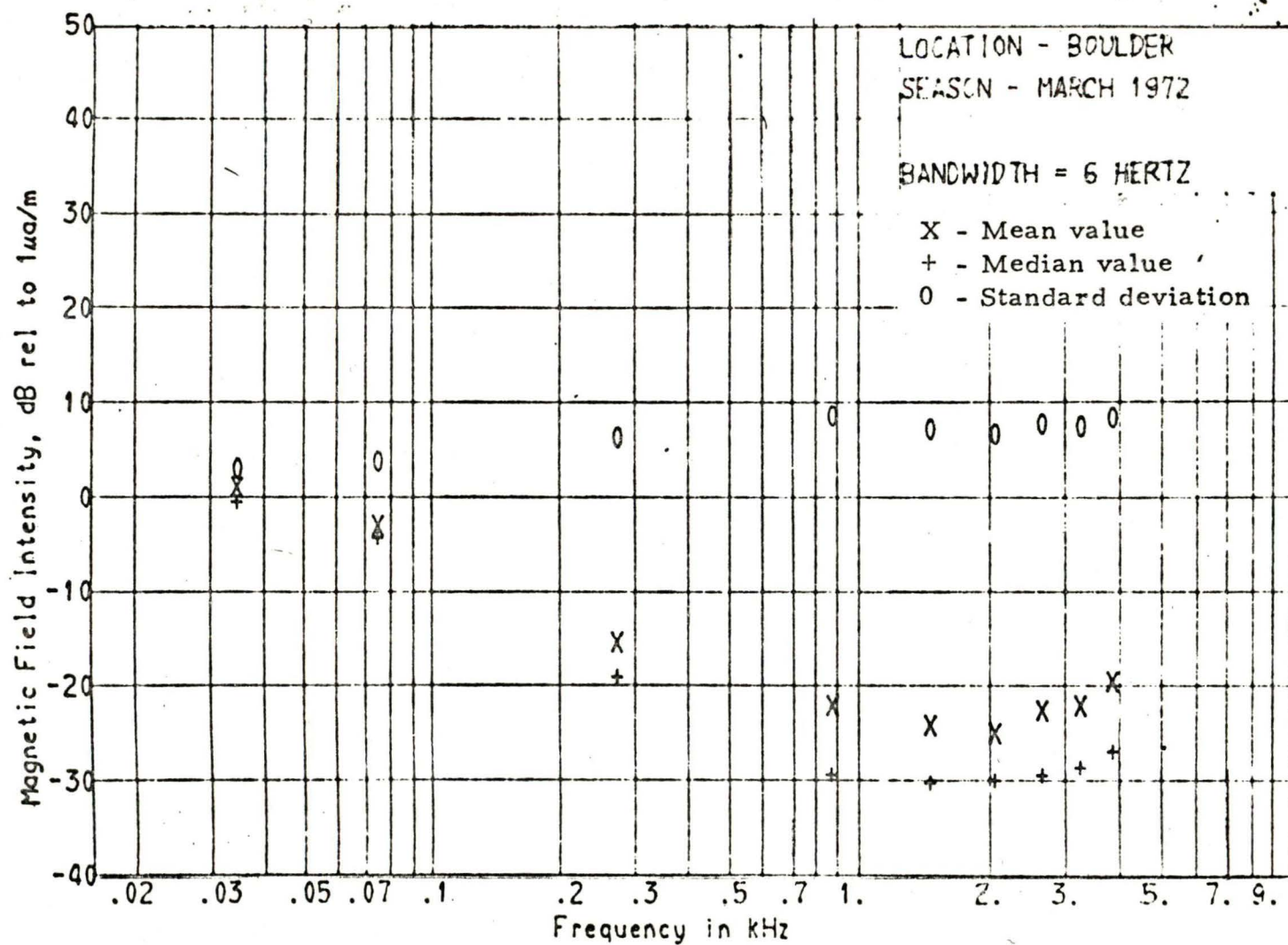


Figure 2.4-2. FREQUENCY VARIATION OF ATMOSPHERIC NOISE (AVG VALUES)

### 3.0 EQUIPMENT DESIGN

#### 3.1 INSTRUMENTATION

The electromagnetic location and direction finding equipment consists of two transmitters and one receiver and associated antennas. Each transmitter generates a near ramp current pulse of 300 microseconds duration (figure 3.1-1) and the pulse recurrence frequencies are 470.5 Hz and 510.5 Hz. The purpose was to determine separate identification capabilities of two sources 40 Hz apart in frequency. Both transmitters operate from the 4.0 volt miners battery (MSA and Koehler).

#### 3.2 TRANSMITTER

The transmitter developed under this contract for the U.S. Bureau of Mines was designed to operate from the 4.0 volt DC supply of the lamp battery used by the miner to light his lamp. The equipment\* was installed in a 4" x 1-1/2" x 2-1/2" aluminum box cemented to the side of the miners battery. The basic circuit is given in figure 3.2-1. The operation is as follows:

The 4.0 VDC is applied to a battery of 8 capacitors in parallel (module  $A_1$ ). The capacitors are used to reduce the drain on the battery by providing the necessary high average current. The capacitors discharge into the antenna by way of transistor switches and are partially recharged by the current fall in the antenna. The capacitors minimize the effect of the battery resistance. In effect we have a system permitting high average current in the antenna (and a high transmitting moment) without excessive battery drain. Experiment bore this out with 2 cases where the transmitter operated continuously for at least 24 hours.

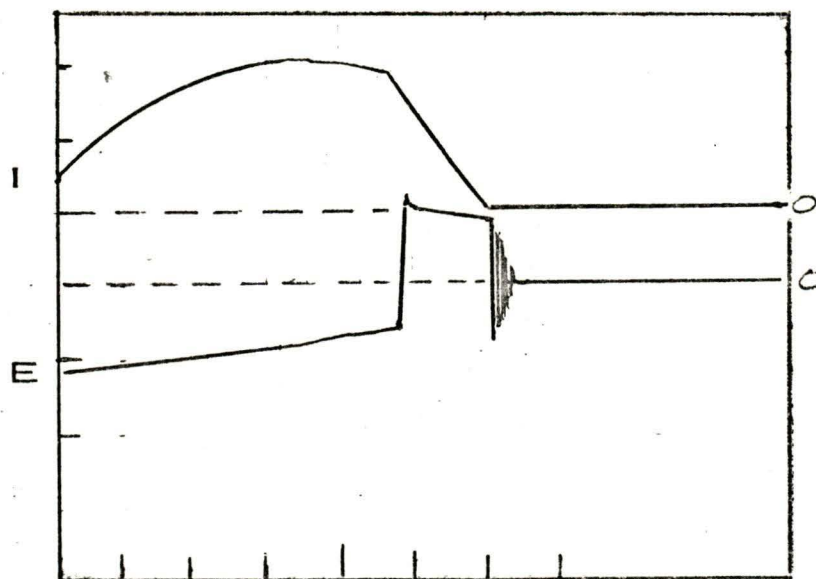
##### 3.2.1

Referring to figure 3.2-1, we see that the operating repetition rate of the system is set precisely by the operating frequency of microfork A2Z with amplifier  $A_2U_1$ . The frequency may be trimmed

---

\* Weight - 1/2 lb.





I - Antenna Current      5 Amperes/Div.  
 E - Antenna Voltage      4 Volts/Div.

Time Scale: 50  $\mu$ s/Div  
 Measured Transmitter Waveform

Figure 3.1-1

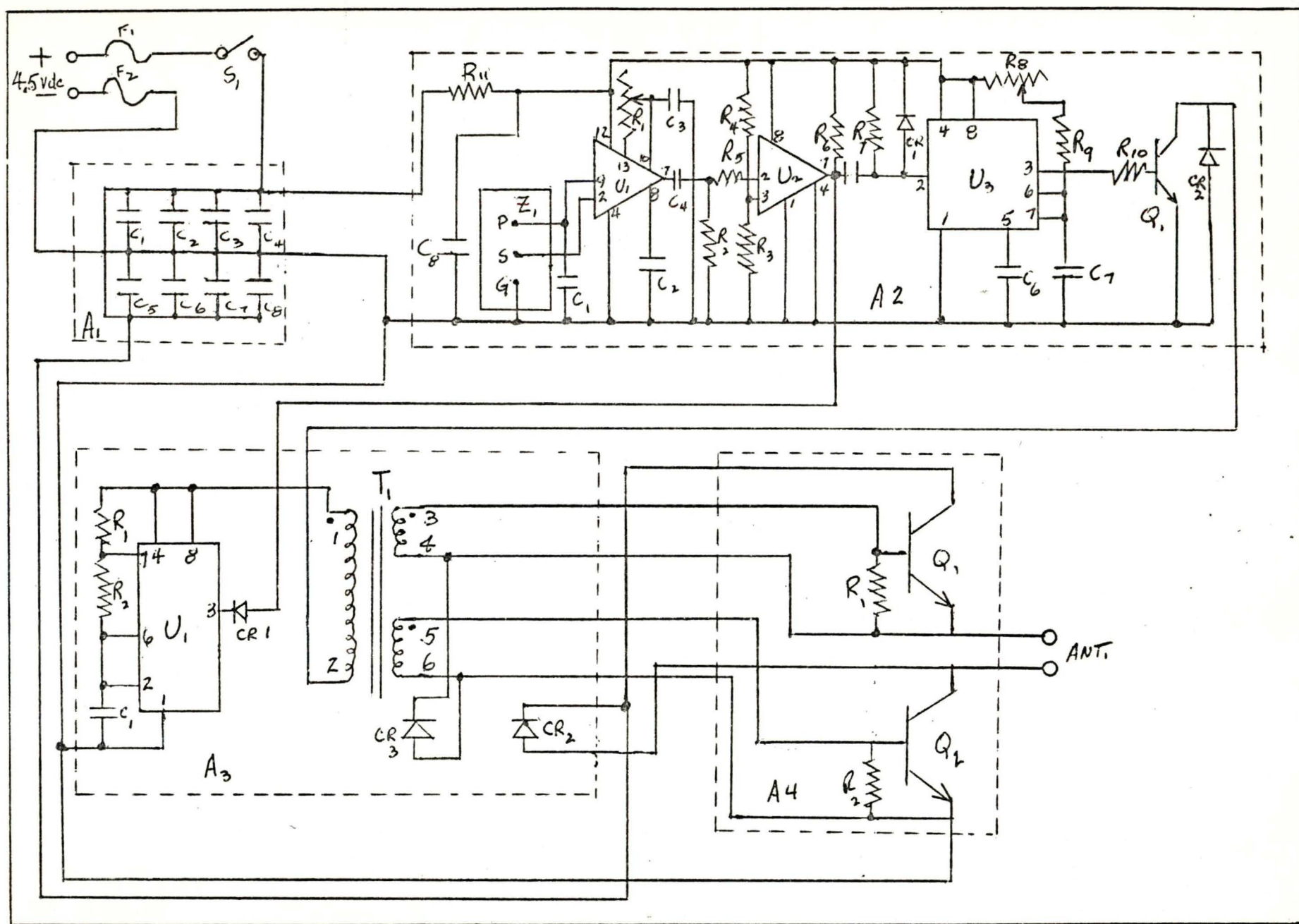


Figure 3.2-1. Mine Location Transmitter



to within .01% by A2R1. The output of A2U1 is a sine wave which is converted to a square wave and amplified by comparator A2U2. The output of A2U2 is clamped to ground for 0.5 seconds every 2.0 seconds by interruptor module A3U1. The purpose of the interruptor is to facilitate identification of the received signal. When A2U2 is not clamped to ground, its output is differentiated to provide trigger pulses to A2U3 which sets the output pulse width as selected by A2R8. Its output is amplified by A2Q1 through A3T1 to turn on A4Q1 and A4Q2. When these two transistors are turned on, current flows in to the antenna from the A1 capacitor storage bank. During this time energy is stored in the inductance and a portion dissipated in the line resistance. When A4Q1 and A4Q2 are turned off, the current in the inductance must continue to flow. Diodes A3CR2 and A3CR3 provide that path. The inductive energy is then used to recharge the storage bank. The use of low saturation drop transistors and low forward drop-hot carrier diodes improve circuit efficiency. The average battery current drain is approximately 300 milliamperes while the average antenna current is 1.3 amperes. Peak antenna current is 10 amperes (figure 3.1-1).

### 3.3 TRANSMITTER ANTENNA

The antenna use consisted simply of 100 feet of #12 stranded copper wire in a PVC jacket. This wire has an inductance of 40 microhenries and a resistance of .16 ohms.\* When laid out in a circle the area is approximately 75 square meters. This is the optimum deployment of the antenna (one turn loop). The size was selected to provide the largest area (75 sq. m) consistent with physical mine structures, required location accuracy and ease of carrying and deployment.

### 3.4 RECEIVER #

The receiver design is centered around four comb filters, one for each of the first four spectral lines in the transmitter pulse frequency spectrum. Two sets of filters are used to correspond to

---

\* Weight - 1.5 lbs.

# Weight - 13.5 lbs.

two transmitters operating at different pulse recurrence frequencies. For multiple channel operation each channel would have its own set of filters. The reason this design was used was to maximize the signal to noise ratio at the receiver output by rejecting unwanted noise in frequency bands containing no intelligence.

#### 3.4.1

Figure 3.4-1 is a block diagram of the overall receiver system. The input signal is amplified in the Input Amplifier (module A) and is applied to modules  $B_1$  and  $B_2$  (470.5 Hz) and modules  $B_3$  and  $B_4$  (510.5 Hz). The output is amplified and fed to an indicating meter and headset.

#### 3.4.2

The input amplifier (figure 3.4-2) uses a high gain, low noise integrated circuit operational amplifier (uA 739) followed by another high performance I.C. operational amplifier (uA741). Two configurations are used to connect these two stages, one a simple potentiometer for continuous voltage control and the other a step attenuator to permit calibration of the received signal to a 1 DB precision.

#### 3.4.3

Filter modules  $B_1$  (470.5 Hz) and  $B_3$  (510.5 Hz) are shown in figure 3.4-3. Illustrated schematically is the fundamental frequency filter consisting essentially of a tuning fork (.01% precision) precisely matched to the one in the corresponding transmitter ( $Z^1$ ) and a hybrid amplifier ( $Z^2$ ) to amplify the signal. The active signal filter is tuned to the 2nd harmonic (941 Hz or 1021 Hz as the case may be). Bandwidth of the active filter is 25 Hz (3 db). Circuit details are shown in figure 3.4-4.

#### 3.4.4

Circuit information for the active filter configuration is shown in figure 3.4-4. Component values that vary with frequency are  $R_1$ ,  $R_4$ ,  $R_{13}$ ,  $R_{16}$ ,  $C_1$ ,  $C_2$ ,  $C_7$ ,  $C_8$  and  $C_0$ . All other components are the same for all filters. Values are given in the parts list in Appendix A.



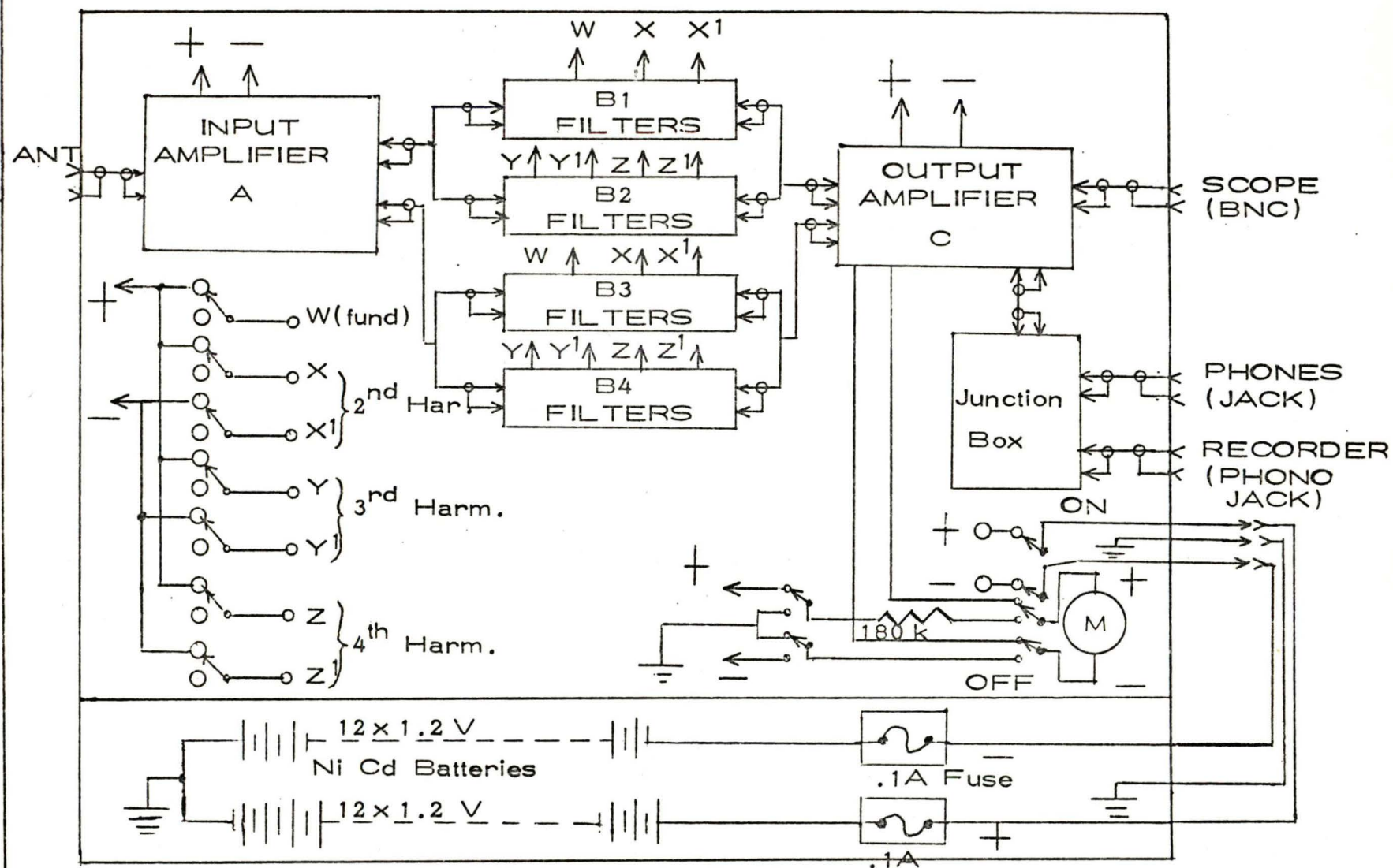


Figure 3.4-1. Mine Location Receiver Main Frame

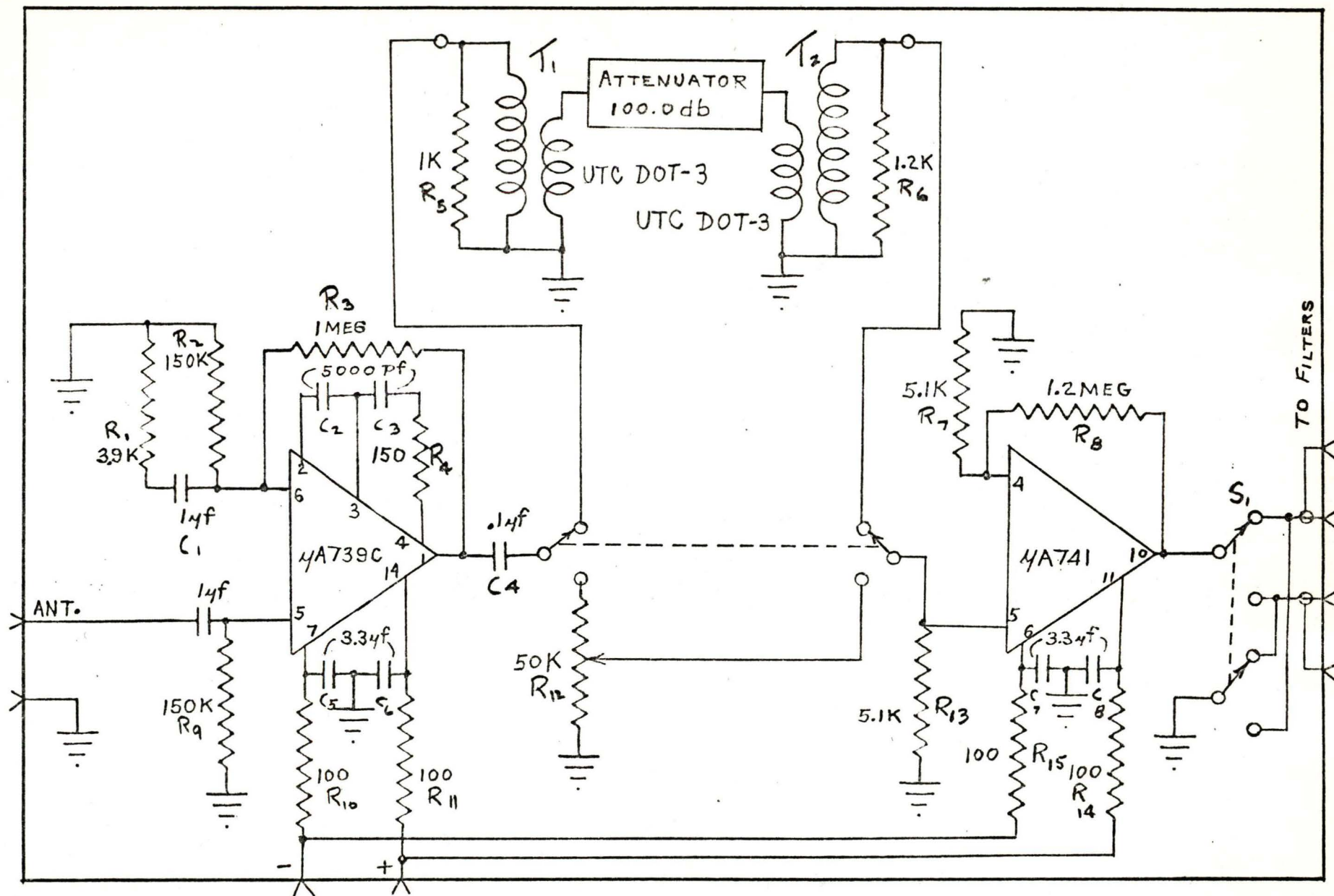
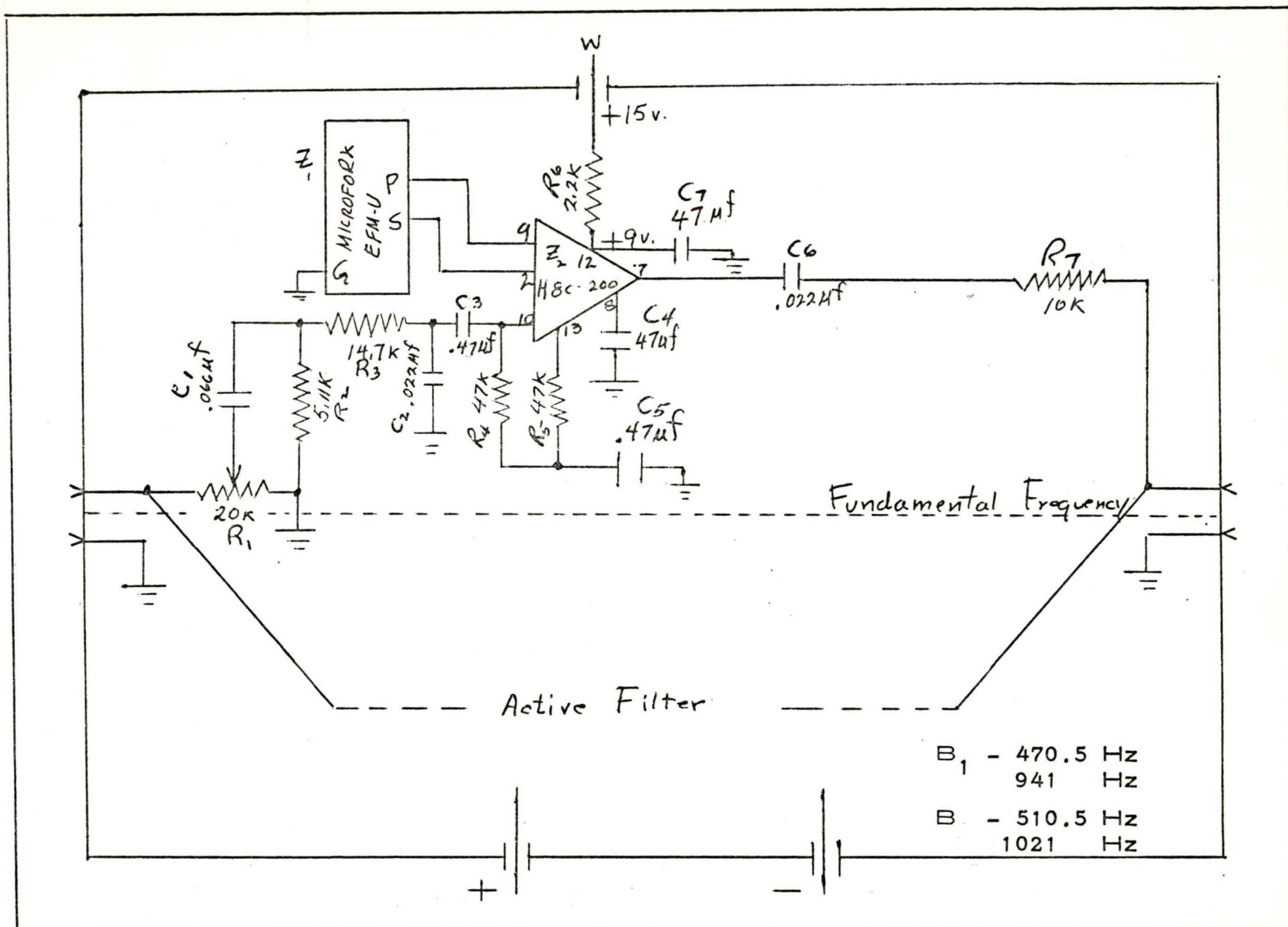


Figure 3.4-2. Input Amplifier A



Figure 3.4-3. Filter Modules B<sub>1</sub> and B<sub>3</sub>

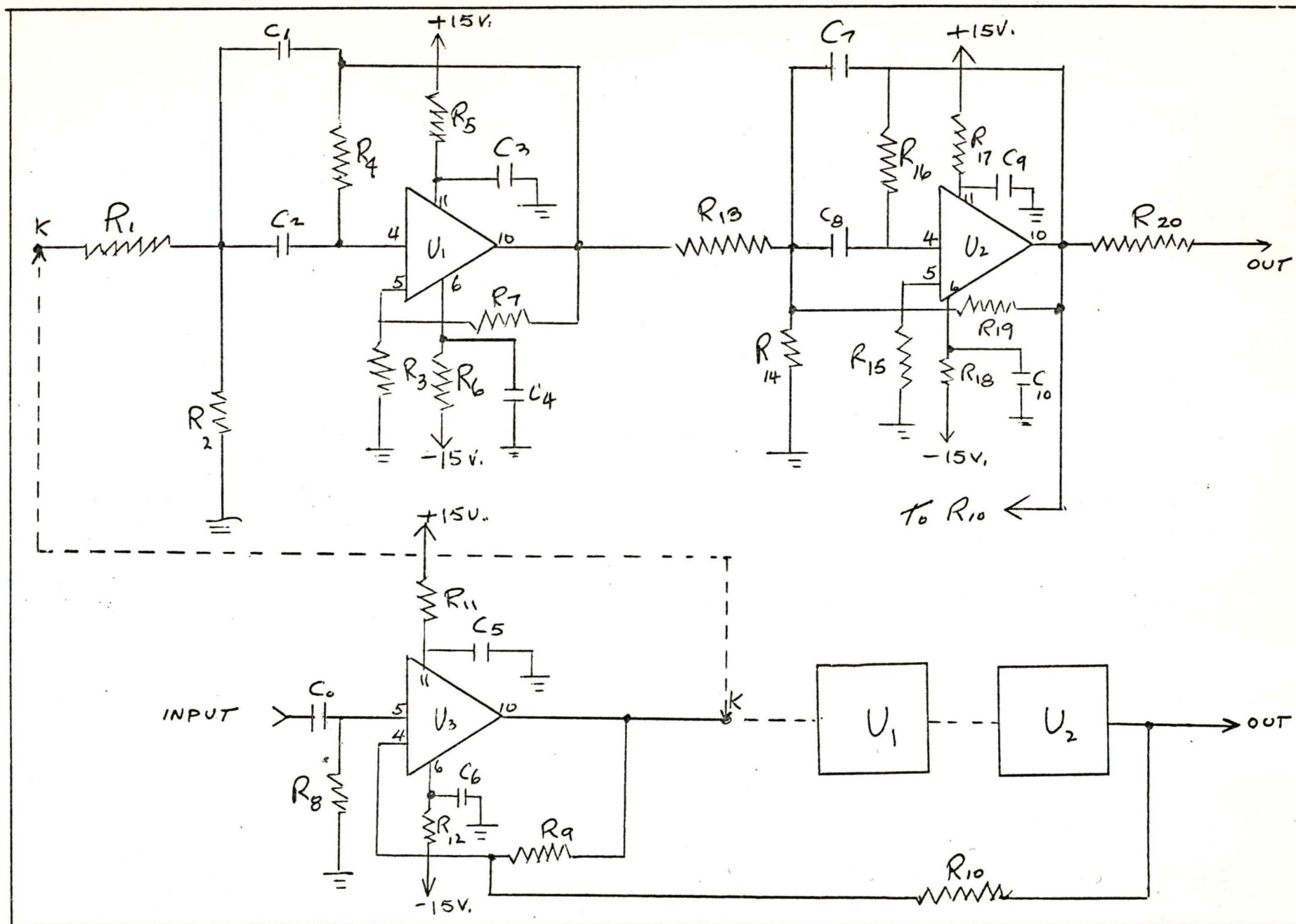


Figure 3.4-4. Typical Active Filter



#### 3.4.5

Modules  $B_2$  and  $B_4$  contain the 3rd and 4th harmonic filters corresponding to fundamental frequencies, 470.5 Hz and 510.5 Hz respectively. (Figure 3.4-5).

#### 3.4.6

All the filter outputs are combined and applied to the output amplifier (figure 3.4-6). The composite received signal is amplified and rectified for indication on a field strength meter (M), figure 3.4-1. As seen in the figure this dc signal is applied through the on-off switch. This is done to permit the meter to indicate the voltage of the battery supply, both positive and negative via  $S_1$ , figure 3.4-1. Other outputs of the output amplifier, module  $C_1$ , are used to operate a headset (Murdock crystal headset, B-800), feed into a tape recorder and provide a presentation on an oscilloscope (figure 3.4-1).

#### 3.4.7 Receiving Antenna

The receiver can operate with any good high impedance antenna. Both ferrite loops and air core antennas have been used. While the former are small and compact they have certain drawbacks such as weight and changes in electrical characteristics with climatic and temporal changes. The antenna finally used in the system is an air core loop 22" in diameter. It is composed of 2500 turns of #33 insulated magnet wire and is equipped with a Faraday Shield. The antenna gain is such that it provides the receiver with an overall sensitivity of better than .1  $\mu\text{A}/\text{m}$  for a 10 db signal to noise ratio at the output. The loop weighs 3.8 lbs.

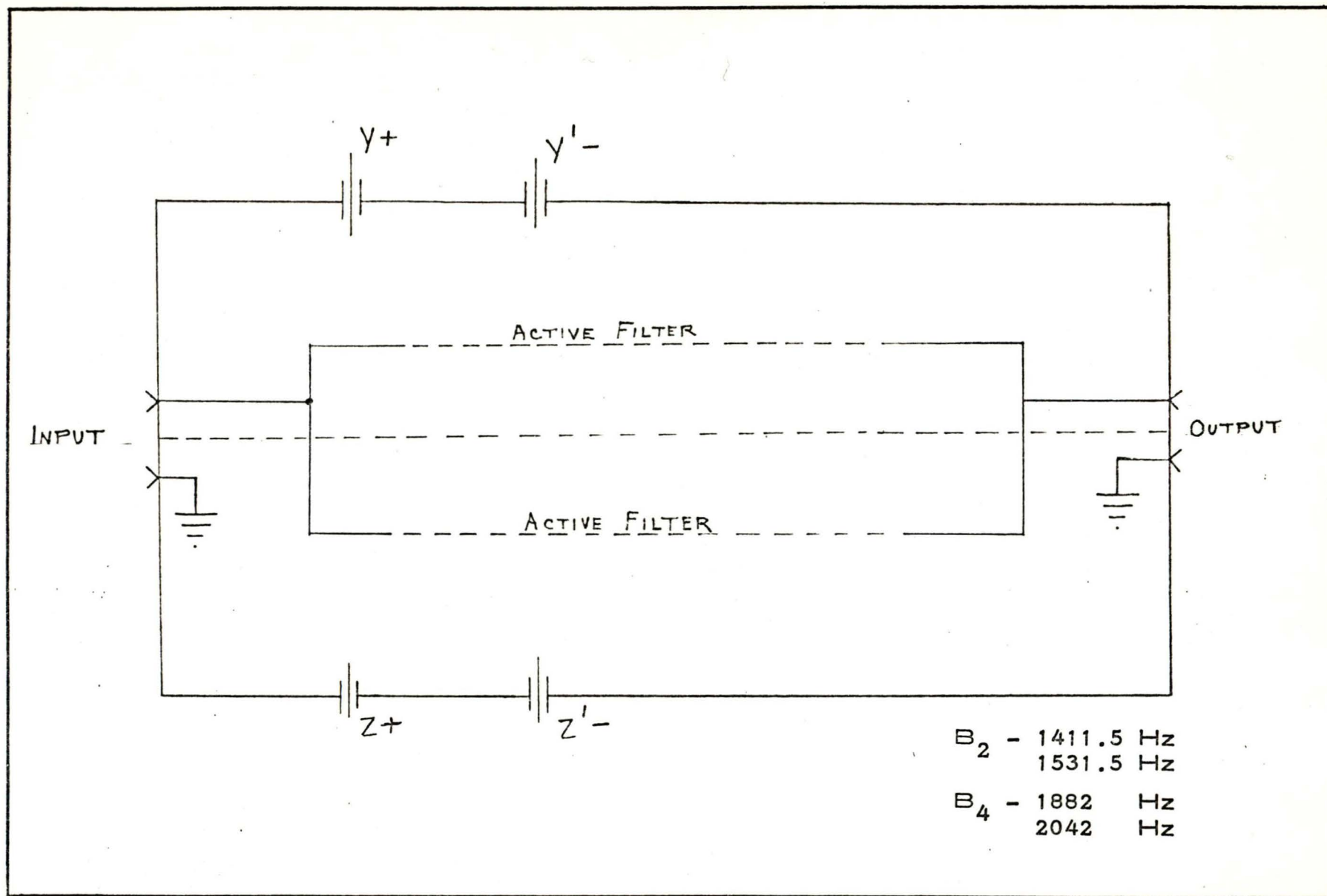


Figure 3.4-5. B2 and B4 Filter Module



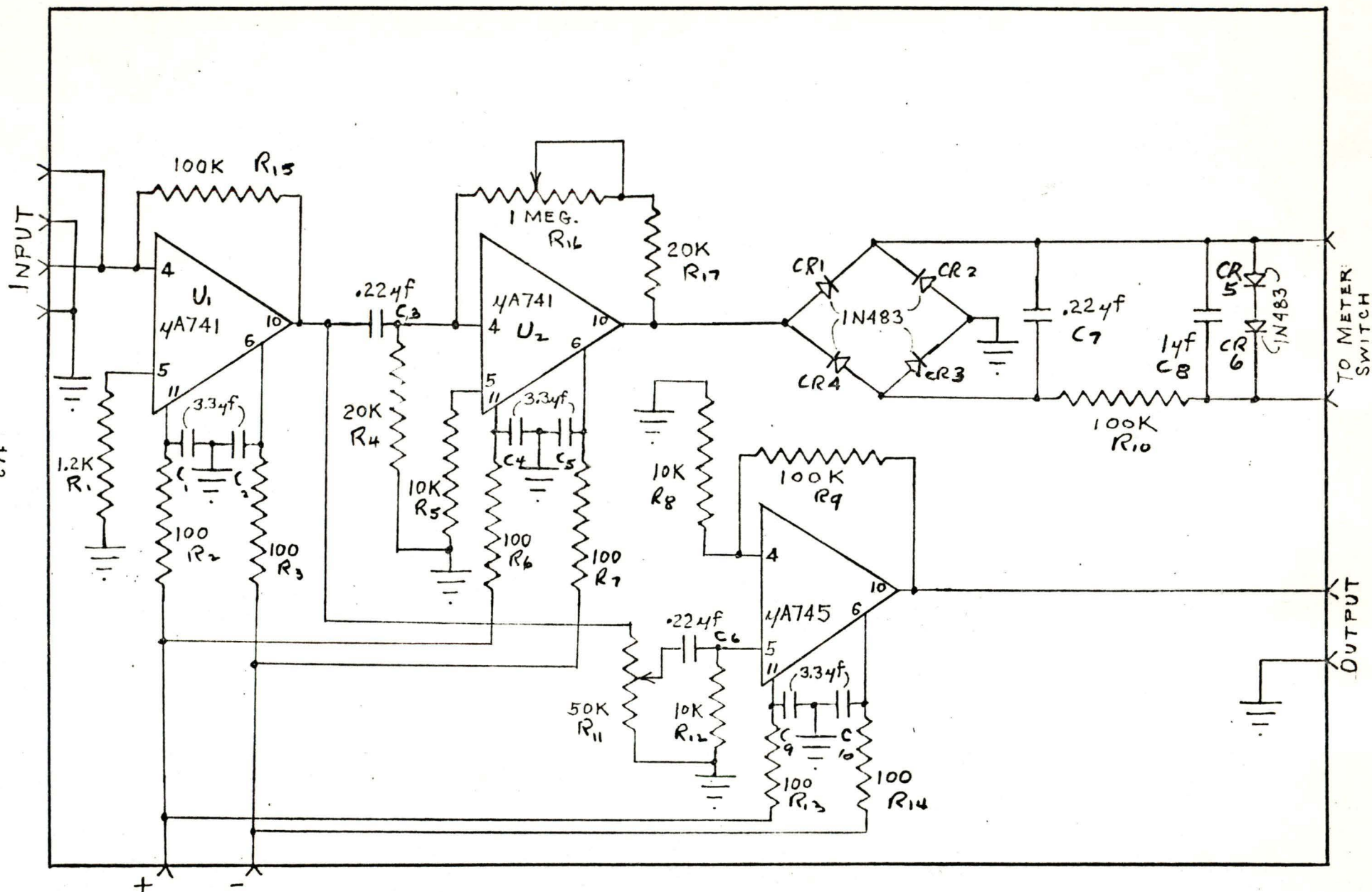


Figure 3.4-6. Output Amplifier (Module C)

#### 4.0

#### EXPERIMENTAL RESULTS

Field tests on the system were performed at two mines; the Island Creek 1A mine at Blair, W.Va., 11/28 to 12/8/72 and the Union Carbide Putnam mine at Leon, W.Va., 12/13 to 12/15/72. Results were generally as follows:

#### 4.1 ISLAND CREEK MINE 1A, BLAIR, W.VA.

- a. Two transmitters were deployed in adjacent crosscuts 425 feet below the surface (80 feet apart). Frequencies (p.r.f.) were 470.5 Hz and 510.5 Hz. The receiver clearly distinguished between the two signals and was able to home on each separately. Each channel in the receiver consisted of four (fundamental and three harmonics) frequency comb filters sharp enough to avoid adjacent channel interference. Good discrimination was achieved even when the receiver was midway between the two sources. (Figure 4.1-1).
- b. Profiles were performed in North-South and East-West directions approximately to determine the structure of the magnetic field strength and to assess the accuracy of the system. There were two problems associated with this site, the terrain was very difficult to traverse and a nearly high voltage power line (figure 4.1-1). The latter resulted in induced signals in the receiver such that the dynamic range and null depth measurements were noise limited. Nevertheless strong signals were received because of:
  - 1) High transmitter moment
  - 2) High receiver sensitivity.

The identification of the source signal was further facilitated by the use of a low duty cycle keying frequency (2 seconds on, 1/2 second off).

Figures 4.1-2 and 4.1-3 show measured profiles North-South and East-West respectively of the 510.5 Hz transmitter at Location 1 (figure 4.1-1). Since this was the initial measurement the first step



145

Figure 4.1-2

Island Creek Mine, W.Va.

Ferrite Loop

North South Radial

Depth: 425 Feet

$\sigma = 3.5 \times 10^{-3}$  mhos/m

Pulse System

PRF 510.5 Hz

Location #1

Solid line - Horizontal H

Dotted line - Vertical H

H  
(db above  
1 ua/m)

146

50

45

40

35

30

25

20

15

10

5

Offset Distances (Ft.)

300

250

200

150

100

50

0

50

100

150

200

250

300

350

400

Noise

S

Noise

True  
Location

Estimated  
Location

K

Noise

Z

Y

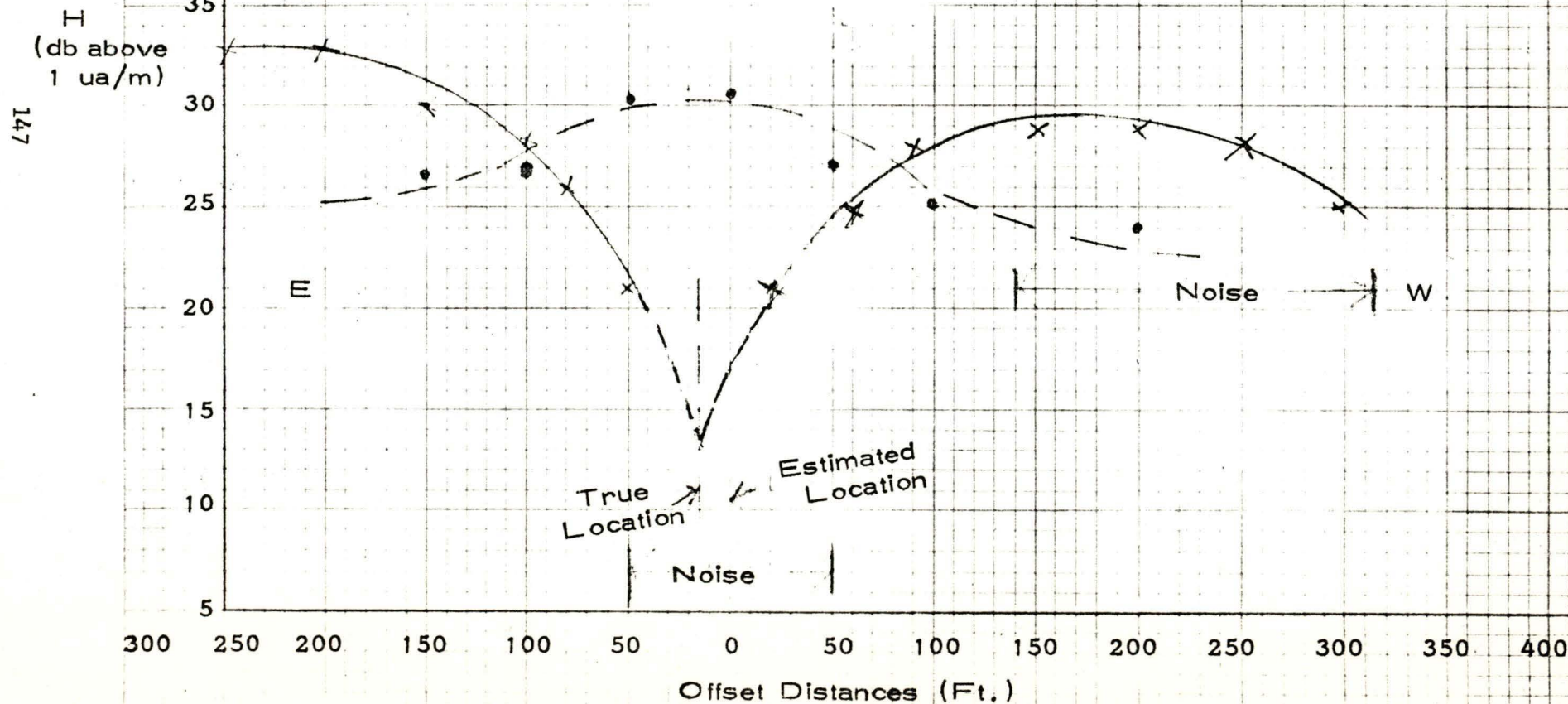


Figure 4.1-3

Island Creek Mine  
 Ferrite Loop  
 East West Radial  
 Depth: 450 Feet

$\sigma = 3.5 \times 10^{-3}$  mhos/m  
 Pulse System 510.5 Hz  
 Location #1  
 Solid line - Horizontal H  
 Dotted line - Vertical H

Measurements of horizontal  
 magnetic field below 20dB  
 are estimated only, due to  
 local noise level at the  
 operating frequency.



involved the electronic detection of the null in the horizontal magnetic field. Profile measurements indicated that the true null was about 30 feet south of the estimated null and about 15 feet east. The true transmitter position as shown on figure 4.1-1 bears this out. As seen from figures 1 and 2, however, the noise in the null region made actual null determination difficult. The measurement was repeated with profiles run from the known true source location and the results were much better (figure 4.1-4).

Figures 4.1-5 and 4.1-6 represent profiles on the 470.5 Hz transmitter located at site #2 (figure 4.1-1). These measurements were made from the true transmitter location site and the results show errors of less than 10 feet in any direction. Again the dynamic range of the measurements was severely limited by the ambient environmental noise.

- c. One of the experiments was to determine the maximum distance a reliable usable signal could be received. Figure 4.1-7 shows the location of the transmitter in the mine and the location of the high voltage surface power line. The latter precluded any distance measurements in all directions except to the west of the transmitter. Reliable strong signals with high directivity were received at approximately 1200 feet west of the transmitter as shown in figure 4.1-7. The receiver was located close to the house as shown. The implications are that course direction finding is possible even in the presence of power lines to distances of 1200 feet. It also implies that direction finding in overburdens of 1000 feet or more should be possible with this equipment.
- d. Another experiment was to determine the useful life of the transmitter signal on one battery charge. A transmitter installed at 8 A.M. was still operating satisfactorily at 8 A.M. the next day. Thus the system is operable for 24 hours at least.



Figure 4.1-4

Island Creek, W. Va.

Ferrite Loop

North South Radial

Depth: 425 Feet

$\sigma = 3.5 \times 10^{-3}$  mhos/m

Pulse: System

PRF - 510.5 Hz

Location #1

Solid line - Horizontal H

Dotted line - Vertical H

H  
(db above  
1 ua/m)

149

55

50

45

40

35

30

25

20

15

10

5

300

250

200

150

100

50

0

50

100

150

200

250

300

350

400

Offset Distances (Ft.)

S

N

True  
Location

137

Figure 4.1-5

Island Creek Mine, W.Va.

Ferrite Loop

North-South Radial

Depth: 425 Feet

$\sigma = 3.5 \times 10^{-3}$  mhos/m

Pulse System - PRF 470.5 Hz

Location #2

Solid line - Horizontal H

Dotted line - Vertical H

150

H  
(db above  
1 ua/m)

55

50

45

40

35

30

25

20

15

10

5

300

250

200

150

100

50

0

50

100

150

200

250

300

250

Offset Distances (Ft.)

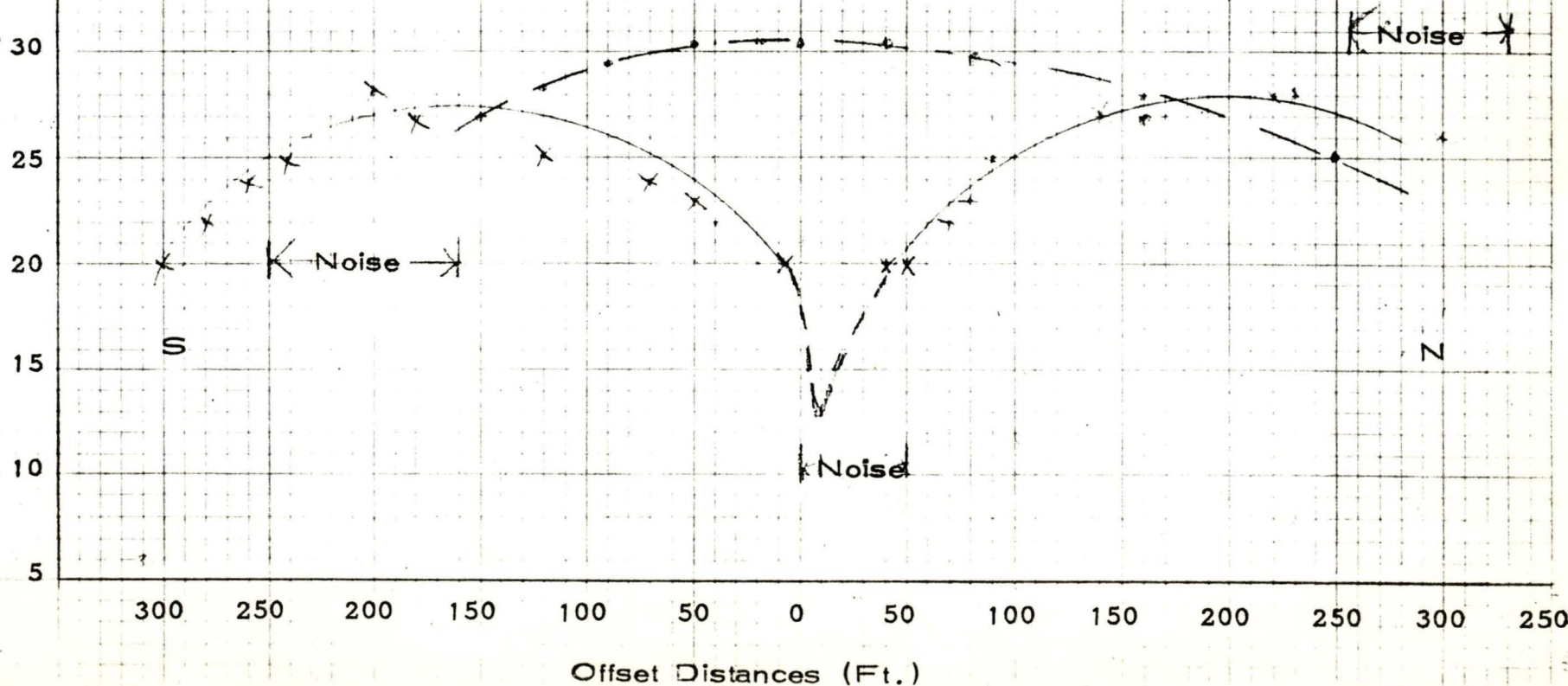




Figure 4.1-6

Island Creek Mine, W.Va.  
 Ferrite Loop  
 East-West Radial  
 Depth: 425 Feet

$\sigma 3.5 \times 10^{-3}$  mhos/m  
 Pulse System - PRF - 470.5 Hz  
 Location #2  
 Solid line - Horizontal H  
 Dotted line - Vertical H

151

H  
 (db above  
 1 ua/m)

55  
 50  
 45  
 40  
 35  
 30  
 25  
 20  
 15  
 10  
 5

300 250 200 150 100 50 0 50 100 150 200 250 300

Offset Distances (Ft.)

E

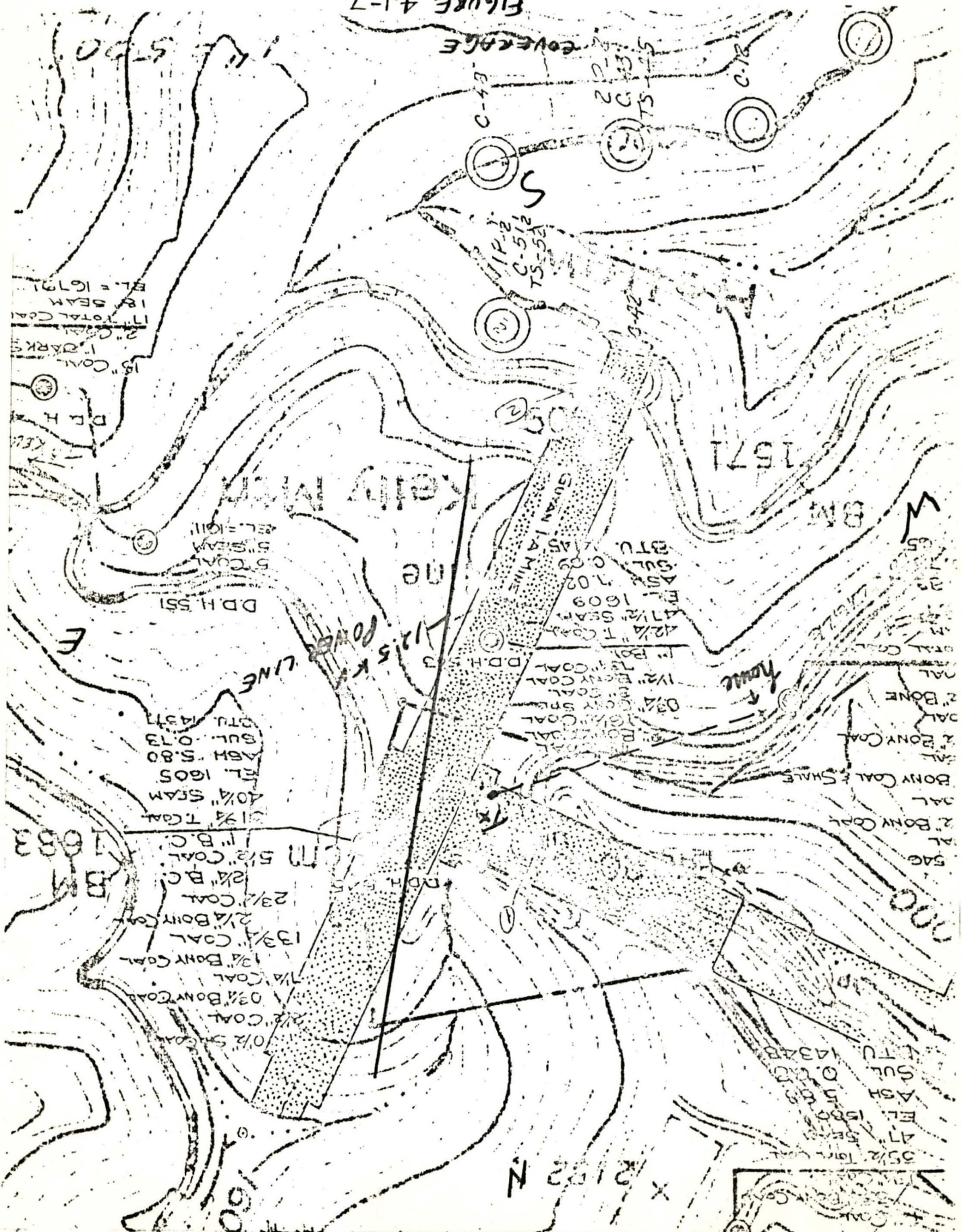
W

Noise

True  
 Location



FIGURE 4.1-7





#### 4.2 UNION CARBIDE MINE, LEON, W.VA.

- a. The tests at this mine were made after some modification\* to the receiver to permit accurate field strength measurements using a calibrated attenuator. This plus the fact that the site offered a far less noisy environment than the Island Creek Mine produced much better results. In figure 4.1-8 we see the East-West profile of the 510.5 Hz transmitter located at site #1 (figure 4.1-9). Surface area was fairly level. Measurements were made from the indicated null which had an error of approximately 10 ft. from the true equipment location (figure 4.1-9). Time permitted only one radial to be run. Note the symmetry and dynamic range of the measurements.
- b. Figures 4.1-10 and 4.1-11 represent two profiles on the 470.5 Hz transmitter located at site #2. (Figure 4.1-9) The error here was less than 5 feet as seen in figure 4.1-9. Again we note the symmetric structure of the fields and the dynamic range of the received signal. All measurements were made from the indicated null.
- c. The life test was repeated here and again a 24 hour operation was observed on a transmitter left in the mine overnight.

#### 4.3 OPERATION

Operationally it appears that to achieve maximum accuracy two orthogonal profiles should be measured and the indicated null should be used for the miner location identification. This is more satisfactory than just looking for a null. The use of slope correction factors is indicated in terrain having a smooth uniform slope. Such correction factors are available in computer programs developed by Westinghouse Georesearch Laboratories, Boulder, Colo. These programs require a knowledge of the conductivity of the overburden as well as the slope of the surface terrain. Correction factors were not applied in the current measurement program as the terrain did not have any slope to speak of in the Union Carbide case and the Island Creek mine did not meet the criterion for a uniform slope correction.

---

\* Modification of the receiver implies that the earlier mine measurements were less accurate, in terms of absolute values. This does not negate the null location at those earlier measurements, however.

Figure 4.1-8

Putman (Union Carbide) Mine,  
Leon, W. Va.  
Air Core Loop  
East-West Radial  
Depth: 400 Feet  
Pulse System-PRF 510.5 Hz  
Location #1  
Solid line - Horizontal H  
Dotted line - Vertical H

154

H  
(db above  
1 ua/m)

45

40

35

30

25

20

15

10

5

0

300

250

200

150

100

50

0

50

100

150

200

250

300

Offset Distances (Ft.)

E

W



FIGURE 4.1-9, UNION CARBIDE MINE, LEON, W. Va.

155





Figure 4.1-10

Putman (Union Carbide) Mine,  
Leon, W.Va.

Air Core Loop

East-West Radial

Depth: 400 Feet

Pulse System - PRF - 470.5 Hz

Location #2

Solid line - Horizontal H

Dotted line - Vertical H

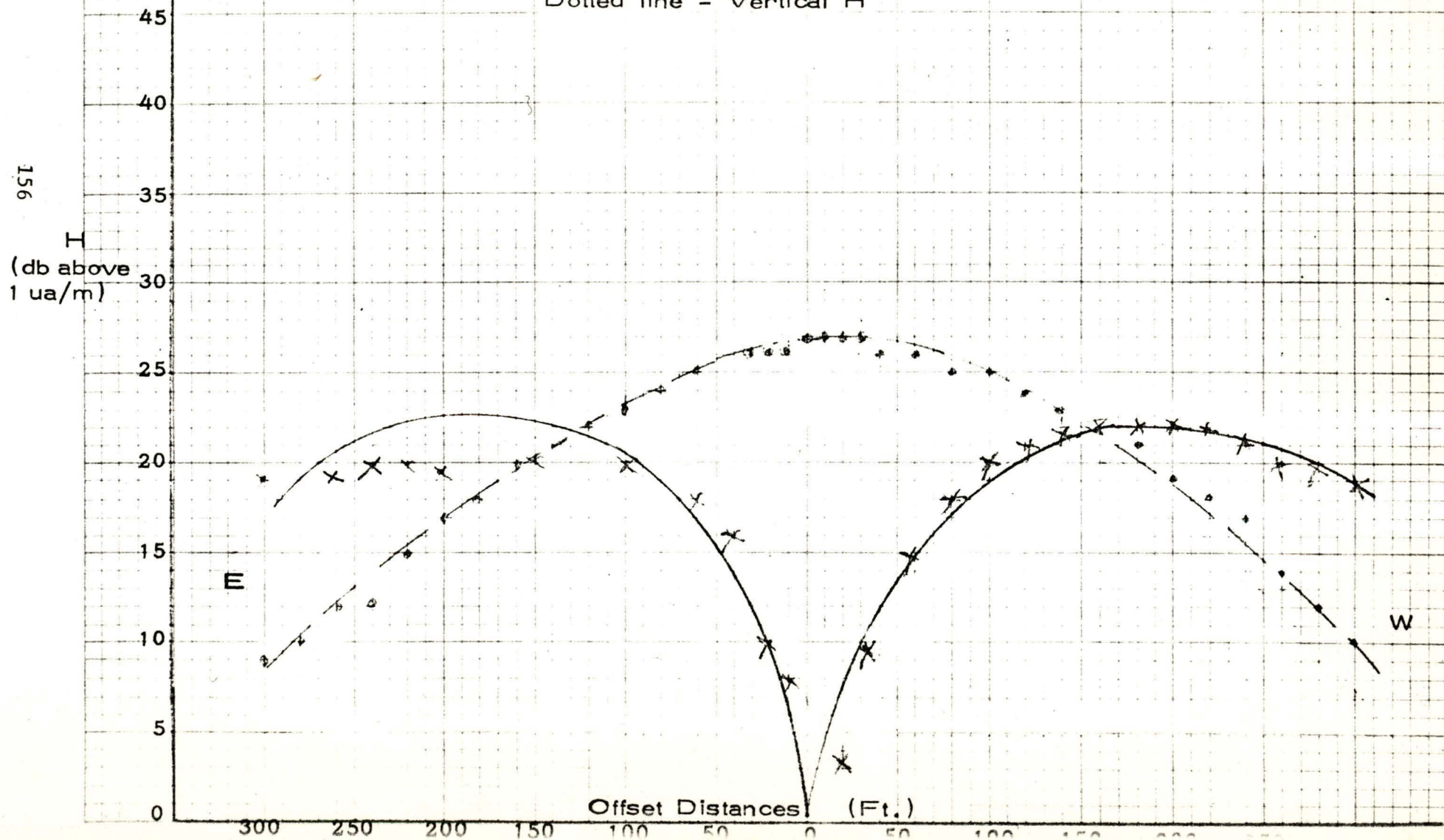




Figure 4.1-11

Putman (Union Carbide) Mine,  
Leon, W. Va.

Air Core Loop

North-South Radial

Depth: 400 Feet

Pulse System-PRF=470.5 Hz

Location #2

Solid line - Horizontal H

Dotted line - Vertical H

157

H  
(db above  
1 ua/m)

45

40

35

30

25

20

15

10

5

0

300

250

200

150

100

50

0

50

100

150

200

250

300

Offset Distances (Ft.)

S

Z

#### 4.4 INTRINSIC SAFETY

The system as tested in the two mines was judged to be intrinsically safe, both from a review of the component sizes, use of limiting resistors and the current and voltage distributions in the circuit. Based upon official BuMines specifications and the actual transmitter voltage and current waveforms used, no explosion could occur in an 8-8.6% methane-air mixture (figure 4.1-12). As we see in this figure a peak to peak voltage of 8 volts (as measured) and a peak current of 8 amperes will not cause an explosion. Similarly, the storage capacitor bank (figure 3.2-1) is also within tolerance as we have a capacitance of 2640 uf (8-330uf capacitors in parallel) whose maximum voltage is 4.0 volts. According to figure 4.1-13 this value at 4.0 volts is a safe combination. Finally figure 4.1-14 indicates that if we extrapolate the inductance threshold below 1000 uh, the 40 uh antenna inductance is readily compatible with the 8 amp antenna peak current and the transformer inductance (100 uh) (Figure 3.2-1) is also compatible with the .1 Amp flowing in the circuit. \*

The above results were borne out in a test performed on the pulse transmitter on 1/17/73 at the U.S. Bureau of Mines Approval and Testing Laboratory, Pittsburgh, Pa.

#### 4.5 ENDURANCE

The pulse system transmitter as presently designed has demonstrated phenomenal endurance capabilities. Operating from the miner's 4.0 volt battery rated at 12 ampere hours at a 1.2 ampere average current drain, the transmitter operated in a 400 foot deep mine for 24 hours with only a 5 db signal loss. Usable signals were received at an offset of 300 feet on the surface. The attenuation increases rapidly with increasing time (Table 4.1.5).

---

\*Due to very low current levels, the receiver was judged to be intrinsically safe under any conditions.



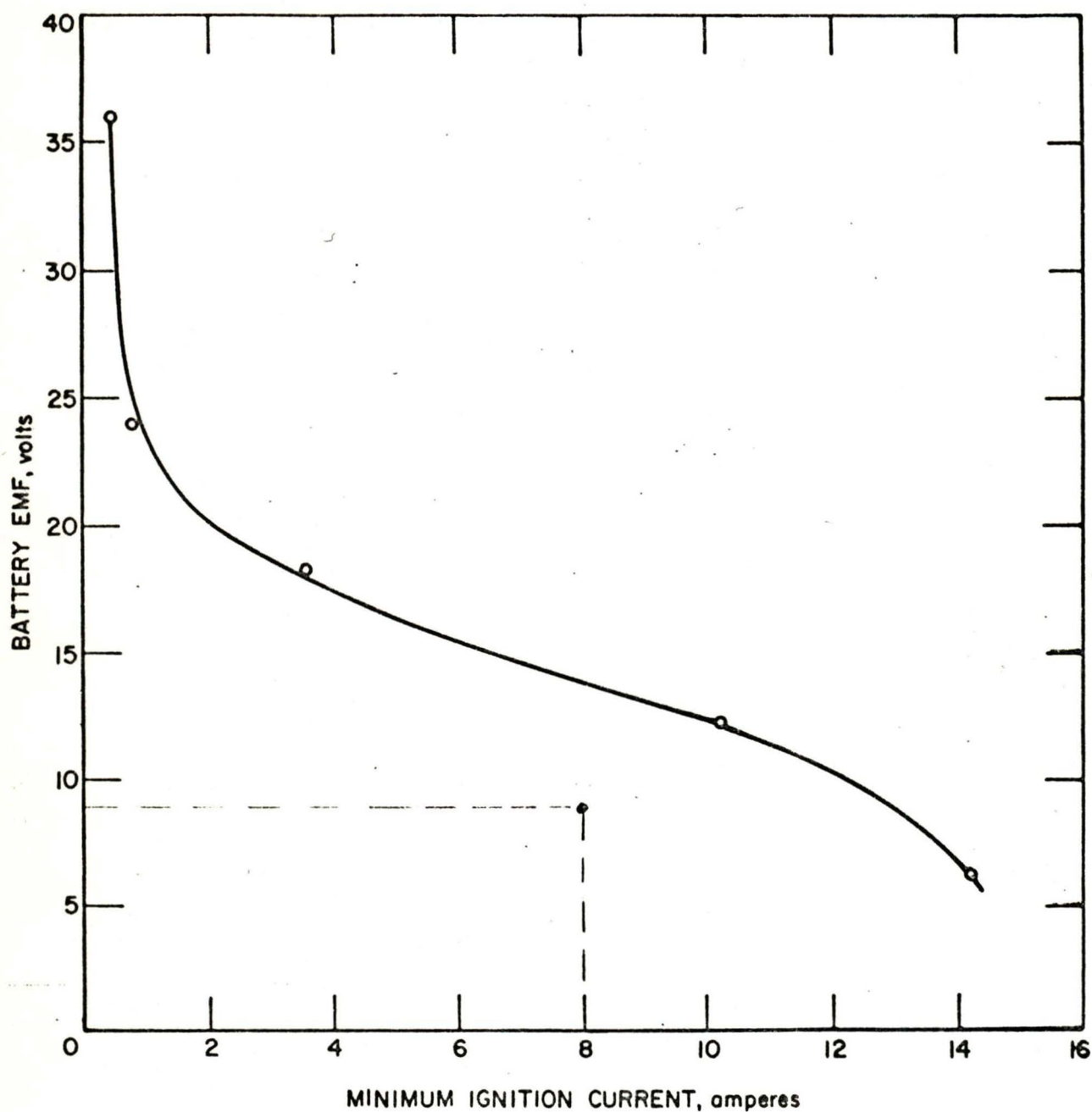


Fig. 4.12. Minimum ignition current as a function of voltage in explosive methane-air mixtures (8.0-8.6 percent  $\text{CH}_4$  by volume).

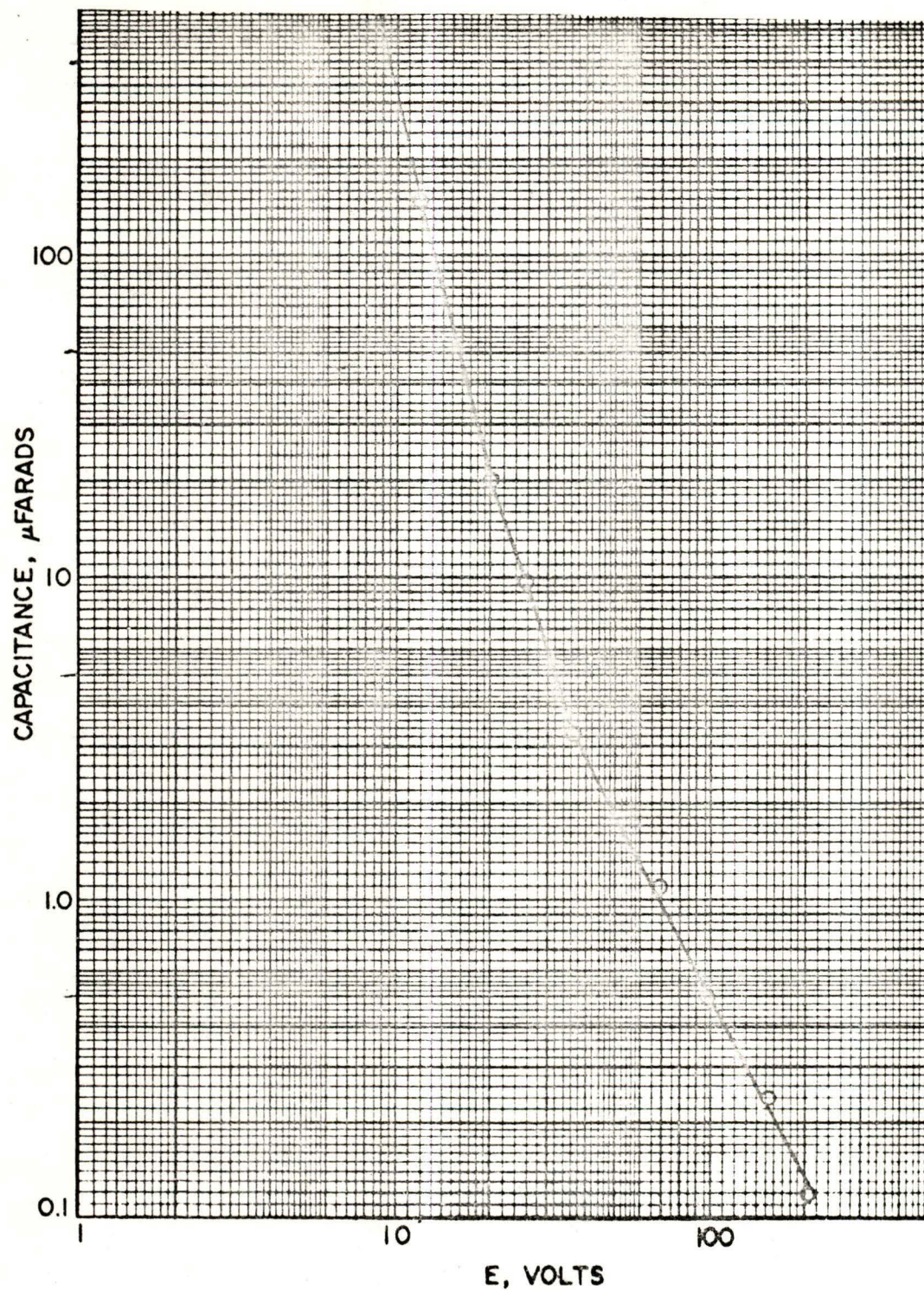


Fig. 4.1-13 Minimum ignition current as a function of voltage in explosive methane-air mixtures (8.1–8.6 percent  $\text{CH}_4$  by volume).



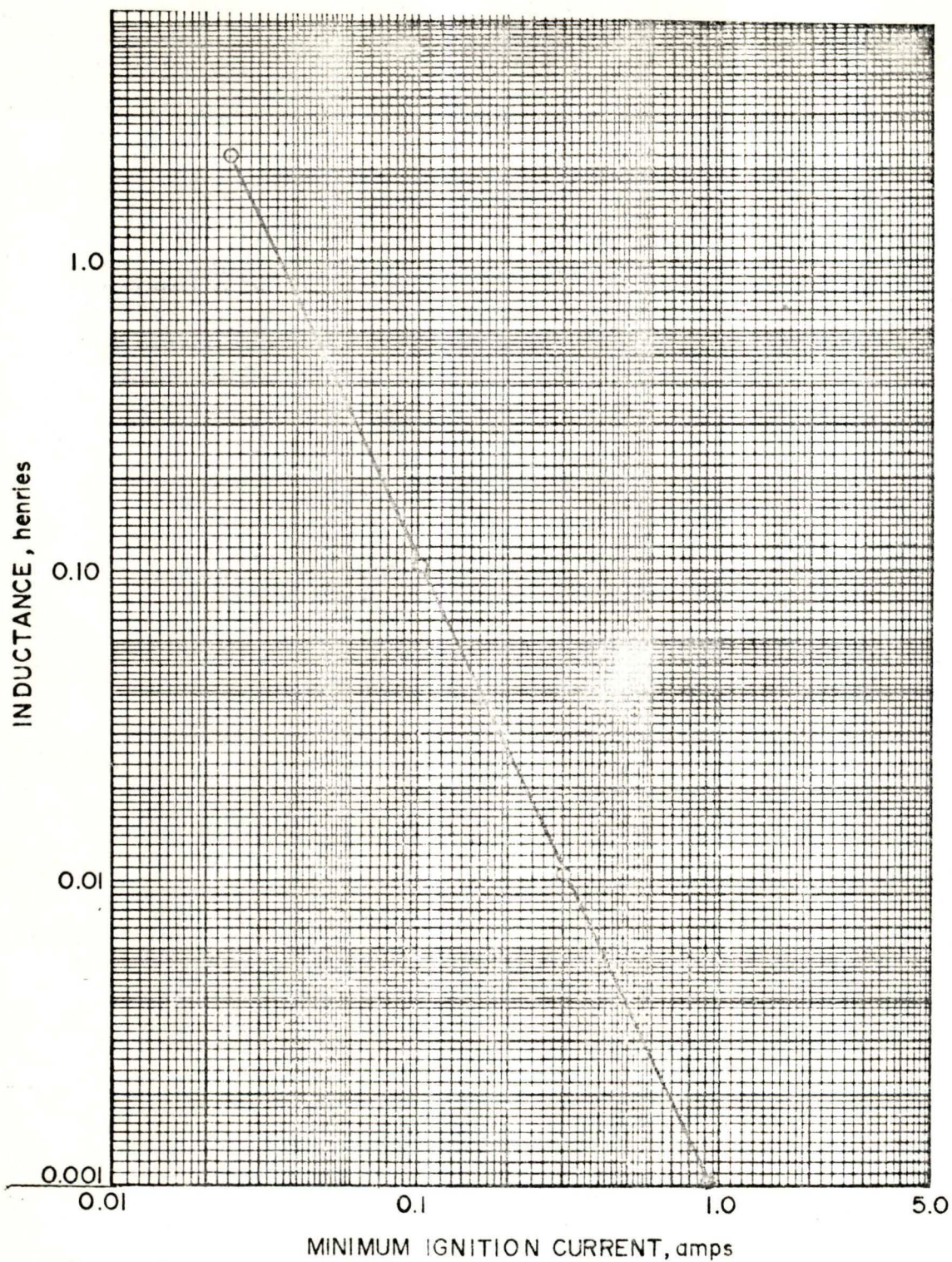


Fig 4.1-14 Minimum ignition current as a function of voltage in explosive methane-air mixtures (8.1-8.6 percent CH<sub>4</sub> by volume).

TABLE 4.1.5  
PULSE TRANSMITTER ENDURANCE CAPABILITIES

<u>Time</u>	<u>Voltage</u>	<u>Signal Attenuation</u>
0	4.5	
24 hrs	3.6	5 db
32 hrs	2.8	10 db
36 hrs	2.7	15 db
42 hrs	2.6	22 db
50 hrs	2.5	40 db



## 4.6

## EQUIPMENT CALIBRATION

In order to assess the received signal amplitude in absolute terms the receiving equipment (antenna and receiver proper) must be calibrated. This is done by establishing a known current in a known loop and placing the receiver and loop to be calibrated in the center of the transmitting loop (figure 4.5-1). The electromagnetic field in the center is related to the current by:

$$H = \frac{\sqrt{2} I}{\pi R} \quad (\text{Reference 6})$$

where R is the distance shown in figure 4.5-1. The computed value of H is correlated with the receiver attenuation setting. Two values of current are used to establish two values of field strength. A straight line through these two values provides a calibration curve for calibrating attenuator settings in terms of absolute field strength. This curve is utilized to plot the experimental data described earlier.

The antenna itself (air core-loop) can be treated as a transducer which converts a magnetic field strength into a voltage output (figure 4.5-2). The equation is given in reference 6 as:

$$E = 2 \pi f u_o A N H$$

where:

f = frequency in hertz

$u_o$  = permeability =  $4\pi \times 10^{-7}$

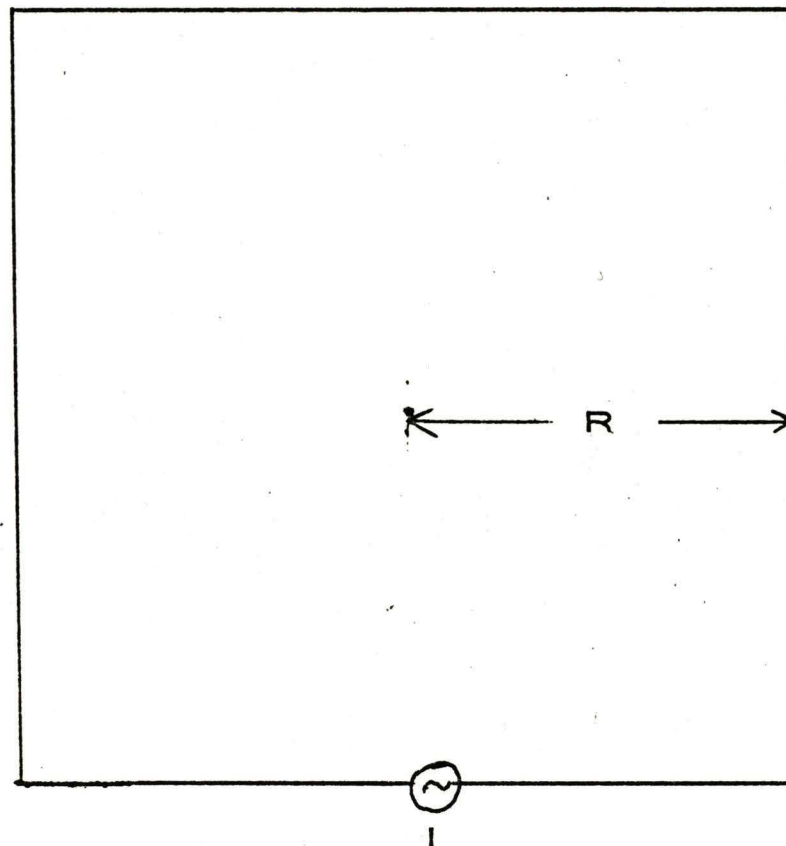
A = loop area in square meters

N = number of turns in loop

H = Electromagnetic Field Intensity in amperes per meter

for the constants used the equation becomes (figure 4.5-2)

$$E = 2.3 H \text{ for } f = 470.5 \text{ Hz (for any other frequency multiply by ratio to 470.5)}$$



CALIBRATION LOOP

Figure 4.5-1



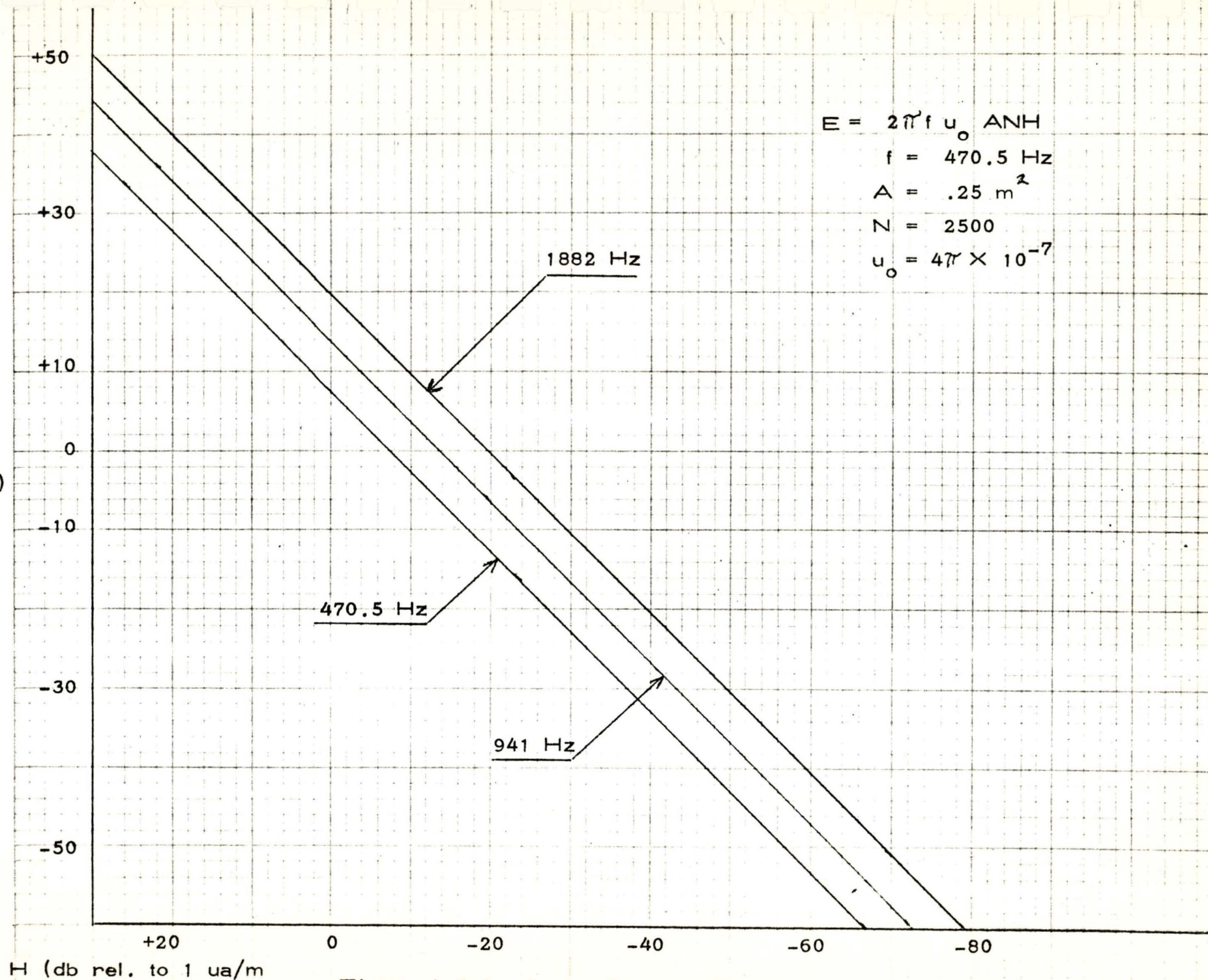


Figure 4.5-2. Loop Characteristics

## 5.0 CONCLUSIONS AND RECOMMENDATIONS

### 5.1 CONCLUSIONS

Based upon the theoretical study and the measured experimental results it appears that the pulse location system is an accurate effective system for the location of trapped miners in an emergency. Accuracies to 10 feet can be achieved in mines to 400' in depth. In addition, signals can be received and homed on for distances to 1200 feet offset from the source. Endurance features are excellent. A usable signal can be received after 24 hours from an underground pulse source powered by the miner's 4 volt battery. Measured attenuation was only 5 db. The system passed intrinsic safety tests and review by the U.S. Bureau of Mines Approval and Testing Office. The identification feature was found satisfactory. Two transmitters 40 Hz apart and 80 feet separation were easily detected without interference at a point midway between them and directly over each site.

### 5.2 RECOMMENDATIONS

It is recommended that:

- a) The equipment be tested at deeper mines.
- b) Additional testing should include tests in which the receiver is deployed from a helicopter.
- c) The system be improved to achieve a better match of the transmitter spectrum and receiver characteristics consistent with intrinsic safety requirements.
- d) The transmitter be redesigned around a hybrid circuit concept to achieve the high reliability and compactness required for deployment to the mining industry.



## 6.0 ADMINISTRATION

### 6.1 RIGHTS IN DATA

Pursuant to Section 2.8 of the contract, all information derived from the performance of the contract is the property of the Government. The results of the work under this contract will not be published or made available to others, except representatives of the contracting officer, without approval in writing from that officer.

### 6.2 INVENTIONS AND DISCLOSURES

Westinghouse submitted the following invention disclosures conceived during the course of this contract:

- "A Receiver System for Use with the Coal Mine Location Project"
- "Transformerless Fullwave Switching Amplifier"

A final detailed Invention Report is being submitted to the Contracting Officer.

REFERENCES

1. "Transient Signals from a Buried Magnetic Dipole" by James R. Wait and David A. Hill. Journal of Applied Physics, Sept. 1971.
2. "Transient Magnetic Fields Produced by a Step Function Excited Loop Buried in the Earth", by James R. Wait and David A. Hill, U.S. Dept. of Commerce, Boulder, Colo. Report submitted to U.S. Bureau of Mines, 15 May 1972.
3. "Electromagnetic Surface Fields Produced by a Pulse-excited Loop Buried in the Earth", by James R. Wait and David A. Hill. Report submitted to U.S. Bureau of Mines, 15 June 1972.
4. "Criteria for Locating an Oscillating Magnetic Dipole Buried in the Earth" by J.R. Wait. Proceedings of the IEEE (Letters) Vol. 59, #6, June 1971, pp. 1033-1035.
5. "Coal Mine Rescue and Survival System", Vol. II, Communications/Location Subsystem, Final Report for Bureau of Mines, Contract H0101262 by Westinghouse Electric Corporation, p. 13.
6. "Mine Emergency Operations Program" Contract H0101262, U.S. Bureau of Mines by Westinghouse Electric Corporation, Appendix III A, Volume I.
7. J. R. Wait, "Electromagnetic Waves in Stratified Media", MacMillan, New York, 1962.



# APPENDIX A

## 1.0 TRANSMITTER PARTS LIST (Figure 3.4-1)

Module A <sub>1</sub>	C <sub>1</sub> -C <sub>8</sub> inclusive	330 uf 6v.	CSRBB337KM
Module A <sub>1</sub>	R11	10 $\Omega$	1/4W
Module A <sub>2</sub>	C <sub>1</sub>	.033 uf	CKO6BX333
	C <sub>2</sub>	47 uf	CSR13B476KM
	C <sub>3</sub>	.033 uf	CKO6BX333
	C <sub>4</sub>	.047 uf	CKO6BX473
	C <sub>5</sub>	1000 pf	CKO5BX102
	C <sub>6</sub>	.01 uf	CKO6BX103
	C <sub>7</sub>	.01 uf	CKO6BX103
	C <sub>8</sub>	150 uf	CSR13B157KM
	R <sub>1</sub>	100K pot.	RJ26CW104
	R <sub>2</sub>	10K, 1/4w	RCR07G103J
	R <sub>3</sub>	1K, 1/4W	RCR07G102J
	R <sub>4</sub>	10K, 1/4W	RCR07G103J
	R <sub>5</sub>	1K, 1/4W	RCR07G102J
	R <sub>6</sub>	10K, 1/4W	RCR07G103J
	R <sub>7</sub>	10K, 1/4W	RCR07G103J
	R <sub>8</sub>	25K, pot.	RJ26CW253
	R <sub>9</sub>	1K, 1/4W	RCR07G102J
	R <sub>10</sub>	330 1/4W	RCR07G331J
	Z1	1 ea. 470.5 Hz	EFM-U Microfork, Murata Corp. of Amer.
		510.5 Hz	
	U1	H8C200 Hybrid Amplifier,	Murata Corp. of Amer.
	U2	LM111	National Semiconductor
	U3	NE555	Signetics National Semiconductor
	Q <sub>1</sub>	2N 2222	Motorola
	CR <sub>1</sub>	1N 4148	Texas Instruments
	CR <sub>2</sub>	1N 968B	Motorola

Module A<sub>3</sub>R<sub>1</sub>

62K

RCR07G623J

R<sub>2</sub>

22K

RCR07G223J

C<sub>1</sub>

33 uf

CSR13B336KM

CR<sub>1</sub>

IN4148

Texas Instruments

CR<sub>2</sub>

MBD 5400

Motorola

CR<sub>3</sub>

MBD 5400

Motorola

V<sub>1</sub>

NE555V

Signetics

T<sub>1</sub>

Local Assembly (See Fig. A-1)

Module A<sub>4</sub>R<sub>1</sub>

220 1/4W

RCR07G221J

R<sub>2</sub>

220 1/4W

RCR07G221J

Q<sub>1</sub>W1743-2N5935

Westinghouse

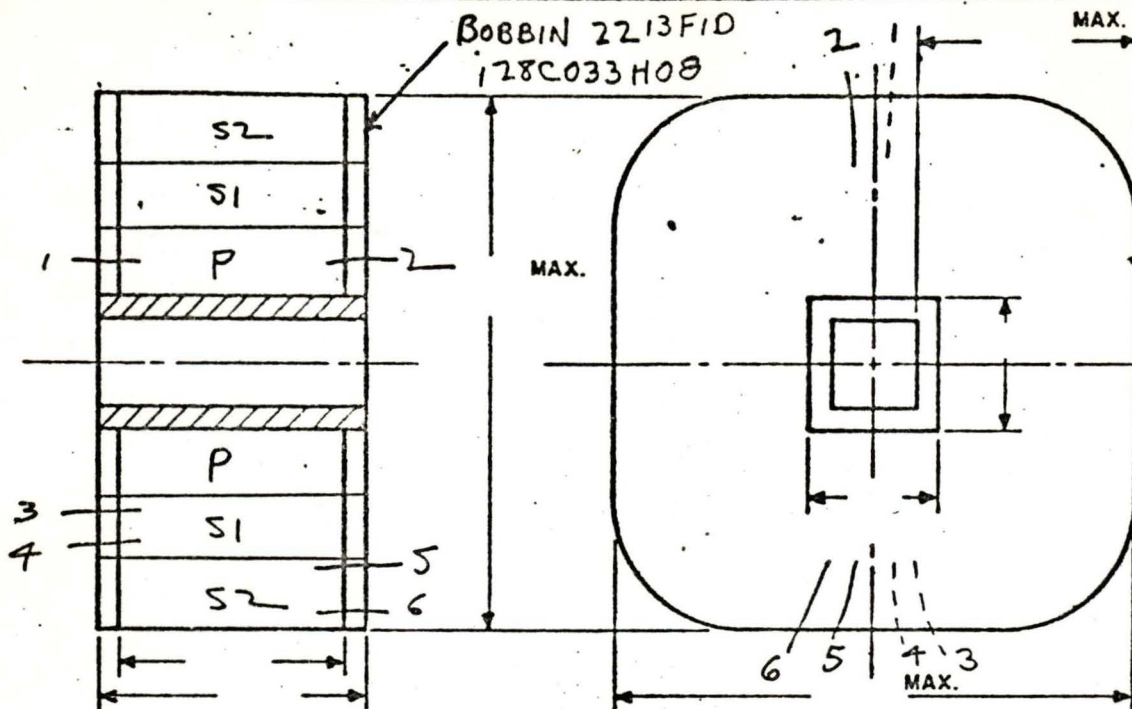
Q<sub>2</sub>W1743-2N5935

Westinghouse



# COIL WINDING AND COIL ASSEMBLY

A3T1



## WINDING DATA

COIL SECTION	P	S1	S2		
TOTAL TURNS	136	34	34		
WIRE SIZE	32	26	26		
WIRE KIND	G12-11PA				
WINDING METHOD	HAND				
NO. OF LAYERS	4	2	2		
URNS/LAYER	34	17	17		
TAPS	NONE			ASSEMBLE IN 387 POT CORE (22MM WITH ZERO GAP)	
MARGIN	NONE				
WDG. TOLERANCE	±1T	±0T	±0T		
LAYER INSULATION	NONE				
WINDING INSULATION	2 LAYERS .005KP	2 LAYERS .005KP	2 LAYERS .005KP		
DIRECTION OF WDG	SAME				
KIND OF LEAD	Wdg Ext	Wdg Ext	Wdg Ext		
LENGTH OF LEAD	2	2	2		
LEAD MARKING	ST-1 FIN-2	ST-3 FIN-4	ST-5 FIN-6		

1. INSULATE PER I-SPEC.

2. FINISH COIL BY

MODULE A3T1

FIGURE A-1

CODE IDENT. NO.	ELEC. SPEC. NO.	REV.	N E M	PAGE
89661	TRANSF 3 REV.	10/25/72		

SD-004

## 2.0

RECEIVER PARTS LIST

Module A

Fig. 3.4-2

R <sub>1</sub>	3.9K	1/4W
R <sub>2</sub>	150K	1/4W
R <sub>3</sub>	1 Meg.	1/4W
R <sub>4</sub>	150	1/4W
R <sub>5</sub>	1K	1/4W
R <sub>6</sub>	1.2K	1/4W
R <sub>7</sub>	5.1K	1/4W
R <sub>8</sub>	1.2 Meg.	1/4W
R <sub>9</sub>	150K	1/4W
R <sub>10</sub>	100	1/4W
R <sub>11</sub>	100	1/4W
R <sub>12</sub>	50K	1/4W
R <sub>13</sub>	5.1K	1/4W
R <sub>14</sub>	100	1/4W
R <sub>15</sub>	100	1/4W
C <sub>1</sub>	1 uf	24V
C <sub>2</sub>	5000 pf	24V
C <sub>3</sub>	5000 pf	24V
C <sub>4</sub>	.1 uf	24V
C <sub>5</sub>	3.3 uf	24V
C <sub>6</sub>	3.3 uf	24V
C <sub>7</sub>	3.3 uf	24V
C <sub>8</sub>	3.3 uf	24V
T <sub>1</sub>	UTC DO-T3	
T <sub>2</sub>	1K - 50 ohms	
	" "	
S <sub>1</sub>	DPDT Switch	

Attenuator, Step 100 db Total

Model 30-0, Kay Electric



Module B<sub>1</sub> and B<sub>3</sub>

Figure 3.4-3

R <sub>1</sub>	20K Pot.	1W
R <sub>2</sub>	5.11K	1/4W
R <sub>3</sub>	14.7K	1/4W
R <sub>4</sub>	47K	1/4W
R <sub>5</sub>	47K	1/4W
R <sub>6</sub>	2.2K	1/4W
R <sub>7</sub>	10K	1/4W
C <sub>1</sub>	.066 uf	24V
C <sub>2</sub>	.022 uf	24V
C <sub>3</sub>	.47 uf	24V
C <sub>4</sub>	47 uf	24V
C <sub>5</sub>	.47 uf	24V
C <sub>6</sub>	.022 uf	24V
C <sub>7</sub>	47 uf	24V
Z <sub>1</sub>	EFM-U Microfork B <sub>1</sub> -470.5 Hz B <sub>2</sub> -510.5 Hz	
Z <sub>2</sub>	H8 C-200	Hybrid Amplifier
Z <sub>1</sub> and Z <sub>2</sub> by Murata Corp. of America		
uA739C	Fairchild Semiconductor	
uA741	Fairchild Semiconductor	

The above parts list is only applicable to the tuning fork circuit of figure 3.4-3. The active filter data is supplied below, (Harmonic filters):

Active filters (all resistors 1/4W, All capacitors 24V).

Figures 3.4-3,4,5

	2nd Harm. 941 Hz	1021 Hz	3rd Harm. 1411.5 Hz	1531 Hz	4th Harm. 1882 Hz	2042 Hz
R <sub>1</sub>	768K	768 K	790K	859K	843K	843K
R <sub>2</sub>	1K	→				
R <sub>3</sub>	196	→				

	2nd Harm.	3rd Harm.		4th Harm.		
	941 Hz	1021 Hz	1411.5 Hz	1531 Hz	1882 Hz	2042 Hz
R <sub>4</sub>	100K	100K	137K	138K	138K	140K
R <sub>5</sub>	100	→				
R <sub>6</sub>	100	→				
R <sub>7</sub>	14.7K	→				
R <sub>8</sub>	5.1K	→				
R <sub>9</sub>	10K	→				
R <sub>10</sub>	10K	→				
R <sub>11</sub>	100	→				
R <sub>12</sub>	100	→				
R <sub>13</sub>	768K	768K	790K	859K	843K	843K
R <sub>14</sub>	1K	→				
R <sub>15</sub>	196	→				
R <sub>16</sub>	100K	100K	137K	138K	138K	140K
R <sub>17</sub>	100	→				
R <sub>18</sub>	100	→				
R <sub>19</sub>	14.7K	→				
R <sub>20</sub>	10K	→				
C <sub>1</sub>	10000 pf	9260 pf	9640 pf	8850 pf	7200 pf	6640 pf
C <sub>2</sub>	10000 pf	9260 pf	9640 pf	8850 pf	7200 pf	6640 pf
C <sub>3</sub>	3.3 uf	→				
C <sub>4</sub>	3.3 uf	→				
C <sub>5</sub>	3.3 uf	→				
C <sub>6</sub>	3.3 uf	→				
C <sub>7</sub>		Same as C <sub>1</sub>				
C <sub>8</sub>		Same as C <sub>1</sub>				
C <sub>9</sub>	3.3 uf	→				
C <sub>10</sub>	3.3 uf	→				
C <sub>0</sub>	.068 uf	.068 uf	.047 uf	.047 uf	.033 uf	.033 uf



# Module C

Figure 3.4-6

R <sub>1</sub>	1.2K	1/4W
R <sub>2</sub>	100	1/4W
R <sub>3</sub>	100	1/4W
R <sub>4</sub>	20K	1/4W
R <sub>5</sub>	10K	1/4W
R <sub>6</sub>	100	1/4W
R <sub>7</sub>	100	1/4W
R <sub>8</sub>	10K	1/4W
R <sub>9</sub>	100K	1/4W
R <sub>10</sub>	100K	1/4W
R <sub>11</sub>	40K Pot.	1W
R <sub>12</sub>	10K	1/4W
R <sub>13</sub>	100	1/4W
R <sub>14</sub>	100	1/4W
R <sub>15</sub>	100K	1/4W
R <sub>16</sub>	1 Meg.	1/4W
R <sub>17</sub>	20 K	1/4W
C <sub>1</sub>	3.3 uf	
C <sub>2</sub>	3.3 uf	
C <sub>3</sub>	.22 uf	
C <sub>4</sub>	3.3 uf	
C <sub>5</sub>	3.3 uf	
C <sub>6</sub>	.22 uf	
C <sub>7</sub>	.22 uf	
C <sub>8</sub>	1 uf	
C <sub>9</sub>	3.3 uf	
C <sub>10</sub>	3.3 uf	
CR1-4	IN 483	Texas Instruments
CR5	IN 483	Texas Instruments

CR6

IN 483

Texas Instruments

U<sub>1</sub>

uA741

Fairchild Semiconductor

U<sub>2</sub>

uA741

Fairchild Semiconductor



# PROPAGATION ATTENUATION

The factors  $|G|$ ,  $|D|$ , and  $|A|$  shown in Figure 2-1, page four of this volume, represent attenuation factors which must be applied in estimating electromagnetic field strengths at the surface from underground transmitting sources. As used here, they are close approximations to the exact values of these factors. Exact values here have been given by Wait\* and Sinha-Bhattacharya\*\*. The latter has shown in the calculation of  $|G|$ , for example, and in the case of both transmitting source and receiver inside the earth, that the electric and magnetic fields can be specified from the potential function, F.

$$\begin{aligned}
 (1) \quad F = & M \left[ \frac{e^{-\gamma R_1}}{R_1} - \frac{e^{-\gamma R_2}}{R_2} + \frac{2}{\gamma} \left\{ B'(z+h)^2 - A' \right\} \right. \\
 & + \frac{2}{\gamma^2} \left\{ (z+h) \left( \frac{3}{2} \frac{\gamma^2 \rho^2}{R_2^4} - \frac{\gamma^2}{R_2^2} \right) I_0(\zeta) K_0(\beta) - (z+h) \left( \frac{3}{2} \frac{\gamma^2 \rho^2}{R_2^4} \right) I_1(\zeta) K_1(\beta) \right. \\
 & + \left[ (z+h) \frac{\gamma^3 \rho^2}{2R_2^3} + \frac{\beta(3\rho^2 - 2R_2^2)}{R_2^5} \right] I_0(\zeta) K_1(\beta) \\
 & \left. \left. - \left[ (z+h) \frac{\gamma^3 \rho^2}{2R_2^3} - \frac{\zeta(3\rho^2 - 2R_2^2)}{R_2^5} \right] I_1(\zeta) K_0(\beta) \right\} \right]
 \end{aligned}$$

\*Wait, J.R. - "The Magnetic Dipole Over the Horizontally Stratified Earth" Can. J. Phys., 29, 577-592.

\*Wait, J.R. - "Mutual Electromagnetic Coupling of Loops Over a Homogeneous Earth", Geophysics, 20, No. 3, 630-637.

\*\*Sinha, A.K. & Bhattacharya, P.K. - "Vertical Magnetic Dipole Buried Inside a Homogeneous Earth", Radio Science, Vol. 1, No. 3, 370-395.

where  $I_0$ ,  $I_1$ ,  $K_0$  and  $K_1$  are modified Bessel functions.

$$(2) \quad \begin{aligned} A' &= \frac{(1 + \gamma R_2)}{R_2^3} \exp(-\gamma R_2) \\ B' &= \frac{(\gamma^2 R_2^2 + 3\gamma R_2 + 3)}{R_2^5} \exp(-\gamma R_2) \end{aligned}$$

$$\zeta = \frac{\gamma}{2} (R_2 - z - h)$$

$$\beta = \frac{\gamma}{2} (R_2 + z + h)$$

$$R_1 = [\rho^2 + (z - h)^2]^{1/2}$$

$$R_2 = [\rho^2 + (z + h)^2]^{1/2}$$

$$M = \frac{i \omega \mu_0}{4\pi} (INA)$$

$\omega$  = source frequency

$I$  = loop antenna current

$N$  = number of turns in the loop antenna

$A$  = area enclosed by the loop antenna

$\mu_0$  = permeability of the earth, taken as  $4\pi \times 10^{-7}$  henries/meter



Once the potential function F is known, the value of  $H_Z$ , for example, can be established from:

$$\begin{aligned}
 (3) \quad \frac{i\omega\mu H_Z}{M} = & e^{-\mu R_1} \left\{ 2p + (2-a^2) - 3\tau_1 (a+\tau_1) \right\} - \\
 & e^{-q R_2} \left\{ 2q + (2-a^2) - 3\tau_2 (a+\tau_2) \right\} + \\
 & 2e^{-q R_2} \left\{ 15\tau_2^2 (1+q) (1-7L_2^2) + \right. \\
 & 3a^2 (2-15L_2^2) + (5L_2^2-1) [6-q(a^2-6)] - \\
 & 5qa^2L_2^2 - q^2 [2 + L_2^2 (a^2-12)] + \\
 & 2L_2^2q^3 \left. \right\} + L_2R_2^{-3} \left\{ d+2a^2-24 \right\} I_0K_0 - \\
 & L_2R_2^3 \left\{ d-70\tau_2^2 \right\} I_1K_1 + \\
 & L_2R_2^{-3} \left\{ e_1 + \beta (20\tau_2^2-6) + 6\beta L_2^{-1} q^{-2} f \right\} I_0K_1 \\
 & - L_2R_2^{-3} \left\{ e_1 + \alpha (20\tau_2^2-6) - 6\alpha L_2^{-1} q^{-2} f \right\} I_1K_0
 \end{aligned}$$

where

$$p = \gamma R_1$$

$$q = \gamma R_2$$

$$L_1 = \frac{Z - h}{R_1}$$

$$L_2 = \frac{Z + h}{R_2}$$

$$\tau_1 = \frac{\rho}{R_1}$$

$$d = 4a^2 - 10a^2\tau_2^2 + 120\tau_2^2 - 105\tau_2^4$$

$$\tau_2 = \frac{\rho}{R_2}$$

$$a = \gamma \rho$$

$$e = 22a\tau_2 - a^3\tau_2 - 45a\tau_2^3$$

$$f = 40\tau_2^2 - 8 - 35\tau_2^4$$

$h$  = depth of transmitting source

$(\rho, \phi, Z)$  = coordinates at the arbitrary point, inside the earth, of observation of the magnetic field, Hz.

$\gamma$  = propagation constant of the medium.

$$I_n = I_n(\alpha) = I_n \frac{\gamma}{2} (R_2 - Z - h)$$

$$K_n = K_n(\beta) = K_n \frac{\gamma}{2} (R_2 + Z + h)$$

For the case being considered here, the transmitter and receiver are located along a common vertical with the transmitter at a depth  $Z$  and the receiver on the surface<sup>1</sup>, directly above the transmitter. Then,  $\rho = h = 0$ , and some simplification is possible.

$$(4) \quad iw\mu Hz = \frac{2M}{Z^3} \left[ \frac{2}{\gamma^2 Z^2} - (12 + 12\gamma Z + 5\gamma^2 Z^2 + \gamma^3 Z^3) \exp(-\gamma Z) - 3 \left\{ 4K_0(\gamma Z) + \left(\gamma Z + \frac{8}{Z}\right) K_1(\gamma Z) \right\} \right]$$

and

<sup>1</sup>Here reciprocity is assumed to hold so that the relation positions of the transmitter and receiver could be reversed.



$$(5) \quad i\omega\mu H_z = \frac{2 \left[ \frac{i\omega\mu_0 I_N A}{\pi^4} \right] |G|}{z^3}$$

where  $G$  is equal to all factors inside the brackets on the right side of equation (4), and the absolute value is taken.

Then

$$(6) \quad H_z = \frac{I_N A |G|}{2 \pi z^3}$$

which is the expression shown in Figure 2-1 for  $|G|$ .

Values for  $|A|$  and  $|D|$  are established in a similar manner.